

# Argonne National Laboratory

DYNAMIC ANALYSIS OF  
LIQUID-METAL-COOLED FAST POWER REACTORS

by

J. A. DeShong, Jr.

The facilities of Argonne National Laboratory are owned by the United States Government. Under the terms of a contract (W-31-109-Eng-38) between the U. S. Atomic Energy Commission, Argonne Universities Association and The University of Chicago, the University employs the staff and operates the Laboratory in accordance with policies and programs formulated, approved and reviewed by the Association.

#### MEMBERS OF ARGONNE UNIVERSITIES ASSOCIATION

The University of Arizona	Kansas State University	The Ohio State University
Carnegie-Mellon University	The University of Kansas	Ohio University
Case Western Reserve University	Loyola University	The Pennsylvania State University
The University of Chicago	Marquette University	Purdue University
University of Cincinnati	Michigan State University	Saint Louis University
Illinois Institute of Technology	The University of Michigan	Southern Illinois University
University of Illinois	University of Minnesota	University of Texas
Indiana University	University of Missouri	Washington University
Iowa State University	Northwestern University	Wayne State University
The University of Iowa	University of Notre Dame	The University of Wisconsin

#### LEGAL NOTICE

This report was prepared as an account of Government sponsored work. Neither the United States, nor the Commission, nor any person acting on behalf of the Commission:

A. Makes any warranty or representation, expressed or implied, with respect to the accuracy, completeness, or usefulness of the information contained in this report, or that the use of any information, apparatus, method, or process disclosed in this report may not infringe privately owned rights; or

B. Assumes any liabilities with respect to the use of, or for damages resulting from the use of any information, apparatus, method, or process disclosed in this report.

As used in the above, "person acting on behalf of the Commission" includes any employee or contractor of the Commission, or employee of such contractor, to the extent that such employee or contractor of the Commission, or employee of such contractor prepares, disseminates, or provides access to, any information pursuant to his employment or contract with the Commission, or his employment with such contractor.

Printed in the United States of America

Available from

Clearinghouse for Federal Scientific and Technical Information  
National Bureau of Standards, U. S. Department of Commerce

Springfield, Virginia 22151

Price: Printed Copy \$3.00; Microfiche \$0.65

ARGONNE NATIONAL LABORATORY  
9700 South Cass Avenue  
Argonne, Illinois 60439

DYNAMIC ANALYSIS OF  
LIQUID-METAL-COOLED FAST POWER REACTORS

by

J. A. DeShong, Jr.

Reactor Physics Division

January 1969



## TABLE OF CONTENTS

	<u>Page</u>
<b>ABSTRACT . . . . .</b>	<b>7</b>
<b>I. INTRODUCTION . . . . .</b>	<b>7</b>
<b>II. LINEAR REACTOR CORE DYNAMICS . . . . .</b>	<b>8</b>
A. Heat Transfer of Core Fuel Element . . . . .	8
B. Coolant Void Effect . . . . .	9
C. Fuel Axial-expansion Effect . . . . .	10
D. Axial Expansion of Control Rod and Subassembly . . . . .	10
<b>III. THERMOMECHANICAL DISTORTION AND MOVEMENT OF THE CORE FUEL ELEMENTS . . . . .</b>	<b>13</b>
A. BOW III Computer Program for Determination of Equilibrium Reactivity . . . . .	14
B. Heat-transfer Dynamics of Reflector Subassemblies . . . . .	15
C. Calculation of Structure Dynamic Reactivity . . . . .	17
<b>IV. SYSTEM BLOCK DIAGRAM OF CORE DYNAMICS . . . . .</b>	<b>20</b>
A. EBR-II System Diagram . . . . .	20
B. Calculated Reactivity Time Response to a Reactor Rod Drop . . . . .	21
<b>V. SUMMARY AND CONCLUSIONS . . . . .</b>	<b>21</b>
<b>APPENDIXES</b>	
A. Dynamic Heat-transfer Calculations . . . . .	23
1. Fuel Subassembly; Rows 1-6 . . . . .	23
2. Blanket Subassembly; Row 9 . . . . .	26
3. Blanket Subassembly; Rows 10-15 . . . . .	27
4. Control Rod Section $L_1$ . . . . .	28
5. Plenum Effect . . . . .	28
6. Control Rod Section $L_2$ . . . . .	29
7. Control Rod Section $L_3$ . . . . .	29
8. Control Rod Section $L_4$ . . . . .	30

## TABLE OF CONTENTS

	<u>Page</u>
B. BOW III Thermomechanical Structure Analysis . . . . .	32
1. Theoretical Bending of Subassemblies due to Combined Nozzle, Button, and Top Loading . . . . .	32
2. BOW III Computer Program . . . . .	35
3. Calculation of Input Quantities . . . . .	38
4. BOW III Sample Run . . . . .	40
C. Reflector Heat-transfer Dynamics . . . . .	60
1. Reflector Subassembly; Row 7 . . . . .	60
2. Reflector Subassembly; Row 8 . . . . .	63
D. PROFILE Temperature Calculations . . . . .	65
E. DYNAMIC Reactivity Calculations . . . . .	77
ACKNOWLEDGMENT . . . . .	89
REFERENCES . . . . .	90

## LIST OF FIGURES

<u>No.</u>	<u>Title</u>	<u>Page</u>
1.	Cross Section of Fuel Element .....	8
2.	Heat-flow Diagram for Fuel Element .....	9
3.	Control-rod Suspension .....	11
4.	Cross Section of Control Drive Rod at L <sub>3</sub> .....	12
5.	Cross Section of Control Drive Rod at L <sub>4</sub> .....	12
6.	Heat-flow Diagram for the Control Drive Rod .....	13
7.	Equilibrium Feedback Reactivity of Structure .....	15
8.	Cross Section of Reflector Subassembly .....	15
9.	Heat-flow Diagram for Reflector Subassembly .....	16
10.	Power Variation with Time for a Rod-drop Experiment .....	17
11.	Dynamic Change in Row Differential Temperature Profiles ..	19
12.	System Block Diagram of EBR-II Core Dynamics .....	20
13.	Calculated Reactivity Variation with Time for a Rod-drop Experiment .....	21
B.1.	Subassembly as a Loaded Beam .....	32
B.2.	Subassembly M/EI Diagram and Radial Displacement .....	33
B.3.	Rotation of Subassembly in Spherical Pivot Support .....	34
B.4.	BOW III Module .....	38
D.1.	PROFILE Input Function .....	65

## LIST OF TABLES

<u>No.</u>	<u>Title</u>	<u>Page</u>
I.	Physical Properties of Type 304 Stainless Steel, Liquid Sodium, and Uranium .....	23
II.	BOW III Bending Modes .....	33
III.	BOW III FORTRAN Quantities .....	36
IV.	Reactivity Evaluation of Sample Output .....	40
V.	PROFILE FORTRAN Quantities .....	66
VI.	C(t) for Rows 6-10 .....	67
VII.	DYNAMIC FORTRAN Quantities .....	77



DYNAMIC ANALYSIS OF  
LIQUID-METAL-COOLED FAST POWER REACTORS

by

J. A. DeShong, Jr.

ABSTRACT

The small-signal dynamic behavior of liquid-metal-cooled fast power reactors is analyzed by means of feedback control theory.

Transfer functions to calculate dynamic feedback reactivity generated by fuel expansion, sodium void effect, and thermal motion of control rods are developed, as well as a computer program to calculate dynamic feedback reactivity produced by thermomechanical distortion and movement of the core fuel elements. A theoretical block diagram of the EBR-II reactor system is constructed from these elements.

I. INTRODUCTION

The dynamic behavior of liquid-metal-cooled fast reactors is sensitive to many factors that influence reactivity, such as sodium void effect, axial thermal expansion of fuel, heat transfer from fuel to coolant, Doppler effect in large cores, and the radial movement and distortion of fuel sub-assemblies due to thermal gradients in the core. This report describes the results of a study made of a specific reactor for the purpose of developing a theoretical description of the reactor core dynamics.

The following sections develop in dynamic form the linear components of feedback reactivity by using heat-transport considerations. The linear treatment is suitable for everything but the structural distortion, where the structural component movements all interact on each other in a complex way. The latter case is attacked by numerical analysis using a computer program, BOW III, developed to analyze a specific reactor core structure as an example. Static heat-transfer calculations were made by Cushman to develop radial differential temperature profiles of the fuel subassembly.<sup>1</sup> These profiles are used as input to the BOW III program to calculate the static power-reactivity coefficient, which is defined as the reactivity generated by structural movement due to a specific change of reactor operating power from one equilibrium value to another.

The dynamic reactivity change due to structural motion is obtained by making heat-transfer calculations to determine dynamic radial and axial temperature response to a rod-drop reactor power-time function. The calculated dynamic temperatures are used to obtain the differential temperature profiles at specified times over the time range of interest. These profiles then are inputed to the BOW III program to determine the structural positions at the specified times. The dynamic motion of the structure in response to a rapid change in reactor power could also be influenced by mechanical inertia, spring constants, and damping. However, for the chosen example, the motions and therefore the inertial forces are small, while the spring constants expressed in force per unit distance are very large. Therefore the mechanical movements are assumed to follow the temperature changes with no time lag.

All the foregoing work is combined to develop a system block diagram to represent the theoretical core dynamics of the EBR-II reactor.

## II. LINEAR REACTOR CORE DYNAMICS

### A. Heat Transfer of Core Fuel Element

The individual fuel element is taken as a right circular cylinder, divided into two annular regions of equal volume, shown as ① and ② in

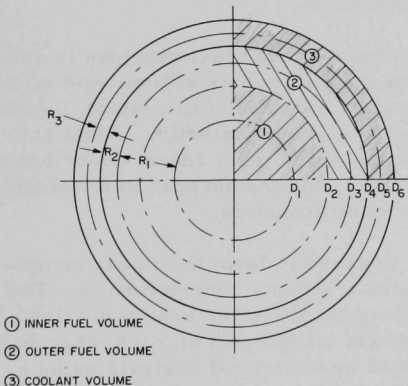


Fig. 1. Cross Section of Fuel Element

Fig. 1, which is a cross section of the cylinder. These are surrounded by another annular region of coolant, shown as ③. Then  $D_2$ , the outside diameter of the inner volume, is 0.707 times  $D_4$ , which is the outside diameter of the outer volume. The heat capacity of each volume can be lumped at  $D_1 = 0.5D_4$  for the inner volume and  $D_3 = 0.866D_4$  for the outer volume. The heat generated in each volume is taken as originating at these same diameters.  $R_1$ , then, is the reciprocal conductivity from the inner to the outer volume, and  $R_2$  is the reciprocal conductivity from the outer volume to the coolant surface, including any film effect.  $R_3$  is the reciprocal conductivity

from the fuel-element surface radially to the center of mass of the coolant. These are reciprocal conductivities evaluated using the fuel-element length ( $L$ ).

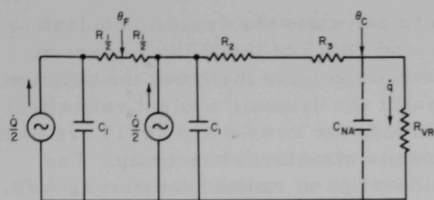


Fig. 2. Heat-flow Diagram for Fuel Element

rate out of the core, as a result of coolant flow, determines  $R_{VR}$ . All of these are evaluated based on the fuel-element length,  $L$ . Average fuel temperature over length  $L$  is  $\theta_F$ ; average coolant temperature over  $L$  is  $\theta_C$ . In this study, heat transport time in the coolant is negligibly small compared to the basic fuel-assembly time constant, since flow velocities are high. The above temperatures, therefore, are those at the core centerline.

### B. Coolant Void Effect

The dynamic void reactivity produced by the thermal expansion of the liquid-metal coolant can be expressed in the Laplace transform as

$$\text{Laplace}[F(K\theta_C/\dot{Q})] = \rho_c K_c \times \text{Laplace}[F(\theta_C/\dot{Q})],$$

where  $\rho_c$  is the reactivity change per unit density change, and  $K_c$  is the coolant density change per unit coolant temperature change. The transform quantity on the right of the above equation is the solution to the heat-flow diagram of Fig. 2. If  $C_{Na}$  is small and can be neglected as in the case considered here, the solution is a quadratic expression of the form

$$\frac{\dot{q}(s)}{\dot{Q}(s)} = \frac{1 + \frac{sR_1C_1}{2}}{1 + s(R_1 + 2R_4) C_1 + s^2 R_1 R_4 C_1^2},$$

where

$$R_4 = R_2 + R_3 + R_{VR}.$$

Then,

$$\theta_C = \dot{q} R_{VR},$$

and

$$\text{Laplace}[F(K\theta_C/\dot{Q})] = \frac{\rho_c K_c R_{VR} \left(1 + \frac{sR_1C_1}{2}\right)}{1 + s(R_1 + 2R_4) C_1 + s^2 R_1 R_4 C_1^2}.$$

Figure 2 shows the above quantities assembled into a heat-flow diagram. The lumped heat capacity of each half-volume is designated  $C_1$ , and the heat generation rate in each half-volume as  $\dot{Q}/2$  calories per second. The coolant heat capacity is represented by  $C_{Na}$ , and the heat deposition rate into the coolant by  $\dot{q}$ . The heat transport

This expression is used in Appendix A to calculate the dynamic coolant temperature response for rows 1-6, 9, and 10-15 of the EBR-II reactor. Since the value of  $\rho_c$  is very small for rows outside the core, the solution for core rows 1-6 was chosen to represent the dynamic coolant void effect in Section IV.A of this report. The solutions for rows 9 and 10-15 are used later in Section III.B to develop the dynamic structural reactivity. The solutions of rows 7 and 8 require consideration of radial heat flow as well, but, since rows 7 and 8 have only minor coolant void effect, their solution will be given in Section III.B, where they have a large influence on the structural reactivity component.

#### C. Fuel Axial-expansion Effect

The fuel axial-expansion effect is considerable with metallic fuel such as that used in EBR-II and similar reactors. The dynamic fuel expansion can be expressed in Laplace transform as

$$\text{Laplace}[F(K\theta_F/\dot{Q})] = \rho_F K_F \times \text{Laplace}[F(\theta_F/\dot{Q})],$$

where  $\rho_F$  is the reactivity change per unit change in core length,  $K_F$  is the thermal-expansion coefficient of the fuel, and  $\theta_F$  is the average fuel temperature, defined as the temperature in the fuel at 0.707 of the fuel outside diameter.

The transform quantity on the right above can be shown to be

$$\frac{\theta_F(s)}{\dot{Q}(s)} = \frac{4R_4 + R_1}{4} \cdot \frac{1 + sC_1 \frac{2R_1R_4}{4R_4 + R_1}}{1 + s(R_1 + 2R_4) C_1 + s^2 R_1 R_4 C_1^2}.$$

Then,

$$\text{Laplace}[F(K\theta_F/\dot{Q})] = \rho_F K_F \cdot \frac{4R_4 + R_1}{4} \cdot \frac{1 + sC_1 \frac{2R_1R_4}{4R_4 + R_1}}{1 + s(R_1 + 2R_4) C_1 + s^2 R_1 R_4 C_1^2}.$$

The above expression is used in Appendix A to calculate the dynamic fuel expansion response for rows 1-6. This solution appears as the fuel axial expansion in Section IV.A.

#### D. Axial Expansion of Control Rod and Subassembly

A reactor whose control subassemblies are suspended from above and immersed in the coolant can generate feedback reactivity due to axial thermal expansion of the rods as the coolant temperature changes with

power. In certain cases, the amount of such reactivity plays a significant part in the total feedback. Such is the case with the EBR-II reactor, where the control-rod drives are calibrated at equilibrium powers to correct for this effect.<sup>2</sup>

The dynamics of such expansion, which forms an important part of the system dynamics, is determined by dividing the length of the rod and the subassembly into sections, each of which possesses characteristic dynamic heat-flow properties. Calculations of the properties of each section are then used in combination to represent the way in which the total drive length, and thereby the feedback reactivity, varies with reactor power.

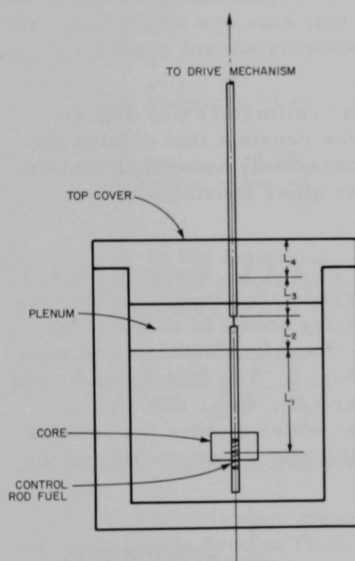


Fig. 3. Control-rod Suspension

The EBR-II control rod and subassembly can be divided into four sections, which possess distinctly different dynamic heat-transfer characteristics. The sections are shown as  $L_1$  through  $L_4$  in Fig. 3, which is a sketch of the control-rod suspension.<sup>3</sup>

The first section ( $L_1$ ) will expand or contract in a way governed by its coolant temperature ( $\theta_c$ ) and by the transport time required for a coolant temperature change to travel the length of the section. The relation of coolant temperature and power can be taken from Section II.A above, and a single time-constant equivalent assumed for the transport lag. The transform of feedback reactivity divided by power change for section  $L_1$  then is

$$\frac{(\delta K/K)(s)}{\Delta P(s)} = \frac{2K_L \left(1 + \frac{sR_1C_1}{2}\right)}{1 + s(R_1 + 2R_3) C_1 + s^2 R_1 R_3 C_1^2} \cdot \frac{C_{L1} W}{1 + \tau_T s}$$

where  $2K_L$  is the equilibrium change in fuel subassembly coolant temperature with power, in units of degrees centigrade per megawatt;  $C_{L1}$  is the expansion of section  $L_1$ , in units of centimeters per degree change in coolant temperature;  $W$  is feedback reactivity in units of  $\delta K/K$  per centimeter of fuel movement; and  $\tau_T$  is 0.63 times the transport time of the coolant through  $L_1$ . The remaining  $R$ 's and  $C$ 's are those defined in Section II.A.

All the remaining sections ( $L_2$ ,  $L_3$ , and  $L_4$ ) respond to plenum coolant temperature, which in EBR-II is delayed with respect to the fuel subassembly coolant temperature by the coolant holdup time of the upper plenum shown in Fig. 3. If a simple lag represents the holdup time, the transform of plenum temperature divided by power change is

$$\frac{\Delta \theta_p(s)}{\Delta P(s)} = \frac{K_p}{1 + \tau_p s},$$

where  $K_p$  is the equilibrium change in plenum coolant temperature with power, in units of degrees centigrade per megawatt, and  $\tau_p$  is 0.63 times the plenum coolant holdup time. This assumes that core coolant transport can be neglected as short compared to plenum holdup time, and that blanket coolant transport time can be neglected because of the small amount of heat it supplies to the plenum. Now that the plenum temperature response is available, the response of control rod section  $L_2$  to power is

$$\frac{(\Delta K/K)(s)}{\Delta P(s)} = \frac{K_p}{1 + \tau_p s} \cdot \frac{C_{L_2} W}{1 + \tau_{L_2} s},$$

where  $C_{L_2}$  is the expansion of section  $L_2$ , in centimeters per degree change in coolant temperature,  $\tau_{L_2}$  is the time constant that relates the internal temperature of the 0.1-cm-thick subassembly hexagonal containment shell to the coolant temperature, and the other constants are as previously defined.

The radial heat transfers of sections  $L_3$  and  $L_4$  shown in Figs. 4 and 5 must be calculated to determine their respective expansion characteristics. Both sections have similar alternating annuli of sodium and stainless steel, but of differing thicknesses. Therefore both may be represented by the radial heat-flow diagram in Fig. 6. The lumped heat capacities of the annuli from inner to outermost are  $C_1$ ,  $C_{Na}$ , and  $C_2$ , respectively. Each is lumped at the diameter which divides the annulus into two equal volumes. The reciprocals of the heat conductivities of the

*Total flow  
Loss through  
copper, sodium  
and carbon  
is 5791*

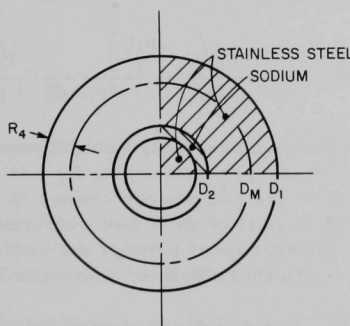


Fig. 4. Cross Section of Control Drive Rod at  $L_3$

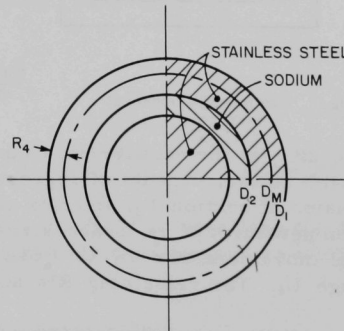


Fig. 5. Cross Section of Control Drive Rod at  $L_4$

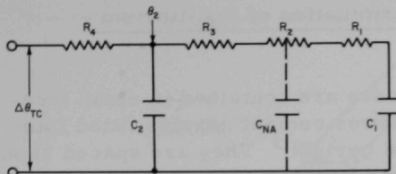


Fig. 6. Heat-flow Diagram for the Control Drive Rod

portions of annuli between these points of lumped heat capacity are designated  $R_1$ ,  $R_2$ ,  $R_3$ , and  $R_4$  (proceeding from inner to outer annuli). The plenum coolant traverses an annulus between the reactor top cover hole and the drive rod that passes through this hole. The quantity  $\Delta\theta_{TC}$ , which represents the temperature of the coolant in this annulus, is assumed to be identical to

$\Delta\theta_p$  but about 10% lower because of heat loss to the surrounding cover. Also, the practical magnitudes of the heat conductivities and capacities of the inner annuli are such that only  $R_4$  and  $C_2$  are needed to obtain a good approximation for the responses of sections  $L_3$  and  $L_4$ .

The response of section  $L_3$  to power is

$$\frac{(\delta K/K)(s)}{\Delta P(s)} = \frac{0.9K_p}{1 + \tau_p s} \cdot \frac{C_{L3} W}{1 + \tau_{L3} s},$$

where  $C_{L3}$  is the expansion of section  $L_3$ , in centimeters per degree change of coolant temperature,  $\tau_{L3}$  is  $R_4$  times  $C_2$  evaluated for section  $L_3$ , and the others are as defined above. Similarly,

$$\frac{(\delta K/K)(s)}{\Delta P(s)} = \frac{0.9K_p}{1 + \tau_p s} \cdot \frac{C_{L4} W}{1 + \tau_{L4} s},$$

with similar definitions to those above but relating to section  $L_4$ .

All the relations appearing in this section are evaluated in Appendix A for use in Section IV.A.

### III. THERMOMECHANICAL DISTORTION AND MOVEMENT OF THE CORE FUEL ELEMENTS

This section is specialized in the sense that any structural treatment must necessarily relate to a specific design, in this case, the EBR-II reactor core design. The effect of the small core is to make reactivity sensitive to fuel subassembly movements as small as one-thousandth of an inch. Small thermomechanical motions of the subassemblies are therefore important to the reactor dynamics and must be calculated to determine the structural feedback reactivity component.

#### A. BOW III Computer Program for Determination of Equilibrium Reactivity

The fuel elements of the EBR-II core are contained in semi-free-standing hexagonal subassemblies, with lower coolant nozzles fitted into holes in two grid plates so that they stand upright.<sup>3</sup> They are spaced about 1/32 in. from each other on all sides of the hexagon, except at the center. At the center, buttons are embossed to reduce spacing to 2 mils to limit movement, but still allow the subassemblies to "flower" outward at the top in response to radial thermal gradients that develop due to heat transfer as reactor power increases. Many combinations of subassemblies such as core and inner and outer blanket types are possible, but the chief interest is in the combination used in reactor run No. 26, where considerable positive structural feedback was observed. This run and its loading are described and analyzed in Refs. 2 and 4, where the bowing problem is discussed in detail.

Bump<sup>5</sup> later developed a method of numerical analysis, known as the BOW II computer program, to compute the structural distortion of the sub-assemblies by treating them as loaded flexible structural beams. The output of this program, which used approximations for the beam formulas, showed positive reactivities corresponding roughly to the amount of positive reactivity that could be postulated from reactor measurements from which other known reactivity effects were subtracted. To make dynamic analysis possible, I calculated the actual beam formulas representing the various modes of bending in the subassemblies and incorporated them into a new program known as BOW III. The bending modes and the formulas are given in Appendix B, along with the method used to calculate the formulas. The FORTRAN description of BOW III appears in the same appendix. The input required for the program includes data about the subassembly mechanical properties and the equilibrium radial differential temperatures of the subassembly evaluated for 10 axial positions along each subassembly. References 1 and 2 describe the method of determining the differential temperatures.

The output of BOW III is a listing of the equilibrium radial locations of each subassembly at 10 axial positions. The core is influenced chiefly by positions 4, 5, and 6, which represent the bottom, center, and top of the core. The weighted position shift of each row of subassemblies is determined from BOW III data, and then the reactivity worth of the shift evaluated by using constants developed for rows 6, 7, 8, and 9. This evaluation assumes that the structure from row 6 to the core center shrank or expanded radially in proportion to the row 6 movement. Thus the entire core reactivity change is evaluated in terms of row 6. The effects of rows 7, 8, and 9 on reactivity are calculated using the respective constants for each row; rows further out have greatly reduced effect and are neglected.

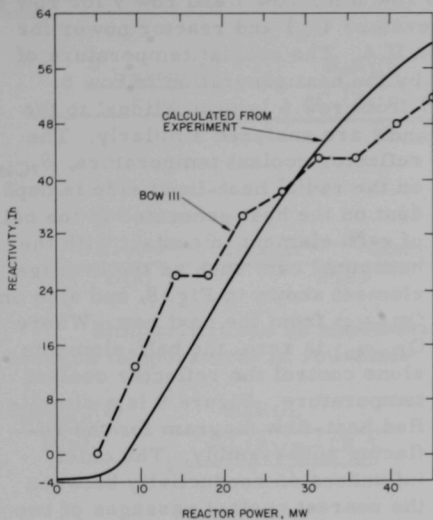


Fig. 7. Equilibrium Feedback Reactivity of Structure

row 8. This transfer of heat must be taken into consideration, and therefore rows 7 and 8 cannot be treated as the other rows were in Section II.A.

An approximate treatment is used, which includes a number of assumptions and is based on the results of equilibrium calculations contained in Ref. 1. The subassemblies of both rows 7 and 8 contain 19 solid stainless steel rods, which are 1.25 cm in outside diameter and 140 cm long, centered about the core axial centerline. Figure 8 shows a subassembly cross section. In this figure,  $Q_{\text{RADIAL}}$  is the heat flow between rows 6 and 7 or between rows 9 and 8. Zero heat flow is assumed between rows 7 and 8. The individual axial coolant passages act as effective heat barriers in the radial direction. Therefore the temperature of the subassembly hexagonal can on the radial heat input side will assume a temperature between that of its own immediately adjacent coolant,  $\theta_7 C_{\text{IN}}$ , and that of the coolant in the adjacent subassembly hexagonal

Appendix B gives the constants for rows 6, 7, 8, and 9, in inhours per mil, together with the differential temperature profiles and subassembly mechanical properties used as input to BOW III to calculate the equilibrium reactivity curve shown in Fig. 7. Also shown in Fig. 7 is an experimental curve taken from Ref. 6. Convergence difficulties cause the lack of smoothness in the calculated curve, although in general the two curves are in good agreement.

#### B. Heat-transfer Dynamics of Reflector Subassemblies

The stainless steel reflector subassemblies in rows 7 and 8 receive an appreciable amount of heat due to radial heat transfer from row 6 to row 7 and from row 9 to

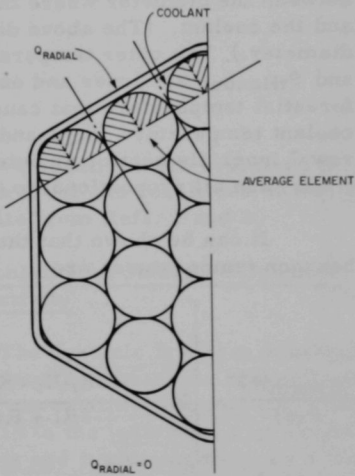


Fig. 8. Cross Section of Reflector Subassembly

can. The adjacent subassembly can is row 6 for row 7 and row 9 for row 8. The relation between the coolant temperature ( $\theta_c$ ) and reactor power for rows 6 and 9 was determined in Section II.A. The coolant temperature of row 6 is controlled almost completely by the heat generation in row 6. Therefore the radial heat flow to row 7 from row 6 is proportional to the coolant temperature of row 6. Rows 9 and 8 are analyzed similarly.

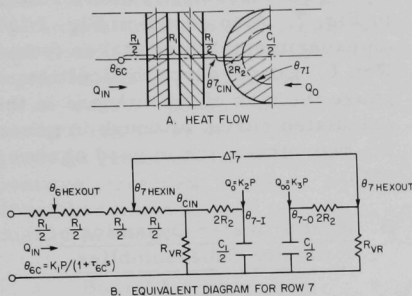
The reflector coolant temperature,  $\theta_{7CIN}$ , on the radial heat-input side is dependent on the heat generated in the half of each element in contact with the hexagonal can, such as the average element shown in Fig. 8, and also on  $Q_{\text{Radial}}$  from the next row. Where  $Q_{\text{Radial}}$  is zero, the half-elements alone control the reflector coolant temperature. Figure 9 is a simplified heat-flow diagram for the reflector subassembly. The chief influences on conductivity between the nearest coolant passages of two adjacent subassemblies are the hex-

Fig. 9. Heat-flow Diagram for Reflector Subassembly

agonal cans themselves. Then the total reciprocal conductivity of two hexagonal thicknesses in series is  $2R_1$ .  $R_{VR}$  is the effective reciprocal conductivity due to heat removal by coolant flow. The reciprocal heat conductivity of one half-element facing an outer coolant passage is twice that of a full element, or  $2R_2$ , where  $R_2$  is the value calculated for heat flow between the diameter where the full element heat capacity ( $C_1$ ) is lumped and the coolant. (The above diameter is 0.707 times the element outside diameter.) The outer temperature of the row 6 hex is  $\theta_{6\text{Hexout}}$ ;  $\theta_{7\text{Hexin}}$  and  $\theta_{7\text{Hexout}}$  are inner and outer temperatures of the row 7 hex. The differential temperature that causes the bowing is designated  $\Delta T_7$ . The row 6 coolant temperature ( $\theta_{6C}$ ) and the heats generated internally in half of a row 7 inner element or an outer element (designated  $Q_0$  and  $Q_{00}$ , respectively) are all proportional to the reactor power (P).

It can be shown that the Laplace transforms of the inner and outer hexagon temperatures are

$$\frac{\theta_{7\text{Hexin}}(s)}{P(s)} = \left[ K_1 - \frac{1.5R_1(K_1 - K_2R_{VR})}{2R_1 + R_{VR}} \cdot \frac{1 + \frac{sC_1(2R_2 + R_{VR})}{2\left(1 - \frac{K_2R_{VR}}{K_1}\right)}}{1 + \frac{sC_1(2R_2 + R_{VR} - R_{VR}^2)}{2}} \right] \cdot \frac{1}{1 + \tau_{6C}s}$$



and

$$\frac{\theta_7 \text{Hexout}(s)}{P(s)} = \frac{K_3 R_{VR}}{1 + \frac{s C_1 (R_{VR} + 2R_2)}{2}}.$$

Then,

$$\frac{\Delta T_7(s)}{P(s)} = \frac{\theta_7 \text{Hexin}(s) - \theta_7 \text{Hexout}(s)}{P(s)}.$$

Similarly it can be shown that the transforms for the inner and outer hexagon temperatures of row 8 are

$$\frac{\theta_8 \text{Hexin}(s)}{P(s)} = \frac{K_6 R_{VR}}{1 + \frac{s C_1 (R_{VR} + 2R_2)}{2}},$$

$$\frac{\theta_8 \text{Hexout}(s)}{P(s)} = \left[ K_4 - \frac{1.5 R_1 (K_4 - K_5 R_{VR})}{2R_1 + R_{VR}} \cdot \frac{1 + \frac{s C_1 (2R_2 + R_{VR})}{2 \left( 1 - \frac{K_5 R_{VR}}{K_4} \right)}}{1 + \frac{s C_1 (2R_2 + R_{VR} - R_{VR}^2)}{2}} \right] \cdot \frac{1}{1 + \tau_9 C s},$$

and

$$\frac{\Delta T_8(s)}{P(s)} = \frac{\theta_8 \text{Hexin}(s) - \theta_8 \text{Hexout}(s)}{P(s)}.$$

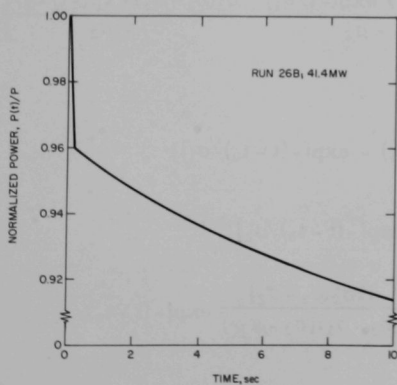


Fig. 10. Power Variation with Time for a Rod-drop Experiment

The above equations are evaluated in Appendix C for the conditions of Run 26, using data from Refs. 1 and 2.

#### C. Calculation of Structure Dynamic Reactivity

The dynamic feedback reactivity is calculated by inputting a rod-drop reactor power-time function<sup>7</sup> like that in Fig. 10 to the individual row dynamic equations and evaluating them as a function of time. Each row time function that results will have a specific value at a given time, which may be used to multiply the starting power differential profile ( $T_\Delta$ ) for the row to obtain the

new profile at the given time. The general form then is

$$(T_{\Delta})_{[t]} = (P/45) \left( (T_{\Delta})_{[P=45 \text{ MW}, t=0]} \right) [1 + C(t)],$$

where  $P$  is the starting power in megawatts, and  $C(t)$  is a function that describes the time behavior of a particular row. When the rod-drop reactor power-time function is represented by a ramp plus an exponential, as in Fig. D.1,  $C(t)$  has two general forms, which can be used to describe all rows. These are:

### 1. Rows 1-6 and 9-15

For  $t \leq t_0$ ,

$$C(t) = \left( \frac{\Delta P}{P} \right)_{t_0} \frac{\sigma_1}{t_0} \left[ \exp(-t/\sigma_1) + \frac{t}{\sigma_1} - 1 \right].$$

For  $t > t_0$ ,

$$C(t) = K_B + \left( \frac{\Delta P}{P} \right)_{t_0} \frac{\sigma_1}{t_0} \left\{ \exp(-t/\sigma_1) - \exp[-(t - t_0)/\sigma_1] \right\}$$

$$+ K \frac{\tau_K \exp[-(t - t_0)/\tau_K] - (\sigma_1) \exp[-(t - t_0)/\sigma_1]}{\sigma_1 - \tau_K}.$$

### 2. Rows 7 and 8

For  $t \leq t_0$ ,

$$C(t) = \frac{(\Delta P/P)_{t_0}}{t_0} \left\{ (t - \sigma_1 - \sigma_2 + \sigma_3) + \frac{\sigma_1(\sigma_1 - \sigma_3) \exp(-t/\sigma_1)}{\sigma_1 - \sigma_2} - \frac{\sigma_2(\sigma_2 - \sigma_3) \exp(-t/\sigma_2)}{\sigma_1 - \sigma_2} \right\}.$$

For  $t > t_0$ ,

$$C(t) = K_B + (\Delta P/P)_{t_0} \frac{\sigma_1(\sigma_1 - \sigma_3)}{t_0(\sigma_1 - \sigma_2)} \left\{ \exp(-t/\sigma_1) - \exp[-(t - t_0)/\sigma_1] \right\}$$

$$+ (\Delta P/P)_{t_0} \frac{\sigma_2(\sigma_2 - \sigma_3)}{t_0(\sigma_2 - \sigma_1)} \left\{ \exp(-t/\sigma_2) - \exp[-(t - t_0)/\sigma_2] \right\}$$

$$+ \frac{K \sigma_1(\sigma_3 - \sigma_1)}{(\sigma_1 - \sigma_2)(\sigma_1 - \tau_K)} \exp[-(t - t_0)/\sigma_1] + \frac{K \sigma_2(\sigma_3 - \sigma_2)}{(\sigma_2 - \sigma_1)(\sigma_2 - \tau_K)} \exp[-(t - t_0)/\sigma_2]$$

$$+ \frac{K \tau_K (\sigma_3 - \tau_K)}{(\tau_K - \sigma_1)(\tau_K - \sigma_2)} \exp[-(t - t_0)/\tau_K].$$

Values for the constants in the above functions are obtained from Appendix D, and  $C(t)$  is then evaluated by means of a computer program, PROFILE, whose output consists of decks of temperature profiles in BOW III format (see Appendix D). These are then inputed to BOW III to obtain the dynamic reactivity response to the specified  $\Delta P/P$  time function. Initial calculations have shown large fluctuations, which are caused by convergence difficulties in the BOW III program. A new BOW IV program is being developed to eliminate these problems.

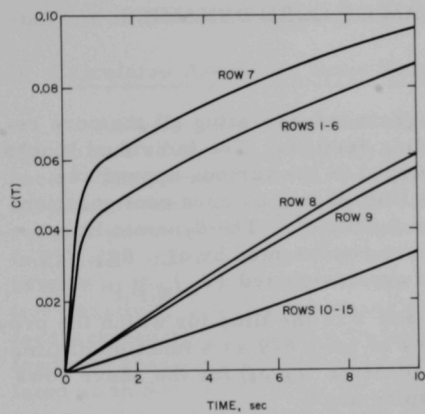


Fig. 11. Dynamic Change in Row Differential Temperature Profiles

curve changes about 54 lh from 0 to 45 MW. This is about 1.2 lh/MW or  $3.7 \times 10^{-3}$  \$/MW. Then the positive structure reactivity change for the rod-drop can be estimated as

$$(\Delta k/k)_t = (3.7 \times 10^{-3})(41.4 \text{ MW})[C(t)],$$

$$(\Delta k/k)_{1\text{sec}} = 3.7 \times 10^{-3} \times 41.4 \times -5.77 \times 10^{-2} = -9.0 \times 10^{-3},$$

$$(\Delta k/k)_{3\text{sec}} = 3.7 \times 10^{-3} \times 41.4 \times -7.00 \times 10^{-2} = -10.8 \times 10^{-3},$$

and

$$(\Delta k/k)_{10\text{sec}} = 3.7 \times 10^{-3} \times 41.4 \times -9.71 \times 10^{-2} = -15.0 \times 10^{-3}.$$

If the above values are added to those in Fig. 13, the total reactivity feedback is

$$(\Delta k/k)_{1\text{sec}} = +3.7 \times 10^{-3} \$,$$

$$(\Delta k/k)_{3\text{sec}} = +5.5 \times 10^{-3} \$,$$

The above  $C(t)$ 's can be used to estimate the structure feedback reactivity. The  $C(t)$ 's plotted in Fig. 11 are for Run 26B (see Table VI in Appendix D) as calculated by PROFILE. The equilibrium starting value for all rows is 1.0, so that the profile differential temperatures for row 7, for example, would all be multiplied by 1.097 at 10 sec. The reactivity worths of rows 6 and 7 dominate rows 8 and 9, and row 6 tends to follow the row 7 position. Therefore, if rows 6 and 7 are assumed to move inward with a position change similar to the temperature changes shown in Fig. 11 for row 7, the reactivity change can be estimated. Figure 7 indicates that the calculated BOW III

and

$$(\Delta k/k)_{10 \text{ sec}} = +10.3 \times 10^{-3} \text{ $.}$$

The corresponding experimental values were  $+5.1 \times 10^{-3}$ ,  $+6.25 \times 10^{-3}$ , and  $+9.2 \times 10^{-3}$  \$, respectively. The agreement is fortuitously good and indicates that the method is sound.

#### IV. SYSTEM BLOCK DIAGRAM OF CORE DYNAMICS

#### A. EBR-II System Diagram

Figure 12 is a system block diagram incorporating all the core reactivity feedbacks treated in the preceding sections. The individual blocks are shown in the simplified forms developed in the various appendixes, where each block was evaluated for the EBR-II Run 26 core configuration.  $P(s)$  is the EBR-II zero-power transfer function.<sup>8,9</sup> The dynamic linear expansions of the control-rod sections are represented by  $d_{L1}$ ,  $d_{L2}$ ,  $d_{L3}$ , and  $d_{L4}$ . The row temperature profiles are designated  $(T_\Delta)_{N.P.t}$ , where

N is the row, P is the starting power, and t is the time for which the profile was calculated. The button positions of rows 6-9 as a function of time are shown as  $d_6-d_9$ . The reactivity coefficients ( $\rho_6-\rho_9$ ) for the above rows are expressed in reactivity per unit displacement.

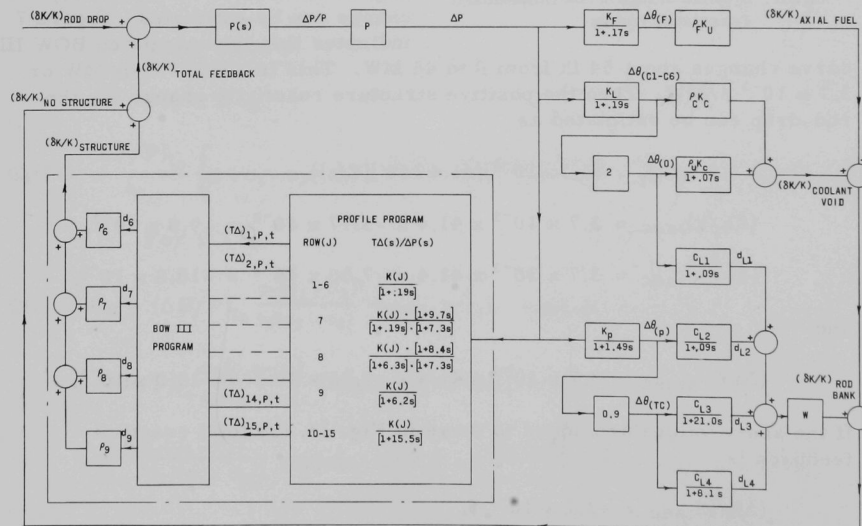


Fig. 12. System Block Diagram of EBR-II Core Dynamics

All elements on Fig. 12 are shown in the linearized transfer function form described in Ref. 9, except for the core structure component, which is the nonlinear element shown within the dot-dash lines. The core component could be shown in approximate transfer function form by the use of artificial time constants and coefficients which would not be directly related to physical heat-transfer phenomena. However, every set of reactor test conditions would lead to a new set of arbitrary constants and coefficients that would not be particularly useful for analytic purposes. Therefore, it is left as a nonlinear element, and the time domain is used for analysis in the following sections.

### B. Calculated Reactivity Time Response to a Reactor Rod Drop

As mentioned in Section III, the EBR-II reactor experimental run No. 26 was of special interest because of the large positive structure feedback.<sup>2</sup> Therefore, from here on, the analysis is based on a specific rod-drop experiment done at 41.4 MW during run No. 26. The variation in reactor power with time which occurred during this experiment is shown in Fig. D.1. The continued falloff in reactor power after the fast ramp insertion of the control rod, as shown in Fig. D.1, will persist until the negative reactivity inserted by means of the rod is just compensated by the feedback reactivity regained by reduction in power. The total dynamic feedback reactivity generated by the remaining parts of Fig. 12 was calculated as in Section III.C for the structure by inputting the above rod-drop reactor power-time function into the point marked  $\Delta P/P$  after opening the loop by removing  $P(s)$ , the zero-power function. Time functions were cal-

culated for each part by inverse Laplace transformation using the DYNAMIC computer program described in Appendix E. The power reactivity coefficients used for sodium expansion and for axial fuel expansion were those derived for Run 26B by Persiani *et al.*<sup>6</sup> Figure 13 is a plot of the individual functions and their sum.

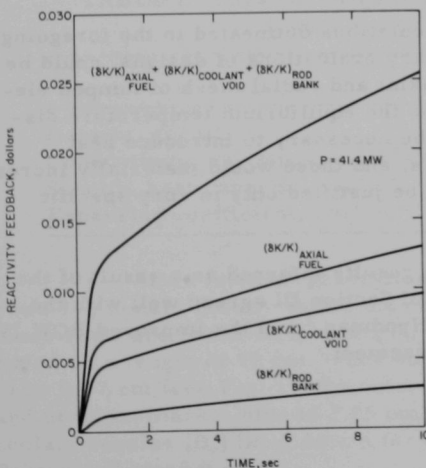


Fig. 13. Calculated Reactivity Variation with Time for a Rod-drop Experiment

### V. SUMMARY AND CONCLUSIONS

The direct systems approach used in the preceding sections of this report has led to a theoretical description of the power behavior of a small liquid-metal-cooled fast breeder reactor. Although a detailed analysis of a particular reactor

(EBR-II) was made using the theory, it is emphasized that the time domain approach is a very powerful tool for the analysis of any reactor and that the methods described here have general application. These methods are particularly useful for determining the theoretical performance of preliminary reactor designs before construction. This would apply especially to a reactor whose cores are constructed of large numbers of long, slender fuel elements, which are loaded vertically into the core and which interact on each other as a result of the core axial and radial thermal gradients.

The analysis of the EBR-II reactor points up the need to consider carefully the thermal gradients in a core and the resulting thermomechanical core-movement effects on reactivity. The BOW III program permits a systematic evaluation of the effects of thermal and mechanical parameter variations on core reactivity, where the calculated final core subassembly positions are accurate to about 1 mil. This is not sufficient resolution for determining core thermomechanical dynamics, and, in fact, about another factor of ten improvement to 0.1 mil is required. An approach to this problem has been instituted in the BOW IV program presently being developed. In this program, the entire group of core subassemblies is considered as a large three-dimensional interacting array of springs with gradual increase in the number of subassemblies treated as a group as power is raised. This is unlike BOW III, where each subassembly is treated individually as if imprisoned between the subassemblies directly adjacent to it. Interaction information from more distant subassemblies is required, and BOW IV will provide this. The added information entering into the calculation should provide the desired position resolution.

The dynamic heat-transfer calculations delineated in the foregoing sections, while sufficient for preliminary evaluations of designs, could be based on a much more finely divided axial and radial mesh of lumped elements of the type used by Cushman<sup>1</sup> for the equilibrium temperature distributions used for BOW III. It would be necessary to introduce heat capacities and axial heat flow dynamics, and these would materially increase the labor required and would probably be justified only in very specific design cases.

The overall dynamic reactivity results inferred as a result of the calculated row 7 movement at the end of Section III agreed well with the experimental measurements made by Hyndman,<sup>7</sup> and the improved BOW IV program should lead to even better agreement.

APPENDIX A  
Dynamic Heat-transfer Calculations

1. Fuel Subassembly; Rows 1-6

a. Dynamic Coolant Response

Since the heat generation rate ( $\dot{Q}$ ) is proportional to reactor power ( $P$ ), the expression for reactor coolant temperature on p. 9 can be rewritten as

$$\frac{\Delta\theta_C(s)}{\Delta P(s)} = \frac{K_L \left( 1 + \frac{sR_1C_1}{2} \right)}{1 + s(R_1 + 2R_4) C_1 + s^2 R_1 R_4 C_1^2},$$

where (as before)

$$R_4 = R_2 + R_3 + R_{VR}.$$

The various reciprocal heat conductivities ( $R$ 's) and heat capacities ( $C$ 's) can be calculated from the physical properties of the materials used. In all the examples given, liquid sodium (~700°F), Type 304 stainless steel (~700°F), or uranium are the main constituents. Their physical properties are listed in Table I.

TABLE I. Physical Properties of Type 304 Stainless Steel,  
Liquid Sodium, and Uranium

	304 SS	Sodium	Uranium
Density, g/cm <sup>3</sup>	7.7	0.97	19.0
Conductivity, cal-cm/sec-cm <sup>2</sup> -°C	0.048	0.174	0.082
Specific heat capacity, cal/g°C	0.115	0.305	0.038
Expansion coefficient, cm/cm°C	$1.8 \times 10^{-5}$	-	-

Since internal generation of heat in the core subassemblies in rows 1-6 occurs chiefly within the core length of 36 cm, the calculations for these rows are based on this length, but the calculations for rows 9-15 are based on a length of 70 cm.<sup>1</sup> The outer diameter of the fuel pin ( $D_4$ ) is taken to be 0.37 cm (see Fig. 1); the outer diameter of the stainless steel reflector and uranium blanket pins is 1.25 cm. The outside diameter of the effective coolant annulus ( $D_6$ ) is ~0.54 cm for the fuel pin and ~1.33 cm for the reflector and blanket pins.

The heat capacity ( $C_1$ ) of the equal inner and outer volumes (see Fig. 1) is

$$C_1 = \text{volume} \times \text{density} \times \text{specific heat capacity}.$$

For rows 1-6,

$$C_1 = \pi \left( \frac{0.707 \times 0.37}{2} \right)^2 \times 36 \times 19.0 \times 0.038 = 1.40 \text{ cal}/^{\circ}\text{C}.$$

Since the heat capacities are lumped at diameters  $D_1$  and  $D_3$ , the reciprocal heat conductivity ( $R_1$ ) between these points is calculated using the mean cylindrical area and the radial distance between the two diameters. The reciprocal conductivity between  $D_3$  and  $D_1$  is

$$R_1 = \frac{\log_e (D_3/D_1)}{2\pi \times \text{conductivity} \times \text{length}}.$$

For rows 1-6,

$$R_1 = \frac{\log_e (0.866/0.50)}{2\pi \times 0.082 \times 36} = 0.0282^{\circ}\text{C}/\text{cal-sec}^{-1}.$$

Similarly, for  $R_2$ ,

$$R_2 = \frac{\log_e (1/0.866)}{2\pi \times 0.082 \times 36} = 0.0078^{\circ}\text{C}/\text{cal-sec}^{-1}.$$

Then, for  $R_3$ , for a clad pin of the type used in EBR-II, the film and cladding total temperature drop can be approximated at power by making  $R_3 = (R_1/2) + R_2$ , or

$$R_3 = 0.0282/2 + 0.0078 = 0.0219^{\circ}\text{C}/\text{cal-sec}^{-1}.$$

The core coolant temperature ( $\theta_C$ ) is taken as the average temperature or one-half the core outlet temperature, so that  $R_{VR}$  is compatible with the previously calculated  $R$ 's, which are all mean values.

Then, for  $R_{VR}$ ,

$$Q_{\text{Element}} = (509 \text{ kW}/91)(238.9 \text{ cal-sec}^{-1}/\text{kW}) = 1342 \text{ cal-sec}^{-1};$$

$$R_{VR} = (T_{\text{out}}/2)/Q_{\text{Element}}$$

$$= [134/(2 \times 1.8)]/1342 = 0.026^{\circ}\text{C}/\text{cal-sec}^{-1} \text{ (see Ref. 1).}$$

The coolant heat capacity ( $C_{Na}$ ) is calculated in the same way that  $C_1$  was treated.

For rows 1-6,

$$C_{Na} = (65/500) \times 36 \times 0.97 \times 0.305 = 1.38 \text{ cal/}^{\circ}\text{C.}$$

The time constant represented by

$$\tau = \frac{RVR(R_2 + R_3)}{RVR + R_2 + R_3} C_{Na} = 0.019$$

is so small that it was possible to neglect  $C_{Na}$  in deriving the expression for  $\Delta\theta_C(s)/\Delta P(s)$  given on p. 23. The evaluation of this expression for rows 1-6 is

$$\begin{aligned} \frac{\Delta\theta_C(s)}{\Delta P(s)} &= \frac{K_L[1 + s(0.0282 \times 1.4/2)]}{1 + s(0.0282 + 0.1114) \cdot 1.4 + s^2(0.0202 \times 0.0557)(1.4)^2} \\ &= \frac{K_L(1 + 0.02s)}{1 + 0.195s + 0.0032s^2}. \end{aligned}$$

The denominator may be factored to give, for the average coolant in the core,

$$\begin{aligned} \frac{\Delta\theta_C(s)}{\Delta P(s)} &= \frac{K_L(1 + 0.02s)}{(1 + 0.173s)(1 + 0.018s)} \\ &\approx \frac{K_L}{1 + 0.17s}. \end{aligned}$$

#### b. Dynamic Coolant Void Response

The above expression for  $\Delta\theta_C(s)/\Delta P(s)$  may be applied to the sodium expansion effect in the core, which is one-half the total effect. The remaining one-half of the effect comes from the coolant volume between the core and the upper plenum. The transport time through this region is

$$t_u = \frac{25.5 \times 2.54 \text{ cm}}{500 \text{ cm/sec}} = 0.13 \text{ sec, or } \tau_u \approx 0.07 \text{ sec.}$$

Then, as a first approximation, for the coolant directly above the core,

$$\frac{\Delta\theta_u(s)}{\Delta P(s)} \approx \frac{2K_L}{(1 + 0.19s)(1 + 0.07s)}.$$

c. Dynamic Fuel Expansion Response

The fuel expansion effect, which is largely due to rows 1-6, will be considered next before proceeding to the outer rows.

The expression for reactor average fuel temperature on p. 12 can be rewritten as

$$\frac{\Delta \theta_F(s)}{\Delta P(s)} = K_L \frac{4R_4 + R_1}{4R_{VR}} \cdot \frac{1 + sC_1 \frac{2R_1R_4}{4R_4 + R_1}}{1 + s(R_1 + 2R_4) C_1 + s^2 R_1 R_4 C_1^2}.$$

Substituting the values derived above and noting that the right-hand denominator is like that for  $\Delta\theta_C(s)$ , we obtain, for the average fuel in the core,

$$\begin{aligned} \frac{\Delta \theta_F(s)}{\Delta P(s)} &= \frac{0.0639}{0.026} \cdot \frac{(1 + 0.014s) K_L}{(1 + 0.173s)(1 + 0.018s)} \\ &\approx \frac{2.4K_L}{1 + 0.17s}. \end{aligned}$$

2. Blanket Subassembly; Row 9

a. Dynamic Coolant Response

The response of row 9 may be obtained in the same way as for a fuel pin. The main differences are in dimensions. The length of the elements in rows 7-15 requires use of a length of 70 cm to calculate the heat transfer in place of the core length of 36 cm used above for the fuel sub-assemblies. The results are

$$C_1 = \pi \times \left( \frac{0.707 \times 1.25}{2} \right)^2 \times 70 \times 19.0 \times 0.038 = 30.9 \text{ cal}/^\circ\text{C},$$

$$R_1 = \frac{\log_e (0.866/0.5)}{2\pi \times 0.082 \times 70} = 0.0145^\circ\text{C}/\text{cal}\cdot\text{sec}^{-1},$$

$$R_2 = \frac{\log_e (1.0/0.866)}{2\pi \times 0.082 \times 70} = 0.0039^\circ\text{C}/\text{cal}\cdot\text{sec}^{-1},$$

$$R_3 = 0.0145/2 + 0.0039 = 0.0112^\circ\text{C}/\text{cal}\cdot\text{sec}^{-1},$$

$$Q_{Element} = (36 \text{ kW}/19)(238.9 \text{ cal}\cdot\text{sec}^{-1}/\text{kW}) = 452 \text{ cal}\cdot\text{sec}^{-1},$$

$$\text{Average } T_{Out} = (125 + 145)/(2 \times 1.8) = 75^\circ\text{C},$$

$$R_{VR} = (T_{Out}/2) \div Q_{Element} = 75/(2 \times 452) = 0.083^{\circ}\text{C}/\text{cal}\cdot\text{sec}^{-1}$$

and

$$C_{Na} = (19.1/130) \times 70 \times 0.97 \times 0.305 = 3.04 \text{ cal}/^{\circ}\text{C}.$$

Again neglecting  $C_{Na}$ , we obtain

$$\begin{aligned} \frac{\Delta\theta_C(s)}{\Delta P(s)} &= \frac{(R_{VR}\dot{Q}_9/45)[1 + s(0.0145 \times 30.9/2)]}{1 + s(0.0145 + 0.1962)(30.9) + s^2(0.0145 \times 0.0981)(30.9)^2} \\ &= \frac{(R_{VR}\dot{Q}_9/45)(1 + 0.224s)}{1 + 6.53s + 1.36s^2}, \end{aligned}$$

where  $(\dot{Q}_9)$  is the cal/sec output of a row 9 subassembly for a reactor equilibrium power of 45 MW. The denominator may be factored to give

$$\begin{aligned} \frac{\Delta\theta_C(s)}{\Delta P(s)} &= \frac{(R_{VR}\dot{Q}_9/45)(1 + 0.224s)}{(1 + 6.2s)(1 + 0.22s)} \\ &\approx \frac{R_{VR}\dot{Q}_9/45}{1 + 6.2s}. \end{aligned}$$

This equation will be used later for row 8 structural effects, depending on heat transfer between rows 8 and 9. It will also be used for the row 9 structural effect.

### 3. Blanket Subassembly; Rows 10-15

#### a. Dynamic Coolant Response

The response of rows 10-15 is like that of row 9, except that  $R_{VR}$  is altered because the flow is reduced from 6 to 2.5 gpm, giving

$$R_{VR} = (6/2.5)(0.083) = 0.210^{\circ}\text{C}/\text{cal}\cdot\text{sec}^{-1},$$

and

$$\begin{aligned} \frac{\Delta\theta_C(s)}{\Delta P(s)} &= \frac{(R_{VR}\dot{Q}_J/45)(1 + 0.224s)}{1 + s(0.0145 + 0.449)30.9 + s^2(0.0145 \times 0.224)(30.9)^2} \\ &= \frac{(R_{VR}\dot{Q}_J/45)(1 + 0.224s)}{1 + 14.4s + 3.11s^2}. \end{aligned}$$

The denominator, when factored, gives

$$\frac{\Delta \theta_c(s)}{\Delta P(s)} = \frac{(RVR \dot{Q}_J / 45)(1 + 0.224s)}{(1 + 15.5s)(1 + 0.219s)}$$

$$\approx \frac{RVR \dot{Q}_J / 45}{1 + 15.5s}.$$

#### 4. Control Rod Section L<sub>1</sub>

The expression for  $(\delta K/K)(s)/\Delta P(s)$  for Section L<sub>1</sub> shown on p. 11 may be written directly using the fuel subassembly dynamics already calculated:

$$8 \frac{Ih}{in} \times 14 = 112$$

$$\tau_T = 0.63 \times 71 \text{ cm}/500 \text{ cm-sec}^{-1} = 0.09 \text{ sec}$$

$$\frac{(\delta K/K)(s)}{\Delta P(s)} = \frac{2K_L}{1 + 0.19s} \cdot \frac{C_{L1}W}{1 + 0.09s},$$

where  $(\delta K/K)(s) = \left[ \frac{2K_L(1.19)}{(1.19+s)} \right] \left[ \frac{C_{L1}W(1.09)}{1.09+s} \right] \Delta P(s)$

$$2K_L = (225^\circ F \times 5/9)/62.5 \text{ MW} = 2.0^\circ C/\text{MW},$$

$$W = (\Delta K/K)/d = \frac{8 \text{ Ih/in.} \times 12 \text{ rods}}{2.54 \times 430 \text{ Ih}/0.01(\delta K/K)} \text{ (see Ref. 2)}$$

$$= 8.8 \times 10^{-4}(\delta K/K)/\text{cm} = 0.118 \text{ $}/\text{cm},$$

and

$$0.098 \text{ $}/\text{cm} \quad \text{for} \quad 10 \text{ control rods}$$

$$C_{L1} = \text{Length} \times \text{expansion coefficient} = L_1 \alpha$$

$$= 128 \text{ cm} \times 1.8 \times 10^{-5} \text{ cm/cm}^\circ C = 2.3 \times 10^{-3} \text{ cm}/^\circ C.$$

#### 5. Plenum Effect

The plenum holdup time is approximately 2.37 sec, and  $\tau_p = 0.63 \times 2.37 = 1.49$  sec. Then,

$$\frac{\Delta \theta_p(s)}{\Delta P(s)} = \frac{K_p}{1 + 1.49s}.$$

## 6. Control Rod Section L<sub>2</sub>

The quantity  $\tau_{L_2}$  is the time constant associated with the 0.1-cm-thick hexagonal subassembly containment shell when heated from the outside by plenum sodium with the temperature of the inner side assumed constant. It may be determined by evaluating  $C_s$  and  $R_s$  using an area of 1 cm<sup>2</sup>. Thus,

$$C_s = \text{volume} \times \text{density} \times \text{specific heat capacity}$$

$$= 1 \times 1 \times 0.1 \times 7.7 \times 0.115 = 0.089 \text{ cal/}^{\circ}\text{C},$$

$$R_s = \frac{\text{thickness}/2}{\text{conductivity} \times \text{area}}$$

$$= \frac{0.1/2}{0.048 \times 1 \times 1} = 1.04^{\circ}\text{C/cal-sec}^{-1},$$

and

$$\tau_{L_2} = R_s C_s = 0.089 \times 1.04 = 0.093 \text{ sec.}$$

Then,

$$\frac{(\Delta K/K)(s)}{\Delta P(s)} = \frac{K_p}{1 + 1.49s} \cdot \frac{C_{L_2} W}{1 + 0.093s},$$

where

$$K_p = (183^{\circ}\text{F} \times 5/9)/62.5 \text{ MW} = 1.63^{\circ}\text{C/MW} \text{ (see Ref. 2)},$$

and

$$\begin{aligned} C_{L_2} &= L_2 \alpha = 46 \text{ cm} \times 1.8 \times 10^{-5} \text{ cm/cm}^{\circ}\text{C} \\ &= 8.3 \times 10^{-4} \text{ cm}/^{\circ}\text{C}. \end{aligned}$$

## 7. Control Rod Section L<sub>3</sub>

Trial calculations of the magnitudes of the inner annuli heat conductivities and capacities for Section L<sub>3</sub> shown in Fig. 4 showed that only  $R_4$  and  $C_2$  need be considered. The outer and inner diameters of the outermost stainless steel annulus are 6.35 and 2.54 cm, respectively. Hence,

$$C_2 = (\pi/4)(D_1^2 - D_2^2) \times L_3 \times 7.7 \times 0.115$$

$$= (\pi/4)(6.35^2 - 2.54^2) \times 50.8 \times 7.7 \times 0.115 = 1179 \text{ cal}/^{\circ}\text{C}.$$

$C_2$  may be lumped at the mean diameter  $D_M$  of the annulus; thus,

$$D_M = \sqrt{\frac{D_1^2 + D_2^2}{2}} = 4.83 \text{ cm},$$

$$R_4 = \frac{\log_e (D_1/D_M)}{2\pi \times 0.048 \times L_3}$$

$$= \frac{\log_e (6.35/4.83)}{2\pi \times 0.048 \times 50.8} = 0.0178^\circ\text{C/cal-sec}^{-1},$$

and

$$\tau_{L_3} = R_4 C_2 = 1179 \times 0.0178 = 21.0 \text{ sec.}$$

Then,

$$\frac{(\delta K/K)(s)}{\Delta P(s)} = \frac{0.9K_p}{1 + 1.49s} \cdot \frac{C_{L_3}W}{1 + 21.0s},$$

where

$$C_{L_3} = L_3 \alpha = 50.8 \times 1.8 \times 10^{-5}$$

$$= 9.14 \times 10^{-4} \text{ cm}^\circ\text{C} \times \frac{1m}{2.54 \text{ cm}} \times \frac{54}{12.2} \times \frac{C}{1.870} \quad (2.926 \times 10^{-5})$$

#### 8. Control Rod Section $L_4$

Again as in Section 7 of this appendix, only  $R_4$  and  $C_2$  need be considered. The outer and inner diameters of the outermost stainless steel annulus are 6.35 and 4.45 cm, respectively.

$$\begin{aligned} C_2 &= (\pi/4)(D_1^2 - D_2^2) \times L_4 \times 7.7 \times 0.115 \\ &= (\pi/4)(6.35^2 - 4.45^2) \times 50.8 \times 7.7 \times 0.115 \\ &= 725 \text{ cal}^\circ\text{C} \end{aligned}$$

$C_2$  may be lumped at the mean diameter of the annulus, which is

$$D_M = \sqrt{\frac{D_1^2 + D_2^2}{2}} = 5.48 \text{ cm},$$

to give

$$R_4 = \frac{\log_e (6.35/5.48)}{2\pi \times 0.048 \times 50.8} = 0.0112^{\circ}\text{C/cal-sec}^{-1}$$

(0.009617)

and

$$\tau_{L4} = R_4 C_2 = 725 \times 0.0112 = \cancel{8.1 \text{ sec.}}$$

6.972

Then,

$$\frac{(\delta K/K)(s)}{\Delta P(s)} = \frac{0.9K_p}{1 + 1.49s} \cdot \frac{C_{L4}W}{1 + 8.1s},$$

where

$$C_{L4} = L_4 \alpha = 50.8 \times 1.8 \times 10^{-5}$$

$$= 9.14 \times 10^{-4} \text{ cm}/^{\circ}\text{C.}$$

## APPENDIX B

BOW III Thermomechanical Structure Analysis1. Theoretical Bending of Subassemblies due to Combined Nozzle, Button, and Top Loading

The structural bending of the subassemblies can be determined by treating them as lightly loaded flexible structural beams. The method by

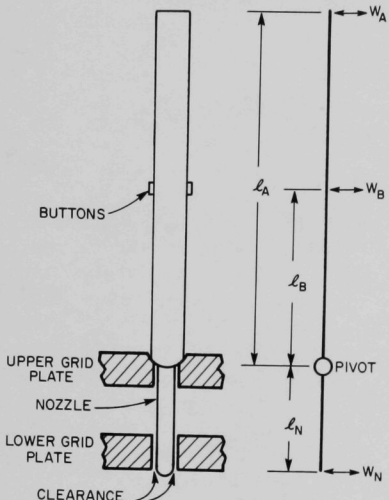


Fig. B.1. Subassembly as a Loaded Beam

depicted as a loaded beam at the right in Fig. B.1. The nozzle is either free or loaded radially inward or outward. The button and the top may be loaded radially either inward or outward, as shown.

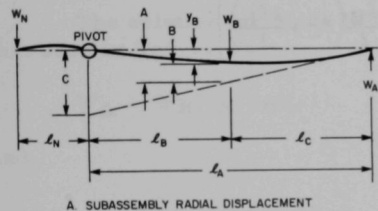
Several different modes of bending can take place because of the different ways that the subassembly can be loaded. I have worked out solutions for radial button displacement in terms of top and button loads for a number of the modes that cannot make use of formulas available in the literature.<sup>10</sup>

Table II lists the various modes with the direction of their radial loading indicated by L or R, where L is a force directed radially outward against the subassembly and R is a force directed inward. There is no contact and therefore no force where 0 appears in the table. Interchange

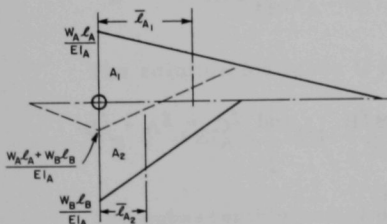
of L's and R's will reverse the direction of bending but not the characteristic mode shape, which is simply a mirror image along the axis.

TABLE II. BOW III Bending Modes

Mode	Force Direction		
	Nozzle	Button	Top
II Top	R	0	R
II	R	R	0
III	R	R	R
IIIA	R	L	R
IV	0	L	R
V	L	L	R



A. SUBASSEMBLY RADIAL DISPLACEMENT



B. M/EI DIAGRAM

Fig. B.2. Subassembly M/EI Diagram and Radial Displacement

The solution for Mode V is worked out below. The method is general and can be applied to any flexible-beam problems of a similar nature. Figure B.2 shows the radial displacement profile for a subassembly with Mode V loading, along with the corresponding M/EI diagram. In the displacement diagram, forces directed upward are taken as positive and displacement downward is also taken as positive.

The relation between  $y_B$  and the constants of the M/EI diagram can be obtained by noting from the figure that

$$y_B = A - B = (\ell_C C / \ell_A) - B.$$

The values of B and C may be obtained by using the Second Area Moment Proposition.<sup>11</sup>

$$A = \frac{1}{EI_A} \cdot \frac{\ell_C}{\ell_A} (A_1 \bar{l}_{A_1} + A_2 \bar{l}_{A_2})$$

$$= \frac{1}{EI_A} \cdot \frac{\ell_C}{\ell_A} \left( W_A \ell_A \frac{\ell_A}{2} \cdot \frac{\ell_A}{3} + W_B \ell_B \frac{\ell_B}{2} \cdot \frac{\ell_B}{3} \right).$$

Similarly,

$$B = \frac{1}{EI_A} \left( W_A \ell_C \frac{\ell_C}{2} \cdot \frac{\ell_C}{3} \right).$$

Combining the above equations, we obtain

$$y_B = \frac{1}{EI_A} \left( W_A \frac{\ell_C \ell_A^3 - \ell_C^3 \ell_A}{6 \ell_A} + W_B \frac{\ell_B^3 \ell_C}{6 \ell_A} \right).$$

It is necessary to apply the Second Area Moment Proposition again to determine the relation between  $W_A$  and  $W_B$  in the above expression. Thus, from Fig. B.3 it can be seen that

$$\begin{aligned} F &= \frac{1}{EI_A} \left( A_1 \bar{\ell}_{A_1} + A_2 \bar{\ell}_{A_2} \right) \\ &= \frac{1}{EI_A} \left[ W_A \ell_A \frac{\ell_A}{2} \cdot \frac{2 \ell_A}{3} + W_B \ell_B \frac{\ell_B}{2} \left( \ell_C + \frac{2 \ell_B}{3} \right) \right] \end{aligned}$$

and

$$\begin{aligned} D &= -\frac{1}{EI_N} A_3 \bar{\ell}_{A_3} \\ &= -\frac{1}{EI_N} W_N \ell_N \frac{\ell_N}{2} \cdot \frac{2 \ell_N}{3}. \end{aligned}$$

Also,

$$D = \frac{\ell_N}{\ell_A} F, \quad W_N \ell_N = W_A \ell_A + W_B \ell_B, \quad \text{and } \ell_C = \ell_A - \ell_B.$$

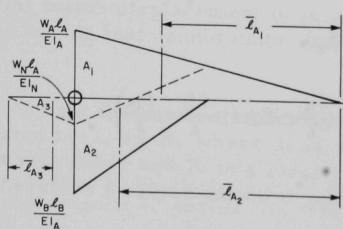
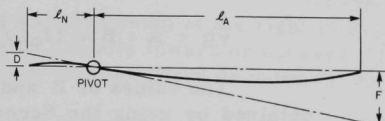


Fig. B.3

Rotation of Subassembly in Spherical Pivot Support

Substituting and solving, we obtain

$$W_A = W_B \frac{\ell_B}{\ell_A} \left[ \frac{\ell_B^2 - 3\ell_B \ell_A + 2\ell_A^2}{2\ell_A^2 \left( 1 + \frac{I_A \ell_N}{I_N \ell_A} \right)} - 1 \right]$$

and

$$W_B = 6EIAYb \frac{\ell_A}{\ell_B^2(\ell_A - \ell_B)} \left[ (2\ell_A - \ell_B) \frac{\ell_B^2 - 3\ell_B \ell_A + 2\ell_A^2}{2\ell_A^2 \left( 1 + \frac{I_A \ell_N}{I_N \ell_A} \right)} + \ell_B \right]^{-1}$$

Similar calculations for Modes III and IIIA result in the same solutions as those for Mode V above.

The solution for Mode IV, written in a slightly different form from that used in Ref. 11, is

$$W_A = W_B (\ell_A / \ell_B)(-1)$$

and

$$W_B = 6EIAYb \frac{\ell_A}{\ell_B^2(\ell_A - \ell_B)} \left[ (2\ell_A - \ell_B)(-1) + \ell_B \right]^{-1}$$

The solution for Mode II in the same form is

$$W_B = -6EIAYb \left[ 2\ell^3 \left( 1 + \frac{I_A \ell_N}{I_N \ell_B} \right) \right]^{-1}$$

The subassembly radial deflection ( $y_x$ ) at any position ( $x$ ) measured upward from the pivot in the axial direction is

$$y_x = \frac{1}{6EI_A} \left\{ W_A \left[ (\ell_A - x) \ell_A^2 - (\ell_A - x)^3 \right] + W_B \left[ (\ell_A - x) \frac{\ell_B^3}{\ell_A} - (\ell_B - x)^3 \right] \right\}$$

The above equation can be evaluated for a specific mode by substituting the relations for  $W_B$  and  $W_A$  developed earlier for that mode.

## 2. BOW III Computer Program

The FORTRAN description of the above program is given later in this appendix. It is similar to the BOW II program developed by Bump,<sup>5</sup> but incorporates the exact relations for the various bending modes as derived

in Part I of this appendix and includes an important mode ignored in BOW II. Also, D. Kucera has added stabilization to produce calculated output positions accurate to about 1 mil. Improvement to about 0.1 mil is necessary for BOW III to be useful in computing accurate dynamic movement of the subassemblies. A new approach conceiving of the subassembly array as a large group of coupled springs is under development by Kucera. This program will be known as BOW IV.

BOW III output includes an input listing as well as the output for chosen iterations. Each quantity printed is identified by its name within the code, and Table III relates program names with physical quantities.

TABLE III. BOW III FORTRAN Quantities

A. Input Quantities

MI	Number of equally spaced vertical nodes on each subassembly
MJ	Number of radial rows of subassembly
LI	Node number corresponding to button level
QQ	Initial fractional power
QD	Fractional-power increment
QT	Final fractional power
TL	Height of each subassembly (in.)
YFL1	Inmost allowed radial position for top of central subassembly
DELY	Maximum position change permitted by one iteration, at top
DL	Maximum position change permitted by one iteration, at button level
B8	Radial distance between vertical-assembly nozzle and grid- plate obstructions, inward or outward (in.)
B9	Length of nozzle (in.)
ALPHA	Coefficient of thermal expansion of buttons (in./in. °F)
D	Distance across flats of a subassembly (in.)
YR	Distance from outmost row centerline L to ring, at top level (in.)
D1	D1(1)
B1	Initial lean slope for all rows
B2	Free-swing distance at top level due to B8 clearance at nozzle
B3	B4(1) + 1
B4	B4(1)
DELT(I,J)	Full-power temperature differential across row J at node I level (°F at 45 MW)
YP(J)	Centerline radial position of row J
B4(J)	$I_A \ell_N / I_N \ell_A$ for row J
B5(J)	$3EIA F(J)/\ell_A^3$ for row J

TABLE III (Contd.)

---

B6(J)	Input as $3EI_{AF}(J)$ , printed as $\frac{3EI_{AF}(J)}{\ell_B^2(\ell_A - \ell_B)^2}$ for row J
D1(J)	Material thickness between centerlines of rows J and J + 1, at top level
DD1(J)	Initial material thickness between centerlines of rows J and J + 1, at button level
F(J)	The number of subassemblies in row J
T(J)	Full-power temperature difference between pivot and top level, for row J ( $^{\circ}\text{F}$ at 45 MW)
F1(J)	Single-button squashing factor for row J (in./lb)

---

B. Output Quantities

YT(I,J)	Thermal deflection at node I of row J, for the power level whose iteration values follow
M	Iteration number
Q	Fractional power
Y(I,J)	Radial position of node I of row J
MODE(J)	Most severe beam-bending formula-type required to fit row J into its constraint positions
ZF(J)	Effective maximum motion at top-level for row J
YFR(J)	Top-level constraint location on outside of row J
YFL(J)	Top-level constraint location on inside of row J
ZL(J)	Effective maximum motion at button level for row J
YFLR(J)	Button-level constraint location on outside of row J
YFLL(J)	Button-level constraint location on inside of row J
PL(J)	Load exerted on top level of row J from inside
PR(J)	Load exerted on top level of row J from outside
WL(J)	Load exerted on button level of row J from inside
WR(J)	Load exerted on button level of row J from outside
DD(J)	Button-level material thickness between row J and row J + 1 centerlines at fractional power Q

---

Some of the input quantities in this table are illustrated in Fig. B.4 with the radial scale greatly enlarged for clarity. Thus,  $\ell_A$  is typically 65 in., and B8 is  $4 \times 10^{-3}$  in. The method of summing DD1(J) and D1(J) between rows J and J + 1 is shown.

All doubly dimensioned arrays are printed so that row number increases with downward motion through each column and node number increases with rightward motion across each column. Thus, values for the top nodes of each row appear in the outermost column.

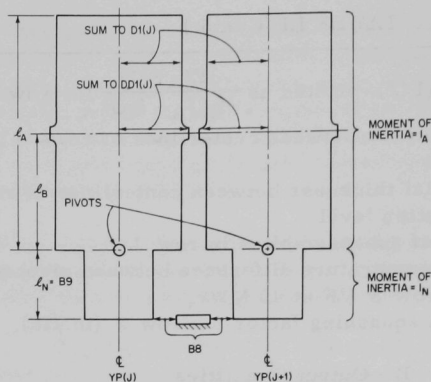


Fig. B.4  
BOW III Module

### 3. Calculation of Input Quantities

#### a. Button Stiffness

The button stiffness can be obtained by assuming a concentrated load on a long, flat, rectangular plate with fixed edges.

Then,

$$\Delta_b = 0.00725 \text{ Pa}^2/D \text{ (see Ref. 12),}$$

where

$\Delta_b$  = deflection at load (in.),

P = load (lb),

a = width of flat = 1.30 in.,

D = flexural rigidity = 130 lb-in. (see Ref. 12),

and

$$E = 24.25 \times 10^6 \text{ lb/in.}^2 \text{ for 304 SS.}$$

Therefore,

$$\Delta_b/P = 0.00725 \times 1.3^2/130 = 1 \times 10^{-4} \text{ mil/lb.}$$

Because of the hexagonal configuration of buttons, the effective stiffness per button per subassembly is 1.5 times as much as the actual stiffness.

Thus,

$$(\Delta b/P)_{\text{eff}} = 1 \times 10^{-4} / 1.5 = 0.7 \times 10^{-5} \text{ mil/lb},$$

and

$$F_1(J) = 2(\Delta b/P)_{\text{eff}} = 1.4 \times 10^{-4} \text{ mil/lb}.$$

The above value was used for rows 1-6. Rows 7-15 were assigned a value one-tenth that of  $F_1(J)$ , or  $1.4 \times 10^{-5}$  mil/lb, because the hexagonal can is supported immediately under the button by the rigid elements contained in the can, and therefore its flexure is greatly reduced.

b. Moment-of-inertia Calculations for Nozzles and Upper Parts of Subassemblies

The nozzles for rows 1-6 are all similar. Their moment of inertia is<sup>13</sup>

$$I_{N,(1-6)} = 0.049(D^4 - d^4) = 0.049(1.683^4 - 1.433^4) = 0.187 \text{ in.}^4.$$

The nozzles for rows 7-15 are similar, and their moment of inertia is

$$I_{N,(7-15)} = 0.049(1.468^4 - 1.068^4) = 0.164 \text{ in.}^4.$$

The hexagonal cans for rows 1-6 and 9-15 will determine the moment of inertia of the portion of the subassembly between the pivot and the top. The hexagon can be calculated, since it has a thin wall, by assigning it an average outside diameter of 2.450 in. The wall thickness of 0.040 in. leads to an inside diameter of 2.370 in.

Then

$$I_{A,(1-6,9-15)} = 0.049(2.450^4 - 2.370^4) = 0.218 \text{ in.}^4.$$

For the stainless steel reflector rows 7 and 8 used in Run 26, the stiffness of the upper part of the subassembly above the pivot is increased by the 19 full-length 0.493-in.-diam rods contained in each subassembly. (Such is not the case in rows 9-15, where the elements are made up of stacked short lengths, which are free to flex.)

Then,

$$\begin{aligned} I_{A,(7-8)} &= 0.049(2.450^4 - 2.370^4) + 19[0.049(0.493^4)] \\ &= 0.275 \text{ in.}^4 \quad (\text{elements free to slip}); \end{aligned}$$

$$\begin{aligned}
 IA_{(7-8)} &= 0.22 + 5 \times 0.049(0.493)^4 + (8 \times \pi \times 0.493^2/4)(0.493 \times 0.866)^2 \\
 &\quad + (6 \times \pi \times 0.493^2/4)(0.493 \times 0.866 \times 2)^2 \\
 &= 1.35 \quad (\text{elements unable to slip}).
 \end{aligned}$$

Since some slippage may occur, the following average value was assumed:

$$IA_{(7-8)} = 0.77 \quad (\text{partial slippage}).$$

Such partial slippage could account for the apparent hysteresis in the EBR-II feedback reactivity, which assumes two values depending upon the direction of power change.

The remaining inputs are combinations of moments of inertia, lengths, numbers of subassemblies per row, and mechanical properties of the materials, all of which are specified in the sample run. The differential temperature profiles for run No. 26B calculated by R. Cushman are used for the input (DELT).

#### 4. BOW III Sample Run

The printed output included on pages 41-59 is that for the computer run that produced the curve plotted in Fig. 7. The data for the curve appear in the last column of Table IV, which is the sum of the reactivity changes in inhours due to rows 6-9. The row displacement from its zero-power position at the button level is represented by  $d_6$ ,  $d_7$ , etc., in mils. It is obtained from the printed output by subtracting Y (in column 5) for a subassembly row from that row's YP. The reactivity due to the row displacement is obtained by multiplying d by the row reactivity constant ( $\rho$ ), which has the units of inhours/mil. The calculated values for  $\rho_6$ ,  $\rho_7$ ,  $\rho_8$ , and  $\rho_9$  are -1.806, -0.989, -0.500, and -0.289, respectively, for the EBR-II run No. 26B configuration. As power is increased from zero to 45 MW, rows 6 and 7 move steadily toward the core center and rows 8 and 9 move away from the center. The combined effect is to increase reactivity as power is increased, yielding positive feedback.

TABLE IV. Reactivity Evaluation of Sample Output

Q, P/45 MW	Row 6		Row 7		Row 8		Row 9		Total, lh
	$d_6$	$\rho_6 d_6$	$d_7$	$\rho_7 d_7$	$d_8$	$\rho_8 d_8$	$d_9$	$\rho_9 d_9$	
0.1	0.09	-0.16	0.46	0.45	0.6	-3.0	0.45	-0.13	-0.14
0.2	5.52	9.97	7.68	7.60	7.42	-3.71	5.08	-1.47	12.25
0.3	11.5	20.77	13.53	13.38	11.30	-5.65	9.04	-2.61	25.89
0.4	14.4	25.54	13.61	13.46	17.88	-8.92	15.66	-4.53	25.55
0.5	17.25	31.15	19.25	19.04	20.95	-10.48	18.85	-5.45	34.26
0.6	19.68	35.54	21.72	21.48	25.73	-12.87	23.71	-6.85	37.30
0.7	22.42	40.49	24.53	24.26	28.66	-14.33	26.73	-7.72	42.70
0.8	24.18	43.67	26.30	26.01	34.82	-17.41	32.97	-9.53	42.74
0.9	26.32	49.53	28.56	28.25	37.02	-18.51	35.25	-10.19	47.08
1.0	28.35	51.20	30.75	30.41	38.45	-19.23	36.76	-10.62	51.76

FORTRAN 5.301

03/06/69

```

PRCGRAM BOW III
DIMENSION CELT(20,20),YP(20),B1(20),D1(20),B3(20),B4(20),B5(20),
1 B6(20),Y(20,20),YI(20,20),YT(20,20),YFR(20),YFL(20),PL(20),
2 PR(20),XDELT(20,20),YY(20),AY(20,20),DD1(20),WR(20),WL(20),
3 F(20),DD(20),T(20),F1(20),A6(20),A7(20),YFL(20),YFLR(20),
4 YZ(20),MA(3C),YPT(20,20),B35(20),XX(20),APL(20),APR(20),
5 AWL(2C),AWR(20),PLB(20),PRB(20),WLB(20),WRB(20),B3L(20),B4L(20),
6 B7(20),B36(20),B35L(20),GL(20),HL(20),PRP(20),PLP(20),ZF(20),
7 ZL(20),MODE(20),B37(20),B38(20),B39(20),B40(20)
TYPE DOUBLE B3,B4,B5,B6,Y,YFR,YFL,PL,PR,YY,AY,WR,WL,DD,A6,A7,
1 YFL,YFLR,YZ,B35,XX,APL,APR,AWR,PLB,PRB,WLB,WRB,B3L,B4L,B7,
2 B36,B35L,GL,HL,PRP,PLP,ZF,ZL,B37,B38,B39,B40,B5L,CL,P,C1,C2,C3,
3 C4,PD,DS,DM,DNOZ,PP,C3M,WB,WA,C2M,YW,C4M
READ 1000,MI,MJ,LI,QQ,QT,TL,YFL1,DELY
REAC 5041,MT,DL,B8,B9,811
5041 FORMAT(1I6,7E10.4)
REAC 5040,(MA(N),N=1,MT)
5040 FORMAT(20I4)
READ 2000,ALPHA
READ 2000,((DELT (I,J),I=1,MI),J=1,MJ)
READ 2000,C
READ 2000,(YP(J),J=1,MJ)
READ 2000,YR
READ 2000,(D1(J),J=1,MJ)
REAC 2000,(B1(J),J=1,MJ)
READ 2000,B2
REAC 2000,(B4(J),J=1,MJ)
READ 2000,(B5(J),J=1,MJ)
REAC 2000,(B6(J),J=1,MJ)
READ 2000,(DC1(J),J=1,MJ)
REAC 2000,(F(J),J=1,MJ)
READ 2000,(T(J),J=1,MJ)
REAC 2000,(F1(J),J=1,MJ)
1000 FORMAT(3I6 ,6E10.4)
2000 FORMAT(8E10.4)
PRINT 5000
5000 FORMAT(6X,2HMI,6X,2HMJ,6X,2HLI,6X,2HQQ,10X,2HQD,10X,2HQT,10X,2HTL,
18 X,4HYFL1,8 X,4HDELY,10X,2HDL)
PRINT 5010,MI,MJ,LI,QQ,QT,TL,YFL1,DELY,DL
5010 FORMAT(3I8,8E12.4)
PRINT 5042,B8,B9
5042 FORMAT(6H B8,B9,6X,9E12.4)
MK=MJ-1
XMI=MI
DELX=TL/XMI
XLI=LI
A4=XLI*DELX
A42=A4**2
A2=TL-A4
A5=A2**2
E2=TL/(A42*A5)
A10=3.*XMI-XLI
A15=XMI-XLI
A11=3.* (XMI**2)*A15
A12=(DELX/XMI)**3/12.
A17=2.* (XMI**3)

```

FORTRAN 5.301

03/06/69

```

A18=A12*(XLI**2)
A20=2.*XMI-XLI
DO240 I=1,MI
XI=I
XX(I)=(1.5*(XMI/XI)-.5)*((XI/XMI)**2)
A1=XI*DELX
A3=TL-A1
A32=A3**2
A8=2.*TL
A6(I)= A1*(A8*A3-A5-A32)/(2.*A42*A2)
GL(I)=((XI/XLI)**2)*(1.5*(XLI/XI)-.5)
HL(I)=(XI-XLI)/XLI
B38(I)=XI*(XMI-XI)*(2.*XMI-XI)
IF(I.GT.LI) GO TO 239
B39(I)=XI*(XI**2-3.*XLI*XI+XLI**2*(3.-XLI/XMI))
GO TO 240
239 B39(I)=XLI**3*(XMI-XI)/XMI
240 A7(I)= A3*(A8*A2-A5-A32)/(2.*A4*A5)
D071 J=1,MJ
B3(J)=B4(J)+1.
B35(J)=B5(J)/B3(J)
B4L(J)=B4(J)*XMI/XLI
B3L(J)=B4L(J)+1.
B5L=B5(J)*((XMI/XLI)**3)
B35L(J)=B5L/B3L(J)
B6(J)=B6(J)*E2
B37(J)=A20*A15*.5/(B3(J)*XMI**2) -1.
B36(J)=2.*B6(J)*A15/(A20*B37(J)+XLI)
B37(J)=B37(J)*XLI/XMI
71 B4C(J)=XLI*A15*(B37(J)*A20+XLI**2/XMI)
PRINT5001
5001 FORMAT(5X,5HALPHA,7X,1HD,11X,2HYR,10X,2HD1,10X,2HB1,10X,2HB2,10X,
12HB3,10X,2HB4)
PRINT5011,ALPHA ,D ,YR ,D1(1),B1(1),B2 ,B3(1),B4(1)
5011 FORMAT(10E12.4)
PRINT 5002,((DELT(I,J),I=1,MI),J=1,MJ)
5002 FORMAT(5H DELT,5X,10E11.4)
PRINT 5003,(YP(J),J=1,MJ)
5003 FORMAT(3H YP,7X,10E11.4)
PRINT 5039,(B4(J),J=1,MJ)
5039 FORMAT (3H B4,7X,10E11.4)
PRINT 5004,(B5(J),J=1,MJ)
5004 FORMAT(3H B5,7X,10E11.4)
PRINT 5025,(B6(J),J=1,MJ)
5025 FORMAT(3H B6,7X,10E11.4)
PRINT5035,(D1(J),J=1,MJ)
5035 FORMAT(3H D1,7X,10E11.4)
PRINT 5027,(D01(J),J=1,MJ)
5027 FORMAT(4H D01,6X,10E11.4)
PRINT 5028,(F(J),J=1,MJ)
5028 FORMAT(2H F,8X,10E11.4)
PRINT 5029,(T(J),J=1,MJ)
5029 FORMAT(2H T,8X,10E11.4)
PRINT 5030,(F1(J),J=1,MJ)
5030 FORMAT(3H F1,7X,10E11.4)
D08C J=1,MJ

```

FORTRAN 5.3C1

03/06/69

```

DO8C I=1,MI
XI=I
80 YI(I,J)=YP(J)+B1(J)*DELX*XI
C=QC
GOTC 60
1 ASSIGN 304 TC MM
GOTC 305
304 Q=Q+QD
IF(L-QT)60,60,61
61 STOP
60 DO50 J=1,MJ
ZF(J)=DELY
ZL(J)=DL
DD(J)=DD1(J)*(1.+ALPHA*T(J)*Q)
DO50 I=1,MI
XDELT(I,J)=Q*DELT(I,J)
M=M-M
K=1
DO 15 J=1,MJ
SUM=0.
SUM2=0.
DO 15 I=1,MI
TERM=ALPHA*XDELT(I,J)*DELX/D
SUM=SUM+TERM
TERM2=(SUM-TERM/2.)*DELX
SUM2=SUM2+TERM2
15 YT(I,J)=SUM2
DO635 J=1,MJ
DO635 I=1,MI
635 YPT(I,J)=YI(I,J)+YT(I,J)
PRINT 5043,((YT(I,J),I=1,MI),J=1,MJ)
5043 FORMAT (3H YT,7X,10E11.4)
DO19 J=1,MK
19 YFR(J)=YP(J+1)-D1(J)
YFR(MJ)=YP(MJ)+YR      +Q*B11
DO18 J=2,MJ
18 YFL(J)=YP(J-1)+D1(J-1)
YFL(1)=YFL1
DO551 J=1,MK
551 YFLR(J)=YP(J+1)-DD1(J)
YFLR(MJ)=YP(MJ)+1.
DO552 J=2,MJ
552 YFLL(J)=YP(J-1)+DD1(J-1)
YFLL(1)=0.
125 M=M+1
IF(M-MA(MT))103,103,304
C
C       FIT TOP-LEVEL CONSTRAINTS
C
103 DO 607 J=1,MJ
MSC=0
PR(J)=PL(J)=0.
IF(YFR(J).LT.YFL(J)) GO TO 612
IF(YPT(MI,J).GE.YFL(J)) GO TO 609
CL=YFL(J)-YPT(MI,J)
GO TO 613

```

FORTRAN 5.301

03/06/69

```

609 IF(YPT(MI,J).GT.YFR(J)) GO TO 611
DO 610 I=1,MI
610 AY(I,J)=YPT(I,J)
GO TO 618
611 CL=YFR(J)-YPT(MI,J)
GO TO 613
612 CL=.5*(YFL(J)+YFR(J))-YPT(MI,J)
MSQ=1
613 SGN=1.
IF(CL.LT.0.) SGN=-1.
B2S=B2-SGN*TL*B1(J)
C
C      MODE 1
C
C1=CL $ ASSIGN 618 TO M1
IF(ABSF(CL).LE.B2S) GO TO 614
C1=SGN*B2S $ ASSIGN 616 TO M1
614 DO 615 I=1,MI
XI=I
615 AY(I,J)=YPT(I,J)+C1*XI/XMI
C2=CL-C1
GO TO M1
C
C      MODE 2
C
616 DO 617 I=1,MI
XI=I
617 AY(I,J)=AY(I,J)+C2*(B4(J)+XX(I))*XI/(XMI*B3(J))
P=-C2*B35(J)
IF(SGN.LT.0.) PR(J)=P
IF(SGN.GT.0.) PL(J)=P
618 PLP(J)=PL(J)
PRP(J)=PR(J)
C
C      SQUASHING
C
IF(MSQ.EQ.0) GO TO 607
PD=(YFL(J)-YFR(J))*F(J)/F1(J)
PL(J)=PL(J)-PD
PR(J)=PR(J)+PD
607 CCNTINUE
DO241 J=1,MJ
WL(J)=0.
241 WR(J)=0.
C
C      SUPERIMPCSE BUTTON-LEVEL CONSTRAINTS
C
DO 900 J=1,MJ
MCCE(J)=0 $ MSQ=0
IF(YFLR(J).LT.YFLL(J)) GO TO 902
IF(AY(LI,J).GE.YFLL(J)) GO TO 901
CL=YFLL(J)-AY(LI,J)
GO TO 903
901 IF(AY(LI,J).LE.YFLR(J)) GO TO 900
CL=YFLR(J)-AY(LI,J)
GO TO 903

```

FORTRAN 5.301

03/06/69

```

902 CL=.5*(YFLL(J)+YFLR(J))-AY(LI,J)
  MSG=1
903 YFF=YFR(J) $ SGN=1.
  IF(CL.GT.0.) GO TO 904
    YFF=YFL(J) $ SGN=-1.
    CHOOSE INITIAL MODE
904 IF(YFR(J).LT.YFL(J)) YFF=AY(MI,J)
  IF(PLP(J).NE.PRP(J)) GO TO 908
C
C      MODE 1
C
C      MOCE(J)=1
DS=A4/B9*(SGN*B8+B9*(4.*AY(1,J)-AY(2,J)-3.*YP(J))/(2.*DELX))
DM=A4/TL*(YFF-AY(MI,J))
  IF(ABSF(DM).LT.ABSF(DS)) GO TO 905
C      1 TO 2
C1=DS
  ASSIGN 916 TO M1
  GO TO 906
C      1 TO 4
905 C1=DM
DNCZ=-B9*(DS-DM)/A4
  ASSIGN 922 TO M1
906 IF(ABSF(C1).LT.ABSF(CL)) GO TO 912
  C1=CL $ ASSIGN 931 TO M1
912 DO 907 I=1,MI
  XI=I
907 AY(I,J)=AY(I,J)+C1*XI/XLI
  CL=CL-C1
  GO TO M1
C
C      MODES 3 AND 3A
C
908 IF(PLP(J).EQ.0.) GO TO 909
  PP=PLP(J)
  IF(CL) 911,900,910
909 PP=PRP(J)
  IF(CL) 910,900,911
C      MODE 3
910 MOCE(J)=3
  C3M=-PP/(B36(J)*B37(J))
  IF(ABSF(C3M).GE.ABSF(CL)) GO TO 914
  C3=C3M
  ASSIGN 916 TO M3
  GO TO 915
C      MODE 3A
911 MOCE(J)=30
  C3M=-PP/(B36(J)*(B37(J)+XLI/XMI))
  IF(ABSF(C3M).GE.ABSF(CL)) GO TO 914
  C3=C3M
  ASSIGN 922 TO M3
  DNCZ=-SGN*2.*B8
  GO TO 915
C      MODES 3,3A
914 C3=CL
  ASSIGN 931 TO M3

```

FORTRAN 5.301

03/06/69

```

915 DO 932 I=1,MI
932 AY(I,J)=AY(I,J)+C3*(B37(J)*B38(I)+B39(I))/B40(J)
WB=C3*B36(J)
WA=WB*B37(J)
IF(CL.LT.0.) WR(J)=WB
IF(CL.GT.0.) WL(J)=WB
IF(PP.LT.0.) PL(J)=PL(J)+WA
IF(PP.GT.0.) PR(J)=PR(J)+WA
CL=CL-C3
GO TO M3
C
C      MODE 2
C
916 MODE(J)=2
C2M=(YFF-AY(MI,J))/(1.+HL(MI)*(1.5+B4L(J))/B3L(J))
IF(ABSF(C2M).GE.ABSF(CL)) GO TO 917
C2=C2M
ASSIGN 929 TO M2
GO TO 918
917 C2=CL
ASSIGN 931 TO M2
918 DO 919 I=1,MI
XI=I
IF(I.GT.LI) GO TO 920
YW=C2*(B4L(J)+GL(I))*XI/(XL1*B3L(J))
GO TO 919
920 YW=C2*(1.+(1.5+B4L(J))*HL(I)/B3L(J))
919 AY(I,J)=AY(I,J)+YW
WB=-B35L(J)*C2
IF(CL.LT.0.) WR(J)=WR(J)+WB
IF(CL.GT.0.) WL(J)=WL(J)+WB
CL=CL-C2
GU TO M2
C
C      MODE 4
C
922 MODE(J)=4
C4M=-DN0Z*2.*XL1*A2/(B9*A20)
IF(ABSF(C4M).GE.ABSF(CL)) GO TO 923
C4=C4M
ASSIGN 929 TO M4
GO TO 924
923 C4=CL
ASSIGN 931 TO M4
924 DO 926 I=1,MI
IF(I.GT.LI) GO TO 925
YW=C4*A6(I)
GO TO 926
925 YW=C4*A7(I)
926 AY(I,J)=AY(I,J)+YW
WB=-C4*B6(J)
WA=-WB*XL1/XMI
IF(CL.LT.0.) GO TO 927
WL(J)=WL(J)+WB
PR(J)=PR(J)+WA
GO TO 928

```

FORTRAN 5.301

03/06/69

```

927  WR(J)=WR(J)+WB
      PL(J)=PL(J)+WA
928  CL=CL-C4
C
C      MCDE 5
C
929  MCDE(J)=5
      WB=CL*B36(J)
      WA=WB*B37(J)
      DO 933 I=1,MI
933  AY(I,J)=AY(I,J)+CL*(B37(J)*B38(I)*B39(I))/B40(J)
      IF(CL.LT.0.) GO TO 930
      WL(J)=WL(J)+WB
      PR(J)=PR(J)+WA
      GO TO 931
930  WR(J)=WR(J)+WB
      PL(J)=PL(J)+WA
C
C      BUTTON-LEVEL SQUASHING
C
931  IF(MSG.EQ.C) GC TO 900
      MCDE(J)=-MCDE(J)
      CM=YFLR(J)-YFLL(J)
      WL(J)=WL(J)+CM*(F(J)-3.)/F1(J)
      WR(J)=WR(J)-CM*(F(J)+3.)/F1(J)
900   CONTINUE
      D0572 N=1,MT
      IF(M-MA(N))572,320,572
572   CONTINUE
      GOTC 3C3
320   ASSIGN 303 TC MM
305   PRINT 5023,M,Q
5023  FORMAT(4H M,Q,1I6,1E12.4)
      PRINT 5005,((AY(I,J),I=1,MI),J=1,MJ)
5005  FORMAT(2H Y,8X,10F11.5)
      PRINT 5006,(MCDE(I),I=1,MJ)
5006  FORMAT(5H MCDE20I4)
      PRINT 5024,(ZF(J),J=1,MJ)
5024  FORMAT(* ZF*7X,10E11.4)
      PRINT 5008,(YFR(J),J=1,MJ)
5008  FORMAT(4H YFR,6X,10F11.5)
      PRINT 5009,(YFL(J),J=1,MJ)
5009  FORMAT(4H YFL,6X,10F11.5)
      PRINT 5026,(ZL(J),J=1,MJ)
5026  FORMAT(* ZL*7X,10E11.4)
      PRINT 5036,(YFLR(J),J=1,MJ)
5036  FORMAT(5H YFLR,5X,10F11.5)
      PRINT 5037,(YFLL(J),J=1,MJ)
5037  FORMAT(5H YFLL,5X,10F11.5)
306   PRINT 5021,(PL(J),J=1,MJ)
5021  FORMAT(3H PL,7X,10E11.4)
      PRINT 5022,(PR(J),J=1,MJ)
5022  FORMAT(3H PR,7X,10E11.4)
      PRINT 5032,(WL(J),J=1,MJ)
5032  FORMAT(3H WL,7X,10E11.4)
      PRINT 5031,(WR(J),J=1,MJ)

```

FORTRAN 5.3D1

03/06/69

```

5031  FORMAT(3H WR,7X,10E11.4)
      PRINT 5033,(CD(J),J=1,MJ)
5033  FORMAT(3H DD,7X,10E11.4)
      GOTC MM
 303  DC 107 J=1,MJ
      IF(ABSF(AY(LI,J)-Y(LI,J)).GT.1.E-5) GO TO 119
107  CONTINUE
      GO TO 1
119  IF(K.GT.1) GO TO 131
      DO 132 J=1,MJ
      PLB(J)=PL(J)
      PRB(J)=PR(J)
132  YY(J)=AY(MI,J)
      GO TO 133
131  DO 132 J=1,MJ
      PLB(J)=(PL(J)+APL(J))/2.
      PRE(J)=(PR(J)+APR(J))/2.
132  YY(J)=(Y(MI,J)+AY(MI,J))/2.
133  DO 701 J=2,MJ
      PMAX=(-PLB(J)+PRB(J))/2.
      IF(PMAX.EQ.0.) PMAX=.1
      P=PRB(J)+PLB(J+1)
      IF(J.EQ.MJ) P=0.
      DEL=(PLB(J)+PRB(J-1)+P)/PMAX
      IF(DEL.EQ.0.) GO TO 701
      FAC=1.
      IF(DEL/ZF(J).LT.0.) FAC=-.8
      ZF(J)=FAC*ZF(J)
      DELF=ZF(J)
      DELA=ABSF(CEL)
      IF(DELA.LT.1.) DELF=DELA*DELF
      YY(J)=YY(J)+DELF
7C1  CCNTINUE
    750  IF(YY(MJ).GT.YFR(MJ)) YY(MJ)=YFR(MJ)
      DO1C0 J=1,MK
      YFR(J)=YY(J+1)-C1(J)
      DO1C1 J=2,MJ
      YFL(J)=YY(J-1)+C1(J-1)
      IF(K.GT.1) GO TO 559
      DO5C0 J=1,MJ
      WLB(J)=WL(J)
      WRB(J)=WR(J)
560  YZ(J)=AY(LI,J)
      GO TO 561
559  DO 562 J=1,MJ
      WLB(J)=(WL(J)+AWL(J))/2.
      WRB(J)=(WR(J)+AWR(J))/2.
562  YZ(J)=(Y(LI,J)+AY(LI,J))/2.
561  DO 8C1 J=2,MJ
      WMAX=(-WLB(J)+WRB(J))/2.
      IF(WMAX.EQ.0.) WMAX=.1
      W=WRB(J)+WLB(J+1)
      IF(J.EQ.MJ) W=0.
      DEL=(WLB(J)+WRB(J-1)+W)/WMAX
      IF(DEL.EQ.0.) GO TO 801
      FAC=1.

```

FORTRAN 5.301

03/06/69

```

      IF(DEL/ZL(J).LT.0.) FAC=-.8
      ZL(J)=FAC*ZL(J)
      DELF=ZL(J)
      DELA=ABSF(DEL)
      IF(DELA.LT.1.) DELF=DELA*DELF
      YZ(J)=YZ(J)+DELF
 8C1  CONTINUE
 832  IF(YZ(MJ).GT.YFLR(MJ)) YZ(MJ)=YFLR(MJ)
      DD(1)=DD(1)*(1.+ALPHA*Q*T(1))+WL8(2)*F1(1)/6.
      D0547 J=1,MK
 547  YFLR(J)=YZ(J+1)-DD(J)
 548  D0548 J=2,MJ
      YFLL(J)=YZ(J-1)+DD(J-1)
      K=2
      IF(YFR(1).LT.YFL(1)) YFR(1)=YFL(1)
      IF(YFLR(1).LT.YFLL(1)) YFLR(1)=YFLL(1)
      IF(YFL(MJ).GT.YFR(MJ)) YFL(MJ)=YFR(MJ)
      IF(YFLL(MJ).GT.YFLR(MJ)) YFLL(MJ)=YFLR(MJ)
      D0110 J=1,MJ
      APL(J)=PL(J)
      APR(J)=PR(J)
      AWL(J)=WL(J)
      AWR(J)=WR(J)
      D0110 I=1,MI
 110  Y(I,J)=AY(I,J)
      GOTC 125
      END

```

50

Y	14.78015	14.78029	14.78044	14.78058	14.78060	14.78019	14.77692	14.77683	14.77351	14.76905
Y	16.89000	16.89000	16.89003	16.89015	16.89045	16.89088	16.89136	16.89168	16.89173	16.89148
Y	18.99000	18.99000	18.99003	18.99018	18.99066	18.99190	18.99425	18.99786	19.00275	19.00897
Y	21.10000	21.10000	21.10003	21.10012	21.10043	21.10129	21.10297	21.10549	21.10872	21.11255
Y	23.22000	23.22000	23.22000	23.22000	23.22007	23.22038	23.22107	23.22218	23.22366	23.22546
Y	25.34000	25.34000	25.34000	25.34000	25.34000	25.34000	25.34000	25.34000	25.34000	25.34000
Y	27.45000	27.45000	27.45000	27.45000	27.45000	27.45000	27.45000	27.45000	27.45000	27.45000
Y	29.55000	29.55000	29.55000	29.55000	29.55000	29.55000	29.55000	29.55000	29.55000	29.55000
MODE	0	0	0	0	0	0	0	0	0	0
ZF	3.0000-003	3.0000-003	3.0000-003	3.0000-003	3.0000-003	3.0000-003	3.0000-003	3.0000-003	3.0000-003	3.0000-003
ZF	3.0000-003	3.0000-003	3.0000-003	3.0000-003	3.0000-003	3.0000-003	3.0000-003	3.0000-003	3.0000-003	3.0000-003
YFR	0.03265	2.25002	4.29170	6.39170	8.49088	10.61305	12.69608	14.80848	16.93597	19.02955
YFR	21.13246	23.24700	25.36700	27.47700	29.64500					
YFL	-6.00000	2.19100	4.23765	6.33702	8.43770	10.54770	12.65688	14.76905	16.85208	18.96448
YFL	21.09197	23.20555	25.31864	27.42300	29.52300					
ZL	2.0000-003	2.0000-003	2.0000-003	2.0000-003	2.0000-003	2.0000-003	2.0000-003	2.0000-003	2.0000-003	2.0000-003
ZL	2.0000-003	2.0000-003	2.0000-003	2.0000-003	2.0000-003	2.0000-003	2.0000-003	2.0000-003	2.0000-003	2.0000-003
YFLR	0.00240	2.22242	4.26243	6.36240	8.46239	10.57186	12.68299	14.78287	16.89302	18.99282
YFLR	21.1C257	23.22250	25.34250	27.45250	29.55000					
YFLL	0.00000	2.21768	4.25774	6.35776	8.45780	10.56780	12.67775	14.77716	16.88820	18.98809
YFLL	21.09827	23.21793	25.33757	27.44750	29.54750					
PL	0.0000+000	0.0000+000	0.0000+000	0.0000+000	0.0000+000	0.0000+000	0.0000+000	0.0000+000	0.0000+000	0.0000+000
PL	0.0000+000	0.0000+000	0.0000+000	0.0000+000	0.0000+000	0.0000+000	0.0000+000	0.0000+000	0.0000+000	0.0000+000
PR	0.0000+000	0.0000+000	0.0000+000	0.0000+000	0.0000+000	0.0000+000	0.0000+000	0.0000+000	0.0000+000	0.0000+000
PR	0.0000+000	0.0000+000	0.0000+000	0.0000+000	0.0000+000	0.0000+000	0.0000+000	0.0000+000	0.0000+000	0.0000+000
WL	0.0000+000	0.0000+000	0.0000+000	0.0000+000	0.0000+000	0.0000+000	0.0000+000	0.0000+000	0.0000+000	0.0000+000
WL	0.0000+000	0.0000+000	0.0000+000	0.0000+000	0.0000+000	0.0000+000	0.0000+000	0.0000+000	0.0000+000	0.0000+000
WR	0.0000+000	0.0000+000	0.0000+000	0.0000+000	0.0000+000	0.0000+000	0.0000+000	0.0000+000	0.0000+000	0.0000+000
WR	0.0000+000	0.0000+000	0.0000+000	0.0000+000	0.0000+000	0.0000+000	0.0000+000	0.0000+000	0.0000+000	0.0000+000
DD	2.2177+000	2.0377+000	2.0977+000	2.0977+000	2.1077+000	2.1077+000	2.0976+000	2.1076+000	2.0976+000	2.1076+000
DD	2.1175+000	2.1175+000	2.1075+000	2.0975+000	-0.0000+000					
YT	0.0000+000	0.0000+000	0.0000+000	0.0000+000	0.0000+000	0.0000+000	0.0000+000	0.0000+000	0.0000+000	0.0000+000
YT	0.0000+000	0.0000+000	0.0000+000	0.0000+000	0.0000+000	0.0000+000	0.0000+000	0.0000+000	0.0000+000	0.0000+000
YT	0.0000+000	0.0000+000	0.0000+000	0.0000+000	0.0000+000	0.0000+000	0.0000+000	0.0000+000	0.0000+000	0.0000+000
YT	0.0000+000	0.0000+000	0.0000+000	0.0000+000	0.0000+000	0.0000+000	0.0000+000	0.0000+000	0.0000+000	0.0000+000
YT	0.0000+000	0.0000+000	0.0000+000	0.0000+000	0.0000+000	0.0000+000	0.0000+000	0.0000+000	0.0000+000	0.0000+000
YT	0.0000+000	0.0000+000	0.0000+000	0.0000+000	0.0000+000	0.0000+000	0.0000+000	0.0000+000	0.0000+000	0.0000+000
YT	0.0000+000	0.0000+000	0.0000+000	0.0000+000	0.0000+000	0.0000+000	0.0000+000	0.0000+000	0.0000+000	0.0000+000
YT	0.0000+000	0.0000+000	0.0000+000	0.0000+000	0.0000+000	0.0000+000	0.0000+000	0.0000+000	0.0000+000	0.0000+000
YT	0.0000+000	0.0000+000	0.0000+000	0.0000+000	0.0000+000	0.0000+000	0.0000+000	0.0000+000	0.0000+000	0.0000+000
YT	0.0000+000	0.0000+000	0.0000+000	0.0000+000	0.0000+000	0.0000+000	0.0000+000	0.0000+000	0.0000+000	0.0000+000
YT	0.0000+000	0.0000+000	0.0000+000	0.0000+000	0.0000+000	0.0000+000	0.0000+000	0.0000+000	0.0000+000	0.0000+000
YT	0.0000+000	0.0000+000	0.0000+000	0.0000+000	0.0000+000	0.0000+000	0.0000+000	0.0000+000	0.0000+000	0.0000+000
YT	0.0000+000	0.0000+000	0.0000+000	0.0000+000	0.0000+000	0.0000+000	0.0000+000	0.0000+000	0.0000+000	0.0000+000
YT	0.0000+000	0.0000+000	0.0000+000	0.0000+000	0.0000+000	0.0000+000	0.0000+000	0.0000+000	0.0000+000	0.0000+000
M,Q	81	2.0000-001								
Y	0.00000	0.00000	0.00000	0.00000	0.00000	0.00000	0.00000	0.00000	0.00000	0.00000
Y	2.22000	2.22000	2.22000	2.22000	2.22015	2.22086	2.22225	2.22393	2.22562	2.22730
Y	4.26000	4.26000	4.26000	4.26000	4.26017	4.26094	4.26247	4.26433	4.26618	4.26804
Y	6.35970	6.35939	6.35909	6.35879	6.35869	6.35929	6.36078	6.36264	6.36450	6.36636
Y	8.45928	8.45855	8.45783	8.45710	8.45659	8.45677	8.45784	8.45928	8.46072	8.46216
Y	10.56886	10.56772	10.56549	10.56545	10.56448	10.56410	10.56444	10.56509	10.56574	10.56638
Y	12.67844	12.67683	12.67517	12.67355	12.67232	12.67222	12.67420	12.67898	12.68688	12.69798
Y	14.78148	14.78299	14.78453	14.78610	14.78742	14.78791	14.78960	14.78385	14.77855	14.77098
Y	16.89084	16.89167	16.89256	16.89366	16.89508	16.89679	16.89857	16.90006	16.90100	16.90133
Y	18.99035	18.99070	18.99112	18.99176	18.99307	18.99590	19.00095	19.00852	19.01866	19.03144
Y	21.10000	21.10000	21.10005	21.10024	21.10086	21.10258	21.10594	21.11097	21.11743	21.12509
Y	23.22000	23.22000	23.22000	23.22000	23.22014	23.22074	23.22215	23.22436	23.22732	23.23092
Y	25.34000	25.34000	25.34000	25.34000	25.34000	25.34000	25.34000	25.34000	25.34000	25.34000
Y	27.45000	27.45000	27.45000	27.45000	27.45000	27.45000	27.45000	27.45000	27.45000	27.45000
Y	29.55000	29.55000	29.55000	29.55000	29.55000	29.55000	29.55000	29.55000	29.55000	29.55000



ZL	1.3744-004	2.0000-003	2.0000-003	2.0000-003	2.0000-003	2.0000-003	10.55825	12.69343	14.79130	16.89902	18.99712
YFLR	0.00000	2.21709	4.25481	6.35255	8.45038	10.55825	12.66647	14.76414	16.89905	18.99695	
YFLR	21.10479	23.22259	25.34250	27.45250	30.55000	10.55875	12.66647	14.76414	16.89905	18.99695	
YFLR	0.00000	2.21711	4.25534	6.35308	8.45092	10.55875	12.66647	14.76414	16.89905	18.99695	
YFLL	21.10476	23.22244	25.33979	27.44759	29.54750	10.55875	12.66647	14.76414	16.89905	18.99695	
PL	0.0000+000	0.0000+000	0.0000+000	0.0000+000	0.0000+000	0.0000+000	0.0000+000	0.0000+000	0.0000+000	0.0000+000	0.0000+000
PL	0.0000+000	0.0000+000	0.0000+000	0.0000+000	0.0000+000	0.0000+000	0.0000+000	0.0000+000	0.0000+000	0.0000+000	0.0000+000
PR	0.0000+000	0.0000+000	0.0000+000	0.0000+000	0.0000+000	0.0000+000	0.0000+000	0.0000+000	1.4994+002	0.0000+000	0.0000+000
PR	0.0000+000	0.0000+000	0.0000+000	0.0000+000	0.0000+000	0.0000+000	0.0000+000	0.0000+000	0.0000+000	0.0000+000	0.0000+000
WL	0.0000+000-1.2961+001	-3.2909+001	-5.5123+001	-7.8836+001	-9.3532+001	-1.9902+002	0.0000+000	0.0000+000	1.6119+002	0.0000+000	0.0000+000
WL	0.0000+000	0.0000+000	0.0000+000	0.0000+000	0.0000+000	0.0000+000	0.0000+000	0.0000+000	1.2021+002	1.6598+002	0.0000+000
WR	0.0000+000	3.8882+001	5.4849+001	8.3005+001	1.2021+002	1.6598+002	0.0000+000	2.1616+002	1.1453+002	0.0000+000	2.1078+000
CD	2.2177+000	2.0380+000	2.0980+000	2.0981+000	2.1081+000	2.1080+000	2.0979+000	2.1077+000	2.0979+000	2.1077+000	2.1078+000
DD	2.1175+000	2.1175+000	2.1075+000	2.0975+000	-0.0000+000	0.0000+000	0.0000+000	0.0000+000	0.0000+000	0.0000+000	0.0000+000
YT	0.0000+000	0.0000+000	0.0000+000	0.0000+000	0.0000+000	0.0000+000	0.0000+000	0.0000+000	0.0000+000	0.0000+000	0.0000+000
YT	0.0000+000	0.0000+000	0.0000+000	0.0000+000	0.0000+000	0.0000+000	0.0000+000	0.0000+000	1.7175-003	4.4998-003	7.8661-003
YT	0.0000+000	0.0000+000	0.0000+000	0.0000+000	0.0000+000	0.0000+000	0.0000+000	0.0000+000	1.8892-003	4.9463-003	8.6561-003
YT	0.0000+000	0.0000+000	0.0000+000	0.0000+000	0.0000+000	0.0000+000	0.0000+000	0.0000+000	2.2327-003	5.8051-003	1.0133-002
YT	0.0000+000	0.0000+000	0.0000+000	0.0000+000	0.0000+000	0.0000+000	0.0000+000	0.0000+000	2.2327-003	5.8051-003	1.0133-002
YT	0.0000+000	0.0000+000	0.0000+000	0.0000+000	0.0000+000	0.0000+000	0.0000+000	0.0000+000	1.8549-003	4.0809-003	8.3813-003
YT	0.0000+000	0.0000+000	0.0000+000	0.0000+000	0.0000+000	0.0000+000	0.0000+000	0.0000+000	4.3967-003	1.1885-002	2.5007-002
YT	0.0000+000	0.0000+000	0.0000+000	0.0000+000	0.0000+000	0.0000+000	0.0000+000	0.0000+000	8.0035-003	1.7347-002	3.1224-002
YT	0.0000+000	0.0000+000	0.0000+000	0.0000+000	0.0000+000	0.0000+000	0.0000+000	0.0000+000	6.9386-003	5.9081-003	0.0000+000
YT	0.0000+000	0.0000+000	0.0000+000	0.0000+000	0.0000+000	0.0000+000	0.0000+000	0.0000+000	5.4272-003	6.7325-003	7.5878-002
YT	0.0000+000	0.0000+000	0.0000+000	0.0000+000	0.0000+000	0.0000+000	0.0000+000	0.0000+000	1.7003-002	3.1430-002	5.1009-002
YT	0.0000+000	0.0000+000	0.0000+000	0.0000+000	0.0000+000	0.0000+000	0.0000+000	0.0000+000	1.3740-004	2.7134-004	2.6449-003
YT	0.0000+000	0.0000+000	0.0000+000	0.0000+000	0.0000+000	0.0000+000	0.0000+000	0.0000+000	1.0305-004	4.8089-004	1.7175-003
YT	0.0000+000	0.0000+000	0.0000+000	0.0000+000	0.0000+000	0.0000+000	0.0000+000	0.0000+000	5.1524-003	1.1885-002	2.1949-002
YT	0.0000+000	0.0000+000	0.0000+000	0.0000+000	0.0000+000	0.0000+000	0.0000+000	0.0000+000	2.7480-004	1.5114-003	4.2937-003
YT	0.0000+000	0.0000+000	0.0000+000	0.0000+000	0.0000+000	0.0000+000	0.0000+000	0.0000+000	8.7428-003	1.4633-002	2.1846-002
YT	0.0000+000	0.0000+000	0.0000+000	0.0000+000	0.0000+000	0.0000+000	0.0000+000	0.0000+000	0.0000+000	0.0000+000	0.0000+000
YT	0.0000+000	0.0000+000	0.0000+000	0.0000+000	0.0000+000	0.0000+000	0.0000+000	0.0000+000	0.0000+000	0.0000+000	0.0000+000
M,C	312	4.0000-001	0.00000	0.00000	0.00000	0.00000	0.00000	0.00000	0.00000	0.00000	0.00000
Y	0.00000	0.00000	0.00000	0.00000	0.00000	0.00000	0.00000	0.00000	0.00000	0.00000	0.00000
Y	2.21919	2.21839	2.21758	2.21677	2.21627	2.21687	2.21885	2.22141	2.22397	2.22653	
Y	4.25866	4.25729	4.25590	4.25450	4.25344	4.25358	4.25523	4.25753	4.25983	4.26213	
Y	6.35838	6.35656	6.35459	6.35252	6.35081	6.35050	6.35194	6.35414	6.35634	6.35854	
Y	8.45757	8.45514	8.45271	8.45028	8.44826	8.44765	8.44879	8.45069	8.45259	8.45448	
Y	10.56788	10.56524	10.56222	10.55893	10.55586	10.55393	10.55346	10.55359	10.55373	10.55387	
Y	12.67736	12.67440	12.67103	12.66731	12.66387	12.66216	12.66415	12.67138	12.68462	12.70416	
Y	14.78288	14.78612	14.78974	14.79381	14.79784	14.80066	14.80088	14.79733	14.78946	14.77716	
Y	16.89220	16.89478	16.89775	16.90133	16.90566	16.91059	16.91565	16.92013	16.92352	16.92566	
Y	18.99196	18.99415	18.99662	18.99954	19.00370	19.01070	19.01709	19.02199	19.03817	19.05942	
Y	21.10177	21.10372	21.10588	21.10834	21.11161	21.11697	21.12552	21.13733	21.15194	21.16894	
Y	23.22158	23.22330	23.22513	23.22707	23.22938	23.23272	23.23766	23.24430	23.25245	23.26191	
Y	25.34138	25.34279	25.34424	25.34571	25.34721	25.34873	25.35027	25.35182	25.35337	25.35494	
Y	27.454094	27.45189	27.45283	27.45377	27.45471	27.45566	27.45660	27.45754	27.45849	27.45943	
Y	29.551084	29.55168	29.55252	29.55336	29.55420	29.55540	29.55588	29.55672	29.55756	29.55840	
MODE	C	-1	-2	-2	-1	-2	30	-2	-5	5	0
ZF	3.0000-003	3.0000-003	3.0000-003	3.0000-003	3.0000-003	3.0000-003	3.0000-003	3.0000-003	2.4000-004	5.0332-004	5.0332-004
ZF	6.2308-007	1.3194-004	-2.1923-008	3.0000-003	3.0000-003	3.0000-003	3.0000-003	3.0000-003	5.0332-004	5.0332-004	3.0000-003
YFR	0.03552	2.24812	4.28553	6.38147	8.47086	10.62116	12.70416	14.84263	17.01289	19.08591	
YFR	21.16894	23.26191	25.37640	27.48339	29.64500	30.62116	32.70416	34.84263	37.01289	39.08591	
YFL	-0.00000	2.19100	4.24052	6.33512	8.43153	10.53747	12.63686	14.77716	16.86016	18.99863	
YFL	21.16889	23.26191	25.35494	27.43791	29.53240	30.62116	32.70416	34.84263	37.01289	39.08591	
ZL	2.0000-003-6.5536-004	1.3744-004	1.3744-004	1.3744-004	1.3744-004	1.3744-004	1.3744-004	1.3744-004	1.6000-003-1.6000-003	8.7961-005	5.6295-005-1.8093-011
ZL	1.4757-005	1.7614-007	1.4757-005	2.0000-003	2.0000-003	2.0000-003	2.0000-003	2.0000-003	2.0000-003	2.0000-003	2.0000-003
YFLR	0.00000	2.21531	4.25263	6.34999	8.44741	10.55515	12.69986	14.79784	16.90563	19.00368	
YFLR	21.11187	23.22971	25.34920	27.45569	29.55000	30.55000	32.69986	34.79784	36.90563	39.00368	
YFL	0.00000	2.21724	4.25425	6.35163	8.44911	10.55658	12.66387	14.76133	16.90570	19.00372	
YFL	21.11181	23.22910	25.34687	27.45471	29.55420	30.55000	32.69986	34.79784	36.90563	39.00368	
PL	0.0000+000	0.0000+000	0.0000+000	0.0000+000	0.0000+000	0.0000+000	0.0000+000	0.0000+000	0.0000+000	0.0000+000	0.0000+000
PL	0.0000+000	2.2839+001	-5.9416+000	0.0000+000	0.0000+000	0.0000+000	0.0000+000	0.0000+000	0.0000+000	0.0000+000	4.6609+001
PL	0.0000+000	0.0000+000	0.0000+000	0.0000+000	0.0000+000	0.0000+000	0.0000+000	0.0000+000	0.0000+000	0.0000+000	0.0000+000





YT 0.0000+000 0.0000+000 2.4045-004 1.2623-003 4.6286-003 1.3285-002 2.9755-002 5.5002-002 8.9266-002 1.3279-001  
 YT 0.0000+000 0.0000+000 1.8034-004 8.4157-004 3.0056-003 9.0168-003 2.0799-002 3.8411-002 6.1013-002 8.7823-002  
 YT 0.0000+000 0.0000+000 0.0000+000 4.8089-004 2.6449-003 7.5140-003 1.5268-002 2.5608-002 3.8231-002  
 YT 0.0000+000 0.0000+000 0.0000+000 0.0000+000 0.0000+000 0.0000+000 0.0000+000 0.0000+000 0.0000+000 0.0000+000  
 YT 0.0000+000 0.0000+000 0.0000+000 0.0000+000 0.0000+000 0.0000+000 0.0000+000 0.0000+000 0.0000+000 0.0000+000  
 M,Q 500 7.0000-001  
 Y 0.0000 0.0000 0.0000 0.0000 0.0000 0.0000 0.0000 0.0000 0.0000 0.0000  
 Y 2.21859 2.21710 2.21556 2.21399 2.21294 2.21381 2.21700 2.22138 2.22567 2.22997  
 Y 4.25778 4.25545 4.25303 4.25055 4.24865 4.24884 4.25168 4.25566 4.25964 4.26362  
 Y 6.35772 6.35483 6.35144 6.34776 6.34464 6.34397 6.34636 6.35007 6.35378 6.35749  
 Y 8.45732 8.45376 8.44954 8.44489 8.44074 8.43902 8.44036 8.44303 8.44569 8.44836  
 Y 10.56700 10.56293 10.55806 10.55265 10.54758 10.54450 10.54395 10.54448 10.54501 10.54554  
 Y 12.67687 12.67303 12.66811 12.66198 12.65547 12.65100 12.65211 12.66177 12.68149 12.71202  
 Y 14.78385 14.78847 14.79411 14.80105 14.80866 14.81500 14.81753 14.81401 14.80330 14.78502  
 Y 16.89338 16.89766 16.90278 16.90907 16.91673 16.92544 16.93440 16.94233 16.94834 16.95219  
 Y 18.99417 18.99912 19.00426 19.00933 19.01508 19.02385 19.03846 19.06035 19.09026 19.12893  
 Y 21.10358 21.10791 21.11264 21.11758 21.12323 21.13156 21.14463 21.16275 21.18535 21.21189  
 Y 23.22290 23.22650 23.23069 23.23531 23.24071 23.24797 23.25806 23.27114 23.28866 23.30490  
 Y 25.34262 25.34597 25.35006 25.35492 25.36059 25.36705 25.37418 25.38180 25.38975 25.39787  
 Y 27.45271 27.45602 27.45979 27.46385 27.46807 27.47232 27.47657 27.48081 27.48506 27.48931  
 Y 29.55312 29.55624 29.55935 29.56247 29.56559 29.56871 29.57183 29.57495 29.57806 29.58118  
 MODE 0 -2 -2 -2 -2 -2 -30 30 -2 -5 -5 3 30 -2 1  
 ZF 3.0000-003 3.0000-003 3.0000-003 3.0000-003 4.2817-008-1.5360-003 7.8643-004 7.8643-004 3.0000-003 3.4588-005  
 ZF 8.4442-005 8.4442-005 3.4588-005-2.4000-003 3.0000-003  
 YFR 0.03896 2.24911 4.28484 6.37535 8.46253 10.62902 12.71202 14.86914 17.05591 19.12893  
 YFR 21.21187 23.30487 25.40627 27.50815 29.64500 30.62902 32.71202 34.86914 36.05591 38.12893  
 YFL -0.00000 2.19100 4.24396 6.33611 8.43048 10.53135 12.62853 14.78502 16.86802 19.02514  
 YFL 21.21191 23.30493 25.39787 27.48087 29.56227 30.62902 32.71202 34.86914 36.05591 38.12893  
 ZL 2.0000-003-6.5536-004 3.3554-004 8.1920-004 2.1475-004-1.6000-003-1.6000-003 5.2429-004-3.0949-006-7.0369-005  
 ZL -7.5558-006 2.3058-005 1.0889-007 8.1961-005 8.0347-010 8.1961-005 8.0347-010 8.1961-005 8.0347-010 8.1961-005  
 YFLR 0.00000 2.21004 4.24598 6.34193 8.43792 10.54545 12.71047 14.80866 16.91653 19.01497  
 YFLR 21.12321 23.24307 25.36059 27.46807 30.55000 30.55000 30.55000 30.55000 30.55000 30.55000  
 YFLL 0.00000 2.21583 4.25132 6.34736 8.44356 10.54971 12.65547 14.75252 16.91692 19.01519  
 YFLL 21.12325 23.24071 25.35821 27.46807 29.56559 29.56559 29.56559 29.56559 29.56559 29.56559  
 PL 0.0000+000 0.0000+000 0.0000+000 0.0000+000 0.0000+000 0.0000+000 0.0000+000 0.0000+000 0.0000+000 0.0000+000  
 PL -1.6486+002-3.4745+002-2.4091+002-6.6174+024 0.0000+000  
 PR 0.0000+000 0.0000+000 0.0000+000 0.0000+000 0.0000+000 0.0000+000 0.0000+000 0.0000+000 0.0000+000 5.4213+002  
 PR 4.7916+002 3.0505+002 0.0000+000 0.0000+000 0.0000+000 0.0000+000 0.0000+000 0.0000+000 0.0000+000 0.0000+000  
 WL 0.0000+000-1.2059+002-3.3361+002-5.6586+002-8.2318+002-7.9885+002-1.9680+003 0.0000+000-1.4408+003-2.1928+003  
 WL -1.1056+003-1.4221+002 0.0000+000-2.3733+002 0.0000+000  
 WR 0.0000+000 3.6394+002 5.6306+002 8.4863+002 1.1642+003 1.1386+003 0.0000+000 1.8232+003 1.3883+003 8.5216+002  
 WR 1.9290+002 0.0000+000 2.8206+002 1.8574+001 0.0000+000  
 DD 2.2158+000 2.0386+000 2.0987+002 2.0989+002 2.0899+000 2.1087+000 2.0984+000 2.1080+000 2.0985+000 2.1082+000  
 DD 2.1175+000 2.1175+000 2.1075+000 2.0975+000-0.0000+000  
 YT 0.0000+000 0.0000+000 0.0000+000 0.0000+000 0.0000+000 0.0000+000 0.0000+000 0.0000+000 0.0000+000 0.0000+000  
 YT 0.0000+000 0.0000+000 0.0000+000 0.0000+000 0.0000+000 0.0000+000 0.0000+000 0.0000+000 0.0000+000 0.0000+000  
 YT 0.0000+000 0.0000+000 0.0000+000 0.0000+000 0.0000+000 0.0000+000 0.0000+000 0.0000+000 0.0000+000 0.0000+000  
 YT 0.0000+000 0.0000+000 0.0000+000 0.0000+000 0.0000+000 0.0000+000 0.0000+000 0.0000+000 0.0000+000 0.0000+000  
 YT 0.0000+000 0.0000+000 0.0000+000 0.0000+000 0.0000+000 0.0000+000 0.0000+000 0.0000+000 0.0000+000 0.0000+000  
 YT 0.0000+000 0.0000+000 0.0000+000 0.0000+000 0.0000+000 0.0000+000 0.0000+000 0.0000+000 0.0000+000 0.0000+000  
 YT 0.0000+000 0.0000+000 0.0000+000 0.0000+000 0.0000+000 0.0000+000 0.0000+000 0.0000+000 0.0000+000 0.0000+000  
 YT 0.0000+000 0.0000+000 0.0000+000 0.0000+000 0.0000+000 0.0000+000 0.0000+000 0.0000+000 0.0000+000 0.0000+000  
 YT 0.0000+000 0.0000+000 0.0000+000 0.0000+000 0.0000+000 0.0000+000 0.0000+000 0.0000+000 0.0000+000 0.0000+000  
 YT 0.0000+000 0.0000+000 0.0000+000 0.0000+000 0.0000+000 0.0000+000 0.0000+000 0.0000+000 0.0000+000 0.0000+000  
 YT 0.0000+000 0.0000+000 0.0000+000 0.0000+000 0.0000+000 0.0000+000 0.0000+000 0.0000+000 0.0000+000 0.0000+000  
 M,Q 500 8.0000-001  
 Y 0.00000 0.00000 0.00000 0.00000 0.00000 0.00000 0.00000 0.00000 0.00000 0.00000

Y	2.21849	2.21684	2.21510	2.21328	2.21206	2.21302	2.21673	2.22161	2.22649	2.23137
Y	4.25736	4.25471	4.25205	4.24939	4.24741	4.24784	4.25129	4.25605	4.26081	4.26556
Y	6.35755	6.35439	6.35067	6.34660	6.34317	6.34253	6.34539	6.34976	6.35413	6.35850
Y	8.45713	8.45327	8.44866	8.44356	8.43903	8.43728	8.43903	8.44229	8.44555	8.44881
Y	10.56681	10.56244	10.55717	10.55130	10.54582	10.54263	10.54232	10.54326	10.54419	10.54512
Y	12.67681	12.67281	12.66756	12.66088	12.65370	12.64874	12.65008	12.66112	12.68362	12.71844
Y	14.78466	14.79026	14.79713	14.80555	14.81482	14.82271	14.82630	14.82302	14.81155	14.79144
Y	16.89409	16.89937	16.90575	16.91356	16.92297	16.93360	16.94450	16.95423	16.96177	16.96683
Y	18.99531	19.00170	19.00833	19.01468	19.02141	19.03107	19.04692	19.07075	19.10352	19.14618
Y	21.10458	21.11022	21.11640	21.12272	21.12963	21.13925	21.15397	21.17424	21.19947	21.22913
Y	23.22373	23.22851	23.23406	23.24014	23.24703	23.25589	23.26784	23.28309	23.30129	23.32211
Y	25.34284	25.34660	25.35139	25.35731	25.36449	25.37296	25.38253	25.39292	25.40385	25.41506
Y	27.45318	27.45716	27.46175	27.46675	27.47194	27.47717	27.48241	27.48764	27.49288	27.49811
Y	29.555288	29.55643	29.56049	29.56488	29.56945	29.57405	29.57864	29.5823	29.58783	29.59242
MODE	0	-2 -2 -2 -2 -2 30 30 -2 -5 -3 -30 -2 2								
ZF	3.0000-003	3.00G0-003	3.0000-003	3.0000-003	3.1594-010-2-7670-005	7.8643-004	7.8643-004	3.0000-003	1.3194-004	
ZF	1.3194-004	2.2136-005	5.4043-005	1.1224-008-2-4400-003						
YFR	0.04037	2.25156	4.28594	6.37580	8.46210	10.63544	12.71844	14.88377	17.07320	19.14618
YFR	21.22907	23.32204	25.41505	27.51697	29.64500					
YFL	-0.0000C	2.19100	4.24537	6.33856	8.43149	10.53180	12.62810	14.79144	16.87444	19.03977
YFL	21.22920	23.32218	25.41507	27.49804	29.57105					
ZL	2.0000-003-1.0240-003	1.3744-004	8.1920-004	3.3554-004-1.6000-003-1.6000-003	5.2429-004-2.1268-007-2.1268-007					
ZL	-3.0949-006	5.6295-005	4.1538-007	3.6029-005-2.4520-009						
YFLR	0.00000	2.20863	4.24433	6.34006	8.43578	10.54340	12.71651	14.81482	16.92276	19.02125
YFLR	21.12952	23.24696	25.36445	27.47193	30.55000					
YFLF	0.00000	2.21548	4.25050	6.34628	8.44228	10.54824	12.65370	14.75077	16.92318	19.02157
YFLF	21.12973	23.24710	25.36452	27.47196	29.56945					
PL	0.0000+000	0.0000+000	0.0000+000	0.0000+000	0.0000+000	0.0000+000	0.0000+000	0.0000+000	0.0000+000	0.0000+000
PL	-5.2682+002-6.1253+002-4.7969+002-1.3235-023									
PR	0.0000+000	0.0000+000	0.0000+000	0.0000+000	0.0000+000	0.0000+000	0.0000+000	0.0000+000	0.0000+000	0.0000+000
PR	9.7953+002	6.1237+002	8.2556+001	0.0000+000	0.0000+000					
WL	0.0000+000-1.4260+002-3.8555+002-6.4740+002-9.4798+002-9.0820+002-2.3721+003									
WL	-2.1549+003-9.4327+002-3.4367+002-5.507+002-3.0691+002									
WR	0.0000+000	4.3185+002	6.4303+002	9.3499+002	2.0363+002	2.0365+002	0.0000+000			
DD	2.2155+000	2.0388+000	2.0598+000	2.0991+000	2.1091+000	2.1088+000	2.0985+000	2.1081+000	2.0986+000	2.1083+000
DD	7.1175+000	2.1175+000	2.1675+000	2.975+000-0.0000+000						
YT	0.0000+000	0.0000+000	0.0000+000	0.0000+000	0.0000+000	0.0000+000	0.0000+000	0.0000+000	0.0000+000	0.0000+000
YT	0.0000+000	0.0000+000	0.0000+000	0.0000+000	0.0000+000	0.0000+000	0.0000+000	0.0000+000	0.0000+000	0.0000+000
YT	0.0000+000	0.0000+000	0.0000+000	0.0000+000	0.0000+000	0.0000+000	0.0000+000	0.0000+000	0.0000+000	0.0000+000
YT	0.0000+000	0.0000+000	0.0000+000	0.0000+000	0.0000+000	0.0000+000	0.0000+000	0.0000+000	0.0000+000	0.0000+000
YT	0.0000+000	0.0000+000	0.0000+000	0.0000+000	0.0000+000	0.0000+000	0.0000+000	0.0000+000	0.0000+000	0.0000+000
YT	0.0000+000	0.0000+000	0.0000+000	0.0000+000	0.0000+000	0.0000+000	0.0000+000	0.0000+000	0.0000+000	0.0000+000
YT	0.0000+000	0.0000+000	0.0000+000	0.0000+000	0.0000+000	0.0000+000	0.0000+000	0.0000+000	0.0000+000	0.0000+000
YT	0.0000+000	0.0000+000	0.0000+000	0.0000+000	0.0000+000	0.0000+000	0.0000+000	0.0000+000	0.0000+000	0.0000+000
YT	0.0000+000	0.0000+000	0.0000+000	0.0000+000	0.0000+000	0.0000+000	0.0000+000	0.0000+000	0.0000+000	0.0000+000
YT	0.0000+000	0.0000+000	0.0000+000	0.0000+000	0.0000+000	0.0000+000	0.0000+000	0.0000+000	0.0000+000	0.0000+000
YT	0.0000+000	0.0000+000	0.0000+000	0.0000+000	0.0000+000	0.0000+000	0.0000+000	0.0000+000	0.0000+000	0.0000+000
YT	0.0000+000	0.0000+000	0.0000+000	0.0000+000	0.0000+000	0.0000+000	0.0000+000	0.0000+000	0.0000+000	0.0000+000
YT	0.0000+000	0.0000+000	0.0000+000	0.0000+000	0.0000+000	0.0000+000	0.0000+000	0.0000+000	0.0000+000	0.0000+000
YT	0.0000+000	0.0000+000	0.0000+000	0.0000+000	0.0000+000	0.0000+000	0.0000+000	0.0000+000	0.0000+000	0.0000+000
M,Q	500	9.0000-001								
Y	0.00000	0.00000	0.00000	0.00000	0.00000	0.00000	0.00000	0.00000	0.00000	0.00000
Y	2.21840	2.21660	2.21466	2.21263	2.21124	2.21232	2.21649	2.22197	2.22745	2.23294
Y	4.25710	4.25420	4.25130	4.24840	4.24627	4.24684	4.25082	4.25267	4.26171	4.26716
Y	6.35739	6.35394	6.34987	6.34593	6.34163	6.34100	6.34431	6.34932	6.35433	6.35934
Y	8.45691	8.45270	8.44764	8.44202	8.43704	8.43518	8.43727	8.44105	8.44483	8.44861
Y	10.56659	10.56183	10.55608	10.54966	10.54368	10.54027	10.54011	10.54134	10.54257	10.54379
Y	12.67682	12.67271	12.67079	12.65968	12.65141	12.65450	12.66461	12.67565	12.68190	12.71994
Y	14.78468	14.79042	14.79763	14.80675	14.81702	14.82600	14.83037	14.82718	14.81489	14.79294
Y	16.89431	16.89991	16.90671	16.91509	16.92525	16.93678	16.94863	16.95915	16.96721	16.97248





APPENDIX C  
Reflector Heat-transfer Dynamics

1. Reflector Subassembly; Row 7

From Section III.B, the relation between row 7 differential temperature  $\Delta T_7(s)$  and power  $P(s)$  is

$$\frac{\Delta T_7(s)}{P(s)} = \frac{\theta_7 \text{Hexin}(s) - \theta_7 \text{Hexout}(s)}{P(s)}.$$

It is convenient to evaluate the above expression by evaluating the numerator terms separately and then combining them.

From Section III.B,

$$\frac{\theta_7 \text{Hexin}(s)}{P(s)} = \frac{1}{1 + \tau_6 C s} \left\{ K_1 - \frac{1.5 R_1 (K_1 - K_2 R_{VR})}{2 R_1 + R_{VR}} \frac{1 + s C_1 (2 R_2 + R_{VR}) / [2(1 - K_2 R_{VR} / K_1)]}{1 + s C_1 (2 R_2 + R_{VR} - R_{VR}^2 / 2)} \right\},$$

where the C's, R's, and K's are defined in Fig. 9.

The calculations will be based on a unit vertical slice of the subassembly, which is one element wide, as shown in Fig. 9A. The length again will be taken as 70 cm, as for the row 9 calculation in Appendix A. Since the element discharges approximately half its heat to the hexagon side and half towards the subassembly interior, one-half the element helps to determine the hexagon temperature.

Then,

$$C_1/2 = \frac{\pi}{2} (1.25/2)^2 \times 70 \times 7.7 \times 0.115 = 38 \text{ cal}/^\circ\text{C},$$

$$R_1/2 = R_{\text{hex}}/2 + R_{\text{film}},$$

and

$$R_{\text{hex}}/2 = \frac{0.1/2}{0.048 \times 1.25 \times 70} = 0.012.$$

Assume  $r_{\text{film}} \approx 0.008$ . Then,

$$\frac{R_1}{2} \approx 0.012 + 0.008 = 0.020 \text{ } ^\circ\text{C/cal-sec}^{-1}$$

and

$$2R_2 = \frac{2 \log_e [1.25/(0.707 \times 1.25)]}{2\pi \times 0.048 \times 70} = 0.026^\circ\text{C/cal-sec}^{-1}.$$

From the row 9 calculation in Appendix A, one full element has  $R_{VR} = 0.083$ . The value for one-half element then is

$$R_{VR} = 2 \times 0.083 = 0.166^\circ\text{C/cal-sec}^{-1}.$$

The radial constants are considered to be lumped at the average axial condition, which is taken as approximately half the outlet condition.

Then,

$$\theta_{7Cin} = (168/2)(5/9) = 46.7^\circ\text{C} \quad (\text{see Ref. 1, Fig. 5})$$

and

$$Q(R_{VR}) = 46.7/0.166 = 281 \text{ cal/sec.}$$

The heat input per sodium channel in row 7 (six channels on the side of the subassembly in contact with row 6) is

$$Q_{in} = Q_{total}/6 \approx 3 \text{ kW} \times 238.9/6 \approx 119.4 \text{ cal/sec.}$$

where  $Q_{total}$  is the radial heat flow from row 6 to row 7 per subassembly.

Then,

$$Q_0 = K_2 \times 45 = Q(R_{VR}) - Q_{in}$$

and

$$K_2 = (281 - 119)/45 = 3.60 \text{ cal/MW-sec.}$$

Similarly, for a row 7 average half-element facing row 8,

$$\theta_{7Hexout} = (60/2)(5/9) = 16.7^\circ\text{C},$$

where  $60^\circ\text{F}$  is the average of the row 7 outer and row 8 inner channel temperatures of  $81$  and  $43^\circ\text{F}$ , respectively, explained in Ref. 1. Then,

$$Q_{00} = K_3 \times 45 = \frac{\theta_{7Hexout}}{R_{VR}} = 100 \text{ cal/sec}$$

and

$$K_3 = \frac{16.7}{0.166 \times 45} = 2.20 \text{ cal/MW-sec.}$$

(We may treat row 7 outer and row 8 inner channels separately because a check of heat flow between these points indicates a flow of about 14 cal/sec, which is small compared to the value of  $Q_{00}$  above and the value for row 8, which will be seen in Section 2 of this appendix.)

Also,

$$\theta_6 C = Q_{in} \times 2R_1 + \theta_7 C_{in} = K_1 P,$$

$$K_1 = \frac{119.4 \times 2 \times 0.04 + 46.7}{45} = 1.24,$$

and

$$\theta_6 C = \frac{1.24 P}{1 + 0.19 s},$$

where  $\tau_6 C = 0.19$  sec as in Appendix A, but with added transport time of 0.02 sec. To evaluate,

$$\frac{\theta_7 H_{\text{exit}}(s)}{P(s)} = \left\{ 1.24 - \frac{0.156(1 + 14.1s)}{1 + 6.3s} \right\} \frac{1}{1 + \tau_6 C s} = \frac{1.08(1 + 5.1s)}{(1 + 6.3s)(1 + 0.19s)}.$$

From Section III.B,

$$\frac{\theta_7 H_{\text{exit}}(s)}{P(s)} = \frac{K_3 R_{VR}}{1 + \frac{sC_1(R_{VR} + 2R_2)}{2}},$$

To evaluate,

$$\frac{\theta_7 H_{\text{exit}}(s)}{P(s)} = \frac{2.2 \times 0.166}{1 + 38s(0.166 + 0.026)} = \frac{0.365}{1 + 7.3s}.$$

Then,

$$\frac{\Delta T_7(s)}{P(s)} = \frac{1}{1 + 0.19s} \left\{ \frac{1.08(1 + 5.1s)}{1 + 6.3s} - \frac{0.365}{1 + 7.3s} \right\}$$

Rewriting results in

$$\frac{\Delta T_7(s)}{P(s)} = \frac{0.72}{1 + 0.19s} \cdot \frac{(1 + 5.8s)(1 + 9.7s)}{(1 + 6.3s)(1 + 7.3s)}.$$

Also, to a good approximation,

$$\frac{\Delta T_7(s)}{P(s)} = \frac{0.72(1 + 9.7s)}{(1 + 0.19s)(1 + 7.3s)}.$$

## 2. Reflector Subassembly; Row 8

The calculations for row 8 are made in the same way as for row 7, noting that the heat source for row 8 is row 9, but for row 7 the source is row 6, and also noting that the R's and C's are identical to those above for row 7.

As before, the average temperature between rows 7 and 8 is

$$\theta_{8\text{Hexin}} = (60/2)(5/9) = 16.7^\circ\text{C},$$

$$Q_{00} = K_6 \times 45 = \theta_{8\text{Hexin}}/R_{VR} = 100 \text{ cal/sec},$$

$$K_6 = 16.7/(45 \times 0.166) = 2.22 \text{ cal/MW-sec},$$

$$\theta_{8\text{Cout}} = (110/2)(5/9) = 30.6^\circ\text{C},$$

and

$$Q_{(VR)} = 30.6/0.166 = 184 \text{ cal/sec.}$$

The input per sodium channel in row 8 (six channels on side of subassembly in contact with row 9) is

$$Q_{in} = Q_{total}/6 \approx 3 \text{ kW} \times 238.9/6 \approx 119.4 \text{ cal/sec.}$$

Then,

$$Q_0 = K_5 P = Q_{(VR)} - Q_{in},$$

$$K_5 = (184 - 119)/45 = 1.44 \text{ cal/MW-sec},$$

$$\theta_{9C} = Q_{in} \times 2R_1 + \theta_{8\text{Cout}} = K_4 P,$$

and

$$K_4 = (119.4 \times 2 \times 0.04 + 30.6) / 45$$

$$= 0.89 \text{ cal/MW-sec.}$$

From Section III.B,

$$\frac{\theta_{8\text{Hexout}}(s)}{P(s)} = \frac{1}{1 + \tau_9 C s} \left\{ K_4 - \frac{1.5R_1(K_4 - K_5 R_{VR})}{2R_1 + R_{VR}} \frac{1 + sC_1(2R_2 + R_{VR})/[2(1 - K_5 R_{VR}/K_4)]}{1 + sC_1(2R_2 + R_{VR} - R_{VR}^2)/2} \right\}.$$

To evaluate,

$$\begin{aligned} \frac{\theta_{8\text{Hexout}}(s)}{P(s)} &= \frac{1}{1 + 6.2s} \left[ 0.89 - \frac{0.159(1 + 10.0s)}{1 + 6.3s} \right] \\ &= \frac{0.73(1 + 5.5s)}{(1 + 6.3s)(1 + 6.2s)} \approx \frac{0.73}{1 + 6.3s}. \end{aligned}$$

From Section III.B,

$$\frac{\theta_{8\text{Hexin}}(s)}{P(s)} = \frac{K_6 R_{VR}}{1 + \frac{sC_1(R_{VR} + 2R_2)}{2}} = \frac{2.22 \times 0.166}{1 + 38s(0.166 + 0.026)} = \frac{0.37}{1 + 7.3s}.$$

From Section III.B,

$$\begin{aligned} \frac{\Delta T_8(s)}{P(s)} &= \frac{\theta_{8\text{Hexin}}(s) - \theta_{8\text{Hexout}}(s)}{P(s)} = - \left( \frac{0.73}{1 + 6.3s} - \frac{0.37}{1 + 7.3s} \right) \\ &= - \frac{0.36(1 + 8.4s)}{(1 + 7.3s)(1 + 6.3s)}. \end{aligned}$$

The above results are in a form suitable for display in the log-log frequency domain. However, the time domain is more useful for computing temperature profiles with the PROFILE program. Therefore they are transformed into the time domain in Appendix D, which describes PROFILE.

APPENDIX D  
PROFILE Temperature Calculations

The computer program PROFILE calculates the row dynamic temperature-time function  $C(t)$  using a specified rod-drop reactor power-time function as the input. An input like that in Fig. D.1 may be represented by an initial ramp with an exponential following the end of the ramp. The Laplace transform of such an input has the form

$$\frac{\Delta P}{P}(s) = \frac{\left(\frac{\Delta P}{P}\right)_{t_0}}{s^2}, \quad t \leq t_0;$$

$$\frac{\Delta P}{P}(s) = \frac{\left(\frac{\Delta P}{P}\right)_{t_0}}{s^2} - \exp(-t_0 s) \left[ \frac{\left(\frac{\Delta P}{P}\right)_{t_0}}{s^2} - \frac{K}{\tau_K} \cdot \frac{1}{s(s + \frac{1}{\tau_K})} \right], \quad t > t_0.$$

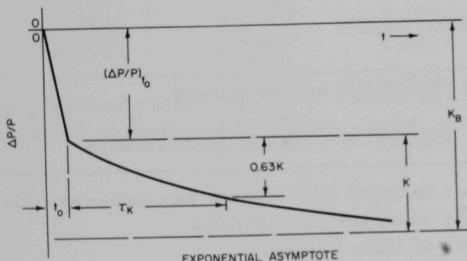


Fig. D.1  
PROFILE Input Function

The function  $C(t)$  resulting when the above input is applied to a row transfer function will have two basic forms as shown in Section III.C. Slightly rearranged, these forms are

$$1. \quad C(t) = C_0 [t - \sigma_1 + \sigma_1 \exp(-t/\sigma_1)], \quad t \leq t_0;$$

$$C(t) = K_B + C_0 \sigma_1 [\exp(-t/\sigma_1) - \exp(-t'/\sigma_1)]$$

$$+ K \frac{\tau_K \exp(-t'/\tau_K) - \sigma_1 \exp(-t'/\sigma_1)}{\sigma_1 - \tau_K}, \quad t > t_0$$

$$2. \quad C(t) = C_0 \left[ t - \sigma_1 - \sigma_2 + \sigma_3 + \frac{\sigma_1(\sigma_1 - \sigma_3) \exp(-t/\sigma_1) - \sigma_2(\sigma_2 - \sigma_3) \exp(-t/\sigma_2)}{\sigma_1 - \sigma_2} \right],$$

$t \leq t_0$

$$C(t) = K_B + C_0 \frac{\sigma_1(\sigma_1 - \sigma_3)[\exp(-t/\sigma_1) - \exp(-t'/\sigma_1)] - \sigma_2(\sigma_2 - \sigma_3)[\exp(-t/\sigma_2) - \exp(-t'/\sigma_2)]}{\sigma_1 - \sigma_2}$$

$$+ K \left[ \frac{\sigma_1(\sigma_3 - \sigma_1)}{(\sigma_1 - \sigma_2)(\sigma_1 - \tau_K)} \exp(-t'/\sigma_1) + \frac{\sigma_2(\sigma_3 - \sigma_2)}{(\sigma_2 - \sigma_1)(\sigma_2 - \tau_K)} \exp(-t'/\sigma_2) \right.$$

$$\left. + \frac{\tau_K(\sigma_3 - \tau_K)}{(\tau_K - \sigma_1)(\tau_K - \sigma_2)} \exp(-t'/\tau_K) \right], \quad t > t_0.$$

Note that  $t' = t - t_0$  in the above expressions. Also, the Type 2 row transfer function was

$$F(s) = \frac{1 + \sigma_3 s}{(1 + \sigma_1 s)(1 + \sigma_2 s)}.$$

The program then calculates temperature values for specified times and punches decks of cards for use with BOW III. Thus

$$T_{\Delta}(t) = (P/P_0)[1 + C(t)] T_{\Delta}(0).$$

Table V defines the PROFILE symbols used.

TABLE V. PROFILE FORTRAN Quantities

---

MI	Number of axial node points per subassembly
MJ	Number of subassembly rows
LT	Number of time values
T(I)	Time values, t
TO	$t_0$ , time duration of input ramp
CO	$C_0$ , slope of input ramp
AK	K, asymptotic value of input exponential
TK	$\tau_K$ , time constant of input exponential
P	P, starting power
PO	$P_0$ , base power, = 45 MW
DPP	$(\Delta P/P)_{t_0}$ , end value of ramp
NT(I)	Function-type, row I
S(I,J)	$\sigma_1, \sigma_2, \sigma_3$ , row I time constants (see F(s) above)
DT(I,J)	Temperature difference across node I of row J for 45-MW equilibrium conditions, $T_{\Delta}(0)$

---

The following pages list the FORTRAN for PROFILE and the output for a typical run, in this case, the 41.4-MW rod drop made during reactor run 26B. The input quantities used appear in the INPUT REVIEW that follows the FORTRAN. Table VI gives  $C(t)$  values for rows 6-10, normalized to a base whose initial value is 1.0.

TABLE VI.  $C(t)^a$  for Rows 6-10

Time	Row				
	6	7	8	9	10
0	0	0	0	0	0
0.1	0.4138	0.5492	0.0165	0.0149	0.0060
0.2	1.4194	1.8815	0.0656	0.0594	0.0239
0.4	3.2019	4.2257	0.2160	0.1965	0.0845
0.6	3.9126	5.1388	0.3587	0.3262	0.1383
0.8	4.2439	5.5443	0.5010	0.4559	0.1931
1.0	4.4415	5.7708	0.6429	0.5854	0.2488
2.0	5.0862	6.4428	1.3436	1.2296	0.5397
3.0	5.6492	7.0049	2.0263	1.8635	0.8485
4.0	6.1709	7.5132	2.6865	2.4826	1.1171
5.0	6.6546	7.9735	3.3213	3.0831	1.5048
6.0	7.1029	8.3907	3.9286	3.6625	1.8462
7.0	7.5186	8.7690	4.5073	4.2189	2.1929
8.0	7.9039	9.1126	5.0566	4.7511	2.5425
9.0	8.2611	9.4247	5.5765	5.2585	2.8931
10.0	8.5923	9.7086	6.0672	5.7407	3.2430

<sup>a</sup>Multiply tabulated values by  $10^{-2}$ . Values are negative and represent the time variation normalized to a base whose initial value is 1.0.

```

*      PROGRAM PROFILE
      DIMENSION S(3,15),T(20),NT(15),C(15),DT(10,15),DT1(10,15)
      PAUSE
      READ 100,MI,MJ,LT
100   FORMAT(12I6)
      READ 110,(T(I),I=1,LT)
110   FORMAT(6E12.5)
      READ 130,TO,CO,AK,TK,P,P0,DPP
      AKB=(DPP+AK)
      DO 1 I=1,MJ
1     READ 120,NT(I),(S(J,I),J=1,3)
120   FORMAT(16,3E12.6)
      READ 130,((DT(I,J),I=1,MI),J=1,MJ)
130   FORMAT(8E10.4)
      PRINT 200
140   FORMAT(13H1INPUT REVIEW//6X,1HP13X,2HT012X,2HC012X,1HK11X,
1       1 6HTAU(K))
      PRINT 201,P,TO,CO,AK,TK
201   FORMAT(1X,5(E12.6,2X))
      PRINT 202
202   FORMAT(//7H NUMBER2X,4HTYPE6X,2HS112X,2HS212X,2HS3/)
      PRINT 203,(I,NT(I),(S(J,I),J=1,3),I=1,MJ)
203   FORMAT(15,I7.3(2X,E12.6))
      PRINT 204
204   FORMAT(/28H1INITIAL TEMPERATURE PROFILE//)
      PRINT 205,((DT(I,J),I=1,MI),J=1,MJ)
205   FORMAT(10(1X,E11.5))
      DO 2 I=1,LT
      T1=T(I)
      T2=T1-T0
      DO 3 J=1,MJ
      E11=EXP(-T1/S(1,J))
      E12=EXP(-T2/S(1,J))
      E21=EXP(-T1/S(2,J))
      E22=EXP(-T2/S(2,J))
      IF(T2) 50,50,52
50    G=0,
      E=0,
      F0=T1-S(1,J)-S(2,J)+S(3,4)
      F1=S(1,J)*E11
      IF(NT(J)=1) 55,55,51
51    F1=(F1*(S(1,J)-S(3,J))-S(2,J)*(S(2,J)-S(3,J))*E21)/(S(1,J)-S(2,J))
      GO TO 55
52    F0=0,
      B=AKB
      F1=S(1,J)*(E11-E12)
      IF(NT(J)=1) 53,53,54
53    G=(TK*EXP(-T2/TK)-S(1,J)*E12)/(S(1,J)-TK)
      GO TO 55
54    F1=(F1*(S(1,J)-S(3,J))-S(2,J)*(S(2,J)-S(3,J))*E21+E22)/
1     ((S(1,J)-S(2,J))
1     G=S(1,J)*(S(3,J)-S(1,J))*E12/((S(1,J)-S(2,J))*(S(1,J)-TK))
1     +S(2,J)*(S(3,J)-S(2,J))*E22/((S(2,J)-S(1,J))*(S(2,J)-TK))
2     +TK*(S(3,J)-TK)*EXP(-T2/TK)/((TK-S(1,J))*(TK-S(2,J)))
55    C(J)=E+(C0*(F0+F1)+AK*B)
      DO 3 K=1,MI
3     DT1(K,J)=DT(K,J)*P*(1.+C(J))/P0
      PRINT 210,T1
210   FORMAT(6H1TIME=F7.2//)
      PUNCH 215,T1
215   FORMAT(9H*** TIME=F7.2)
      PRINT 205,((DT1(K,J),K=1,MI),J=1,MJ)
      PUNCH 130,((DT1(K,J),K=1,MI),J=1,MJ)
2     CONTINUE
      END

```

## MEMORY MAP

## INTEGER VARIABLES

IDENT	LEVEL	OBJECT CODE	LOCATION	UP SUBROUTINE
K	1	1	5244	1 2400
J	1	1	5470	1 2406
I	1	1	5526	1 2426
LT	1	1	5533	NOT USED
MJ	1	1	5535	NOT USED
MI	1	1	5537	NOT USED
IO	0	1	7775	1 2442

## FLOATING POINT VARIABLES

IDENT	LEVEL	OBJECT CODE	LOCATION
F1	1	1	5246
F0	1	1	5251
E	1	1	5254
G	1	1	5262
E22	1	1	5265
E21	1	1	5272
E12	1	1	5275
E11	1	1	5300
T2	1	1	5303
T1	1	1	5306
AKB	1	1	5472
DPP	1	1	5475
P0	1	1	5500
P	1	1	5503
TK	1	1	5506
AK	1	1	5511
CO	1	1	5514
TO	1	1	5517

## INTEGER ARRAYS

IDENT	LEVEL	OBJECT CODE	LOCATION	DIMENSION	DIM1	DIM2
NT	1	1	7422		1	

## FLOATING POINT ARRAYS

IDENT	LEVEL	OBJECT CODE	LOCATION	DIMENSION	DIM1	DIM2
DT1	1	1	5541		2	10
DT	1	1	6443		2	10
C	1	1	7345		1	
T	1	1	7460		1	
S	1	1	7554		2	3

## CONSTANTS

VALUE	OBJECT CODE	LOCATION
-------	-------------	----------

0.1000000 E 01	1	5241
0.0	1	5257
2	1	5270
10	1	7763
20	1	7765
15	1	7767
3	1	7771
1	1	7773

## STATEMENT NUMBERS

## IDENT LEVEL OBJECT CODE LOCATION

54	1	1 1657
53	1	1 1627
51	1	1 1535
55	1	1 2027
52	1	1 1572
50	1	1 1466
3	1	1 2066
2	1	1 2312
1	1	1 0775
0	1	1 0650

## FORMAT STATEMENTS

## IDENT LEVEL OBJECT CODE LOCATION

215	1	1 5220
210	1	1 5231
205	1	1 5311
204	1	1 5320
203	1	1 5342
202	1	1 5354
201	1	1 5403
200	1	1 5413
120	1	1 5462
130	1	1 5456
110	1	1 5522
100	1	1 5530

## LIBRARY FUNCTIONS

## IDENT LEVEL OBJECT CODE LOCATION

(P5230		0 6740
(16120		0 7150
(R405I		0 7230
INPUT		1 0001
EXPF		1 0505

ERASABLE STORAGE 1 2453 TO 1 5220

## INPUT REVIEW

P	T0	C0	K	TAU(K)
.414000E 02	.220000E 00	-.186000E 00	-.870000E-01	,132000E 02

## NUMBER TYPE S1 S2 S3

1	1	,190000E 00	.000000E 00	,000000E 00
2	1	,190000E 00	.000000E 00	,000000E 00
3	1	,190000E 00	.000000E 00	,000000E 00
4	1	,190000E 00	.000000E 00	,000000E 00
5	1	,190000E 00	.000000E 00	,000000E 00
6	1	,190000E 00	.000000E 00	,000000E 00
7	3	,190000E 00	.730000E 01	,970000E 01
8	3	,630000E 01	.730000E 01	,820000E 01
9	1	,620000E 01	.000000E 00	,000000E 00
10	1	,155000E 02	.000000E 00	,000000E 00
11	1	,155000E 02	.000000E 00	,000000E 00
12	1	,155000E 02	.000000E 00	,000000E 00
13	1	,155000E 02	.000000E 00	,000000E 00
14	1	,155000E 02	.000000E 00	,000000E 00
15	1	,155000E 02	.000000E 00	,000000E 00

## INITIAL TEMPERATURE PROFILE

5      6      7      8      9      10

```

.00000E 00 .00000E 00
.00000E 00 .00000E 00 .00000E 00 .00000E 00 .00000E 00 .00000E 01 .23000E 02 .17000E 02 .00000E 00 .00000E 00 .00000E 00 .00000E 00
.00000E 00 .00000E 00 .00000E 00 .00000E 00 .00000E 00 .10000E 02 .25000E 02 .19000E 02 .00000E 00 .00000E 00 .00000E 00 .00000E 00
.00000E 00 .00000E 00 .00000E 00 .00000E 00 .00000E 00 .12000E 02 .29000E 02 .22000E 02 .00000E 00 .00000E 00 .00000E 00 .00000E 00
.00000E 00 .00000E 00 .00000E 00 .00000E 00 .00000E 00 .12000E 02 .29000E 02 .22000E 02 .00000E 00 .00000E 00 .00000E 00 .00000E 00
.00000E 00 .00000E 00 .00000E 00 .00000E 00 .00000E 00 .10000E 02 .24000E 02 .18000E 02 .00000E 00 .00000E 00 .00000E 00 .00000E 00
.00000E 00 .00000E 00 .00000E 00 .00000E 00 .00000E 00 .40000E 01 .20000E 02 .48000E 02 .74000E 02 .90000E 02 .92000E 02 .95000E 02
.00000E 00 .00000E 00 .00000E 00 .00000E 00 .00000E 00 .-15000E 02 .-35000E 02 .-53000E 02 .-66000E 02 .-66000E 02 .-66000E 02
.00000E 00 .00000E 00 .30000E 01 .90000E 01 .10000E 02 .70000E 01 .-30000E 01 .-14000E 02 .-18000E 02 .-76000E 02 .-78000E 02
.00000E 00 .00000E 00 .40000E 01 .90000E 01 .30000E 02 .58000E 02 .72000E 02 .74000E 02 .52000E 02 .45000E 02 .38000E 02 .32000E 02
.00000E 00 .00000E 00 .30000E 01 .50000E 01 .20000E 02 .44000E 02 .52000E 02 .23000E 02 .20000E 02 .18000E 02
.00000E 00 .00000E 00 .00000E 00 .00000E 00 .00000E 01 .20000E 02 .25000E 02 .00000E 00 .00000E 00 .00000E 00 .00000E 00
.00000E 00 .00000E 00 .00000E 00 .00000E 00 .00000E 00 .00000E 00 .00000E 00 .00000E 00 .00000E 00 .00000E 00 .00000E 00 .00000E 00
.00000E 00 .00000E 00 .00000E 00 .00000E 00 .00000E 00 .00000E 00 .00000E 00 .00000E 00 .00000E 00 .00000E 00 .00000E 00 .00000E 00
.00000E 00 .00000E 00 .00000E 00 .00000E 00 .00000E 00 .00000E 00 .00000E 00 .00000E 00 .00000E 00 .00000E 00 .00000E 00 .00000E 00

```

TIME= .00

```

.00000E 00 .00000E 00
.00000E 00 .00000E 00 .00000E 00 .00000E 00 .00000E 00 .82800E 01 .21560E 02 .15640E 02 .00000E 00 .00000E 00 .00000E 00 .00000E 00
.00000E 00 .00000E 00 .00000E 00 .00000E 00 .00000E 00 .92000E 01 .22999E 02 .17480E 02 .00000E 00 .00000E 00 .00000E 00 .00000E 00
.00000E 00 .00000E 00 .00000E 00 .00000E 00 .00000E 00 .11040E 02 .26679E 02 .20240E 02 .00000E 00 .00000E 00 .00000E 00 .00000E 00
.00000E 00 .00000E 00 .00000E 00 .00000E 00 .00000E 00 .11040E 02 .26679E 02 .20240E 02 .00000E 00 .00000E 00 .00000E 00 .00000E 00
.00000E 00 .00000E 00 .00000E 00 .00000E 00 .00000E 00 .92000E 01 .22080E 02 .16560E 02 .00000E 00 .00000E 00 .00000E 00 .00000E 00
.00000E 00 .00000E 00 .00000E 00 .00000E 00 .00000E 00 .36799E 01 .44159E 02 .68080E 02 .82799E 02 .84639E 02 .87399E 02
.00000E 00 .00000E 00 .00000E 00 .00000E 00 .00000E 00 .-13800E 02 .-32200E 02 .-48760E 02 .-60720E 02 .-60720E 02 .-60720E 02
.00000E 00 .00000E 00 .27600E 01 .82800E 01 .92000E 01 .64400E 01 .27600E 01 .-12880E 02 .-16560E 02 .-16560E 02 .-16560E 02
.00000E 00 .00000E 00 .36800E 01 .82800E 01 .27600E 02 .53340E 02 .66240E 02 .68080E 02 .69920E 02 .71760E 02
.00000E 00 .00000E 00 .27600E 01 .46000E 01 .18400E 02 .40480E 02 .47840E 02 .41400E 02 .34960E 02 .29440E 02
.00000E 00 .00000E 00 .00000E 00 .00000E 00 .00000E 00 .73600E 01 .18400E 02 .22999E 02 .21160E 02 .18400E 02 .16560E 02
.00000E 00 .00000E 00
.00000E 00 .00000E 00 .00000E 00 .00000E 00 .00000E 00 .00000E 00 .00000E 00 .00000E 00 .00000E 00 .00000E 00 .00000E 00

```

TIME= .10

```

.00000E 00 .00000E 00
.00000E 00 .00000E 00 .00000E 00 .00000E 00 .00000E 00 .82457E 01 .21072E 02 .15575E 02 .00000E 00 .00000E 00 .00000E 00 .00000E 00
.00000E 00 .00000E 00 .00000E 00 .00000E 00 .00000E 00 .91619E 01 .22904E 02 .17407E 02 .00000E 00 .00000E 00 .00000E 00 .00000E 00
.00000E 00 .00000E 00 .00000E 00 .00000E 00 .00000E 00 .10994E 02 .26569E 02 .20156E 02 .00000E 00 .00000E 00 .00000E 00 .00000E 00
.00000E 00 .00000E 00 .00000E 00 .00000E 00 .00000E 00 .10994E 02 .26569E 02 .20156E 02 .00000E 00 .00000E 00 .00000E 00 .00000E 00
.00000E 00 .00000E 00 .00000E 00 .00000E 00 .00000E 00 .91619E 01 .21988E 02 .16491E 02 .00000E 00 .00000E 00 .00000E 00 .00000E 00
.00000E 00 .00000E 00 .00000E 00 .00000E 00 .00000E 00 .36597E 01 .18298E 02 .43917E 02 .67706E 02 .82345E 02 .84175E 02 .86919E 02
.00000E 00 .00000E 00 .00000E 00 .00000E 00 .00000E 00 .-13797E 02 .-32194E 02 .-48751E 02 .-60709E 02 .-60709E 02 .-60709E 02
.00000E 00 .00000E 00 .27595E 01 .82878E 01 .91986E 01 .64390E 01 .-27595E 01 .-12878E 02 .-16557E 02 .-16557E 02 .-16557E 02
.00000E 00 .00000E 00 .27598E 01 .45997E 01 .18398E 02 .40477E 02 .47837E 02 .41397E 02 .34957E 02 .29438E 02
.00000E 00 .00000E 00 .00000E 00 .00000E 00 .00000E 00 .73595E 01 .18398E 02 .22998E 02 .21158E 02 .18398E 02 .16559E 02
.00000E 00 .00000E 00
.00000E 00 .00000E 00 .00000E 00 .00000E 00 .00000E 00 .00000E 00 .00000E 00 .00000E 00 .00000E 00 .00000E 00 .00000E 00

```

TIME = .20

```

.00000E 00 .00000E 00 .00000E 00 ,00000E 00
.00000E 00 .00000E 00 .00000E 00 ,00000E 00 ,81624E 01 ,20859E 02 ,15418E 02 ,00000E 00 ,00000E 00 ,00000E 00 ,00000E 00
.00000E 00 .00000E 00 .00000E 00 ,00000E 00 ,90694E 01 ,22673E 02 ,17231E 02 ,00000E 00 ,00000E 00 ,00000E 00 ,00000E 00
.00000E 00 .00000E 00 .00000E 00 ,00000E 00 ,10883E 02 ,26301E 02 ,19952E 02 ,00000E 00 ,00000E 00 ,00000E 00 ,00000E 00
.00000E 00 .00000E 00 .00000E 00 ,00000E 00 ,10883E 02 ,26301E 02 ,19952E 02 ,00000E 00 ,00000E 00 ,00000E 00 ,00000E 00
.00000E 00 .00000E 00 .00000E 00 ,00000E 00 ,90694E 01 ,21766E 02 ,16324E 02 ,00000E 00 ,00000E 00 ,00000E 00 ,00000E 00
.00000E 00 .00000E 00 .00000E 00 ,00000E 00 ,36107E 01 ,18053E 02 ,43329E 02 ,66799E 02 ,81242E 02 ,83047E 02 ,85755E 02
.00000E 00 .00000E 00 .00000E 00 ,00000E 00 ,13790E 02 ,32178E 02 ,48728E 02 ,60680E 02 ,60680E 02 ,60680E 02 ,60680E 02
.00000E 00 .00000E 00 ,27583E 01 ,82750E 01 ,91945E 01 ,64361E 01 ,27583E 01 ,12872E 02 ,16550E 02 ,16550E 02 ,16550E 02 ,16550E 02
.00000E 00 .00000E 00 ,36791E 01 ,82787E 01 ,27593E 01 ,53347E 02 ,66224E 02 ,68063E 02 ,69903E 02 ,71742E 02 ,71742E 02 ,71742E 02
.00000E 00 .00000E 00 ,27593E 01 ,45989E 01 ,18395E 02 ,40470E 02 ,47828E 02 ,41390E 02 ,34951E 02 ,29432E 02 ,29432E 02 ,29432E 02
.00000E 00 .00000E 00 .00000E 00 ,00000E 00 ,73582E 01 ,18395E 02 ,22994E 02 ,21154E 02 ,18395E 02 ,16556E 02 ,16556E 02 ,16556E 02
.00000E 00 .00000E 00 .00000E 00 ,00000E 00
.00000E 00 .00000E 00 .00000E 00 ,00000E 00

```

TIME\*, , 40

TIME = , 60

TIME= .80

,00000E 00  
.00000E 00 ,00000E 00 ,00000E 00 ,00000E 00 ,00000E 00 ,79286E 01 ,20261E 02 ,14976E 02 ,00000E 00 ,00000E 00 ,00000E 00  
.00000E 00 ,00000E 00 ,00000E 00 ,00000E 00 ,00000E 00 ,88095E 01 ,22023E 02 ,16738E 02 ,00000E 00 ,00000E 00 ,00000E 00  
.00000E 00 ,00000E 00 ,00000E 00 ,00000E 00 ,00000E 00 ,10571E 02 ,25547E 02 ,19381E 02 ,00000E 00 ,00000E 00 ,00000E 00  
.00000E 00 ,00000E 00 ,00000E 00 ,00000E 00 ,00000E 00 ,10571E 02 ,25547E 02 ,19381E 02 ,00000E 00 ,00000E 00 ,00000E 00  
.00000E 00 ,00000E 00 ,00000E 00 ,00000E 00 ,00000E 00 ,88095E 01 ,21142E 02 ,15857E 02 ,00000E 00 ,00000E 00 ,00000E 00  
.00000E 00 ,00000E 00 ,00000E 00 ,00000E 00 ,00000E 00 ,34759E 01 ,17379E 02 ,41711E 02 ,64305E 02 ,78209E 02 ,79947E 02 ,82554E 02  
.00000E 00 ,00000E 00 ,00000E 00 ,00000E 00 ,00000E 00 ,13733E 02 ,32038E 02 ,48515E 02 ,60415E 02 ,60415E 02 ,60415E 02 ,60415E 02  
.00000E 00 ,00000E 00 ,00000E 00 ,00000E 00 ,00000E 00 ,27474E 01 ,82422E 01 ,91580E 01 ,64106E 01 ,27474E 01 ,12821E 02 ,16484E 02 ,16484E 02  
.00000E 00 ,00000E 00 ,00000E 00 ,00000E 00 ,00000E 00 ,36728E 01 ,82640E 01 ,27546E 02 ,53256E 02 ,66112E 02 ,67948E 02 ,69784E 02 ,71621E 02  
.00000E 00 ,00000E 00 ,00000E 00 ,00000E 00 ,00000E 00 ,27546E 01 ,45911E 01 ,18364E 02 ,40401E 02 ,47747E 02 ,41320E 02 ,34892E 02 ,29383E 02  
.00000E 00 ,00000E 00 ,00000E 00 ,00000E 00 ,00000E 00 ,73457E 01 ,18364E 02 ,22955E 02 ,21119E 02 ,18364E 02 ,18364E 02 ,16528E 02  
.00000E 00 ,00000E 00  
.00000E 00 ,00000E 00  
.00000E 00 ,00000E 00

TIME= 1.00

,00000E 00  
.00000E 00 ,00000E 00 ,00000E 00 ,00000E 00 ,00000E 00 ,79122E 01 ,20220E 02 ,14945E 02 ,00000E 00 ,00000E 00 ,00000E 00  
.00000E 00 ,00000E 00 ,00000E 00 ,00000E 00 ,00000E 00 ,87913E 01 ,21978E 02 ,16703E 02 ,00000E 00 ,00000E 00 ,00000E 00  
.00000E 00 ,00000E 00 ,00000E 00 ,00000E 00 ,00000E 00 ,10549E 02 ,25494E 02 ,19341E 02 ,00000E 00 ,00000E 00 ,00000E 00  
.00000E 00 ,00000E 00 ,00000E 00 ,00000E 00 ,00000E 00 ,10549E 02 ,25494E 02 ,19341E 02 ,00000E 00 ,00000E 00 ,00000E 00  
.00000E 00 ,00000E 00 ,00000E 00 ,00000E 00 ,00000E 00 ,87913E 01 ,21099E 02 ,15824E 02 ,00000E 00 ,00000E 00 ,00000E 00  
.00000E 00 ,00000E 00 ,00000E 00 ,00000E 00 ,00000E 00 ,34674E 01 ,17338E 02 ,41611E 02 ,64151E 02 ,78021E 02 ,79755E 02 ,82356E 02  
.00000E 00 ,00000E 00 ,00000E 00 ,00000E 00 ,00000E 00 ,13711E 02 ,31992E 02 ,48446E 02 ,630329E 02 ,630329E 02 ,630329E 02 ,630329E 02  
.00000E 00 ,00000E 00 ,00000E 00 ,00000E 00 ,00000E 00 ,27438E 01 ,82315E 01 ,91461E 01 ,64022E 01 ,27438E 01 ,12804E 02 ,16463E 02 ,16463E 02  
.00000E 00 ,00000E 00 ,00000E 00 ,00000E 00 ,00000E 00 ,36708E 01 ,82594E 01 ,27531E 02 ,53227E 02 ,66075E 02 ,67910E 02 ,69746E 02 ,71581E 02  
.00000E 00 ,00000E 00 ,00000E 00 ,00000E 00 ,00000E 00 ,27531E 01 ,45885E 01 ,18354E 02 ,40379E 02 ,47720E 02 ,41297E 02 ,34873E 02 ,29366E 02  
.00000E 00 ,00000E 00 ,00000E 00 ,00000E 00 ,00000E 00 ,73416E 01 ,18354E 02 ,22942E 02 ,21107E 02 ,18354E 02 ,16518E 02  
.00000E 00 ,00000E 00  
.00000E 00 ,00000E 00

TIME= 2.00

,00000E 00  
.00000E 00 ,00000E 00 ,00000E 00 ,00000E 00 ,00000E 00 ,78588E 01 ,20083E 02 ,14844E 02 ,00000E 00 ,00000E 00 ,00000E 00  
.00000E 00 ,00000E 00 ,00000E 00 ,00000E 00 ,00000E 00 ,87320E 01 ,21830E 02 ,16590E 02 ,00000E 00 ,00000E 00 ,00000E 00  
.00000E 00 ,00000E 00 ,00000E 00 ,00000E 00 ,00000E 00 ,10478E 02 ,25322E 02 ,19210E 02 ,00000E 00 ,00000E 00 ,00000E 00  
.00000E 00 ,00000E 00 ,00000E 00 ,00000E 00 ,00000E 00 ,10478E 02 ,25322E 02 ,19210E 02 ,00000E 00 ,00000E 00 ,00000E 00  
.00000E 00 ,00000E 00 ,00000E 00 ,00000E 00 ,00000E 00 ,87320E 01 ,20956E 02 ,15717E 02 ,00000E 00 ,00000E 00 ,00000E 00  
.00000E 00 ,00000E 00 ,00000E 00 ,00000E 00 ,00000E 00 ,34429E 01 ,17214E 02 ,41314E 02 ,63693E 02 ,77465E 02 ,79186E 02 ,81768E 02  
.00000E 00 ,00000E 00 ,00000E 00 ,00000E 00 ,00000E 00 ,13614E 02 ,31767E 02 ,48104E 02 ,59904E 02 ,59904E 02 ,59904E 02 ,59904E 02  
.00000E 00 ,00000E 00 ,00000E 00 ,00000E 00 ,00000E 00 ,27260E 01 ,81781E 01 ,90868E 01 ,63608E 01 ,27260E 01 ,12721E 02 ,16356E 02 ,16356E 02  
.00000E 00 ,00000E 00 ,00000E 00 ,00000E 00 ,00000E 00 ,36616E 01 ,82355E 01 ,27451E 02 ,53072E 02 ,65882E 02 ,67712E 02 ,69542E 02 ,71372E 02  
.00000E 00 ,00000E 00 ,00000E 00 ,00000E 00 ,00000E 00 ,27451E 01 ,45751E 01 ,18300E 02 ,40261E 02 ,47581E 02 ,41176E 02 ,34771E 02 ,29281E 02  
.00000E 00 ,00000E 00 ,00000E 00 ,00000E 00 ,00000E 00 ,73202E 01 ,18300E 02 ,22875E 02 ,21045E 02 ,18300E 02 ,16470E 02  
.00000E 00 ,00000E 00  
.00000E 00 ,00000E 00

TIME = 3.00

TIME = 4,00

TIME = 5.00

TIME: 6:00

TIME: 7.00

TIME = 8,00

TIME = 9.00

TIME = 10.00

APPENDIX E  
DYNAMIC Reactivity Calculations

The computer program DYNAMIC calculates the reactivity time function  $C(t)$  of each component on Fig. 12 with up to two denominator roots in the transfer function of the component and using a specified rod-drop reactor power-time function as the input. An input like that in Fig. D.1, which was used in Appendix D, is also used here. The function  $C(t)$  resulting when the Laplace-transformed input is applied to the component transfer function has two basic forms depending upon whether there are one or two denominator roots in the transfer function. These forms are:

Form 1

$$C(t) = PCC_0[t - \sigma_1 + \sigma_1 \exp(-t/\sigma_1)], \quad t < t_0;$$

$$C(t) = PC \left\{ C_0 + \sigma_1 [\exp(-t/\sigma_1) - \exp(-t'/\sigma_1)] + K \left[ 1 + \frac{\tau_K \exp(-t'/\tau_K) - \sigma_1 \exp(-t'/\sigma_1)}{\sigma_1 - \tau_K} \right] \right\}, \quad t \geq t_0.$$

Form 2

$$C(t) = PCC_0 \left( t - \sigma_1 - \sigma_2 + \frac{\sigma_2^2 \exp(-t/\sigma_2) - \sigma_1^2 \exp(-t/\sigma_1)}{\sigma_2 - \sigma_1} \right), \quad t < t_0;$$

$$C(t) = PC \left\{ C_0 \left[ t_0 + \frac{\sigma_2^2 [\exp(-t/\sigma_2) - \exp(-t'/\sigma_2)] - \sigma_1^2 [\exp(-t/\sigma_1) - \exp(-t'/\sigma_1)]}{\sigma_2 - \sigma_1} \right] + K \left[ 1 - \frac{\tau_K^2 \exp(-t'/\tau_K)}{(\tau_K - \sigma_1)(\tau_K - \sigma_2)} - \frac{\sigma_1^2 \exp(-t'/\sigma_1)}{(\sigma_1 - \sigma_2)(\sigma_1 - \tau_K)} - \frac{\sigma_2^2 \exp(-t'/\sigma_2)}{(\sigma_1 - \sigma_2)(\sigma_2 - \tau_K)} \right] \right\}, \quad t \geq t_0.$$

Note that  $t' = t - t_0$  in the above expressions.

Table VII lists DYNAMIC FORTRAN quantities.

TABLE VII. DYNAMIC FORTRAN Quantities

NC	Number of components to be evaluated	AK	K, asymptotic value of input exponential
NS	Number of component subtotals to be calculated	TK	$\tau_K$ , time constant of input exponential
LT	Number of time values	P	P, starting power
NS1(I)	Initial number of components in subtotal I	BCDU,I	18-character BCD identifier for component I
NS2(I)	Final number of components in subtotal I	NTI(I)	Function type for component I
T(I)	Time values	SU,I	$\sigma_1, \sigma_2$ component I time constants
TO	$t_0$ , time duration of input ramp	CII	C component I multiplier in \$/MW
CO	$C_0$ , slope of input ramp		

The following pages list the FORTRAN for DYNAMIC and the output for a typical run, in this case the 41.4-MW rod drop made during reactor run 26B. The input quantities used appear in the INPUT REVIEW which follows the FORTRAN. The various outputs in dollars versus time are plotted in Fig. 13.

```

* PROGRAM DYNAMIC
  DIMENSION S(2,10),T(20),SUM(20),BCD(3,10),NS1(5),NS2(5),NT(10),
  C(10),DK(10)
  READ 100,NC,NS,LT,(NS1(I),NS2(I),I=1,NS)
100  FORMAT(12I6)
      READ 110,(T(I),I=1,LT)
      READ 110,T0,C0,AK,TK,P
110  FORMAT(6E12.5)
      DO 1 I=1,NC
1     READ 120,(BCD(J,I),J=1,3),NT(I),(S(J,I),J=1,2),C(I)
120  FORMAT(3A6,I6,3E12.6)
      PRINT 200
200  FORMAT(13H1INPUT REVIEW//6X,1HP13X,2HT012X,2HC012X,1HK11X,
1 6HTAU(K))
      PRINT 201,P,T0,C0,AK,TK
201  FORMAT(1X,5(E12.6,2X))
      PRINT 202
202  FORMAT(//H NUMBER7X,5HTITLE8X,4HTYPE6X,2HS110X,2WS215X,2HC /)
      PRINT 203,(I,(BCD(J,I),J=1,3),NT(I),(S(J,I),J=1,2),C(I),I=1,NC)
203  FORMAT(3X,I2,3X,3A6,2X,I2,2(2X,E12.6),5X,E12.6)
      DO 2 I=1,LT
      T1=T(I)
      T2=T1-T0
      SUM(I)=0.
      DO 3 J=1,NC
      E11=EXP(-T1/S(1,J))
      E12=EXP(-T2/S(1,J))
      E21=EXP(-T1/S(2,J))
      E22=EXP(-T2/S(2,J))
      IF(T2) 50,50,52
      G=0.
      F0=T1-S(1,J)-S(2,J)
      F1=S(1,J)*E11
      IF(NT(J)>1) 55,55,51
51    F1=(-S(1,J)*F1+S(2,J)**2*E21)/(S(2,J)-S(1,J))
      GO TO 55
52    F0=T0
      F1=S(1,J)*(E11-E12)
      IF(NT(J)-1) 53,53,54
53    G=1.,(TK*EXP(-T2/TK)-S(1,J)*E12)/(S(1,J)-TK)
      GO TO 55
54    F1=(-S(1,J)*F1+S(2,J)**2*(E21-E22))/(S(2,J)-S(1,J))
      G=1.,-TK**2*EXP(-T2/TK)/((TK-S(1,J))*(TK-S(2,J)))
1   -S(1,J)**2*E12/((S(1,J)-S(2,J))*(S(1,J)-TK)) -S(2,J)**2*E22/
2   ((S(2,J)-S(1,J))*(S(2,J)-TK))
55    DK(J)=C(J)*(C0*(F0+F1)+AK*G)*P
      SUM(I)=SUM(I)+DK(J)
      PRINT 210,T1
210  FORMAT(6H1TIME=F7.2//)
      PRINT 220,(J,(BCD(K,J),K=1,3),DK(J),J=1,NC)
220  FORMAT(14H COMPONENT NO.I2,5X,3A6,E12.6,8H DOLLARS)
      PRINT 230,SUM(I)
230  FORMAT(/15X,15HCOMBINED EFFECT5X,E12.6,8H DOLLARS)
      IF(NS) 2,2,56
      PRINT 240
240  FORMAT(//10H SUBTOTALS/)
      DO 4 J=1,NS
      N1=NS1(J)
      N2=NS2(J)
      SM=0.
      DO 5 K=N1,N2
5     SM=SM+DK(K)
4     PRINT 250,N1,N2,SM
250  FORMAT(5X,10HCOMPONENTSI2,3H TOI2,5X,E12.6,8H DOLLARS)
2     CONTINUE
      PRINT 260
260  FORMAT(18H1REVIEW OF RESULTS//)
      PRINT 270,(T(I),SUM(I),I=1,LT)
270  FORMAT(10X,2HT=E12.6,5X,E12.6,8H DOLLARS)
END

```

## INPUT REVIEW

P	T0	C0	K	TAU(K)
.414000E 02	.220000E 00	-.186000E 00	-.870000E-01	.132000E 02

NUMBER	TITLE	TYPE	S1	S2	C
1	AXIAL FUEL EXP.	1	.170000E 00	.000000E 00	.365000E-02
2	CORE NA EXP.	1	.190000E 00	.000000E 00	.135000E-02
3	ABOVE-CORE NA EXP.	2	.190000E 00	.700000E-01	.135000E-02
4	ROD-BANK EXP., L1	2	.190000E 00	.900000E-01	.540000E-03
5	ROD-BANK EXP., L2	2	.149000E 01	.930000E-01	.160000E-03
6	ROD-BANK EXP., L3	2	.149000E 01	.210000E 02	.160000E-03
7	ROD-BANK EXP., L4	2	.149000E 01	.810000E 01	.160000E-03

TIME= .10

COMPONENT NO. 1	AXIAL FUEL EXP.	-.685856E-03 DOLLARS
COMPONENT NO. 2	CORE NA EXP.	-.231277E-03 DOLLARS
COMPONENT NO. 3	ABOVE-CORE NA EXP.	-,.825386E-04 DOLLARS
COMPONENT NO. 4	ROD-BANK EXP., L1	-.274693E-04 DOLLARS
COMPONENT NO. 5	ROD-BANK EXP., L2	-.113584E-05 DOLLARS
COMPONENT NO. 6	ROD-BANK EXP., L3	-.587493E-08 DOLLARS
COMPONENT NO. 7	ROD-BANK EXP., L4	-.164498E-07 DOLLARS

COMBINED EFFECT - .102829E-02 DOLLARS

## SUBTOTALS

COMPONENTS 2 TO 3	-,.313815E-03 DOLLARS
COMPONENTS 4 TO 7	-,.286275E-04 DOLLARS

TIME= .20

COMPONENT NO. 1	AXIAL FUEL EXP.	-.231659E-02 DOLLARS
COMPONENT NO. 2	CORE NA EXP.	-.793319E-03 DOLLARS
COMPONENT NO. 3	ABOVE-CORE NA EXP.	-.443381E-03 DOLLARS
COMPONENT NO. 4	ROD-BANK EXP., L1	-.154759E-03 DOLLARS
COMPONENT NO. 5	ROD-BANK EXP., L2	-.721110E-05 DOLLARS
COMPONENT NO. 6	ROD-BANK EXP., L3	-.502307E-07 DOLLARS
COMPONENT NO. 7	ROD-BANK EXP., L4	-.130717E-06 DOLLARS
	COMBINED EFFECT	-.371544E-02 DOLLARS

SUBTOTALS

COMPONENTS 2 TO 3	-.123670E-02 DOLLARS
COMPONENTS 4 TO 7	-.162151E-03 DOLLARS

TIME= .40

COMPONENT NO. 1	AXIAL FUEL EXP.	-.504875E-02 DOLLARS
COMPONENT NO. 2	CORE NA EXP.	-.178507E-02 DOLLARS
COMPONENT NO. 3	ABOVE-CORE NA EXP.	-.149865E-02 DOLLARS
COMPONENT NO. 4	ROD-BANK EXP., L1	-.561477E-03 DOLLARS
COMPONENT NO. 5	ROD-BANK EXP., L2	-.340613E-04 DOLLARS
COMPONENT NO. 6	ROD-BANK EXP., L3	-.355643E-06 DOLLARS
COMPONENT NO. 7	ROD-BANK EXP., L4	-.914782E-06 DOLLARS
	COMBINED EFFECT	-.892931E-02 DOLLARS

SUBTOTALS

COMPONENTS 2 TO 3	-.328373E-02 DOLLARS
COMPONENTS 4 TO 7	-.596809E-03 DOLLARS

TIME= .60

COMPONENT NO. 1	AXIAL FUEL EXP.	-.603721E-02	DOLLARS
COMPONENT NO. 2	CORE NA EXP.	-.218228E-02	DOLLARS
COMPONENT NO. 3	ABOVE-CORE NA EXP.	-.205710E-02	DOLLARS
COMPONENT NO. 4	ROD-BANK EXP., L1	-.801544E-03	DOLLARS
COMPONENT NO. 5	ROD-BANK EXP., L2	-.641313E-04	DOLLARS
COMPONENT NO. 6	ROD-BANK EXP., L3	-.95n763E-06	DOLLARS
COMPONENT NO. 7	ROD-BANK EXP., L4	-.243467E-05	DOLLARS
	COMBINED EFFECT	-.111456E-01	DOLLARS

## SUBTOTALS

COMPONENTS 2 TO 3	-.423938E-02	DOLLARS
COMPONENTS 4 TO 7	-.869061E-03	DOLLARS

TIME= .80

COMPONENT NO. 1	AXIAL FUEL EXP.	-.647568E-02	DOLLARS
COMPONENT NO. 2	CORE NA EXP.	-.236745F-02	DOLLARS
COMPONENT NO. 3	ABOVE-CORE NA EXP.	-.230701E-02	DOLLARS
COMPONENT NO. 4	ROD-BANK EXP., L1	-.912658E-03	DOLLARS
COMPONENT NO. 5	ROD-BANK EXP., L2	-.921391E-04	DOLLARS
COMPONENT NO. 6	ROD-BANK EXP., L3	-.18n825F-05	DOLLARS
COMPONENT NO. 7	ROD-BANK EXP., L4	-.460526E-05	DOLLARS
	COMBINED EFFECT	-.121613E-01	DOLLARS

## SUBTOTALS

COMPONENTS 2 TO 3	-.467446E-02	DOLLARS
COMPONENTS 4 TO 7	-.101121E-02	DOLLARS

TIME= 1.00

COMPONENT NO. 1	AXIAL FUEL EXP.	-.674254E-02 DOLLARS
COMPONENT NO. 2	CORE NA EXP.	-.247792E-02 DOLLARS
COMPONENT NO. 3	ABOVE-CORE NA EXP.	-.244079E-02 DOLLARS
COMPONENT NO. 4	ROD-BANK EXP., L1	-.97n831F-03 DOLLARS
COMPONENT NO. 5	ROD-BANK EXP., L2	-.117760E-03 DOLLARS
COMPONENT NO. 6	ROD-BANK EXP., L3	-.29n059F-05 DOLLARS
COMPONENT NO. 7	ROD-BANK EXP., L4	-.734888E-05 DOLLARS
	COMBINED EFFECT	-.127600E-01 DOLLARS

SUBTOTALS

COMPONENTS 2 TO 3	-,491871E-02 DOLLARS
COMPONENTS 4 TO 7	-,109884E-02 DOLLARS

TIME= 2.00

COMPONENT NO. 1	AXIAL FUEL EXP.	-.769190E-02 DOLLARS
COMPONENT NO. 2	CORE NA EXP.	-.283825F-02 DOLLARS
COMPONENT NO. 3	ABOVE-CORE NA EXP.	-.281521E-02 DOLLARS
COMPONENT NO. 4	ROD-BANK EXP., L1	-.112342F-02 DOLLARS
COMPONENT NO. 5	ROD-BANK EXP., L2	-.217944E-03 DOLLARS
COMPONENT NO. 6	ROD-BANK EXP., L3	-.111780E-04 DOLLARS
COMPONENT NO. 7	ROD-BANK EXP., L4	-.275755E-04 DOLLARS
	COMBINED EFFECT	-.147255E-01 DOLLARS

SUBTOTALS

COMPONENTS 2 TO 3	-.565347E-02 DOLLARS
COMPONENTS 4 TO 7	-.138012E-02 DOLLARS

TIME= 3.00

COMPONENT NO. 1	AXIAL FUEL EXP.	-.854109E-02	DOLLARS
COMPONENT NO. 2	CORE NA EXP.	-.315290E-02	DOLLARS
COMPONENT NO. 3	ABOVE-CORE NA EXP.	-.313159E-02	DOLLARS
COMPONENT NO. 4	ROD-BANK EXP., L1	-.125018E-02	DOLLARS
COMPONENT NO. 5	ROD-BANK EXP., L2	-.287864E-03	DOLLARS
COMPONENT NO. 6	ROD-BANK EXP., L3	-.228192E-04	DOLLARS
COMPONENT NO. 7	ROD-BANK EXP., L4	-.547931E-04	DOLLARS
COMBINED EFFECT		-.164412E-01	DOLLARS

## SUBTOTALS

COMPONENTS 2 TO 3	-.628449E-02	DOLLARS
COMPONENTS 4 TO 7	-.161566E-02	DOLLARS

TIME= 4.00

COMPONENT NO. 1	AXIAL FUEL EXP.	-.932824E-02	DOLLARS
COMPONENT NO. 2	CORE NA EXP.	-.344448E-02	DOLLARS
COMPONENT NO. 3	ABOVE-CORE NA EXP.	-.342473E-02	DOLLARS
COMPONENT NO. 4	ROD-BANK EXP., L1	-.136762E-02	DOLLARS
COMPONENT NO. 5	ROD-BANK EXP., L2	-.340950E-03	DOLLARS
COMPONENT NO. 6	ROD-BANK EXP., L3	-.366669E-04	DOLLARS
COMPONENT NO. 7	ROD-BANK EXP., L4	-.857018E-04	DOLLARS
COMBINED EFFECT		-.180284E-01	DOLLARS

## SUBTOTALS

COMPONENTS 2 TO 3	-.686921E-02	DOLLARS
COMPONENTS 4 TO 7	-.183093E-02	DOLLARS

TIME= 5.00

COMPONENT NO. 1	AXIAL FUEL EXP.	-.100579E-01 DOLLARS
COMPONENT NO. 2	CORE NA EXP.	-.371479E-02 DOLLARS
COMPONENT NO. 3	ABOVE-CORE NA EXP.	-.369648E-02 DOLLARS
COMPONENT NO. 4	ROD-BANK EXP., L1	-.147648E-02 DOLLARS
COMPONENT NO. 5	ROD-BANK EXP., L2	-.384166E-03 DOLLARS
COMPONENT NO. 6	ROD-BANK EXP., L3	-.52n455E-04 DOLLARS
COMPONENT NO. 7	ROD-BANK EXP., L4	-.118447E-03 DOLLARS
	COMBINED EFFECT	-.195003E-01 DOLLARS

#### SUBTOTALS

COMPONENTS 2 TO 3	-.741128E-02 DOLLARS
COMPONENTS 4 TO 7	-.203114E-02 DOLLARS

TIME= 6.00

COMPONENT NO. 1	AXIAL FUEL EXP.	-.107344E-01 DOLLARS
COMPONENT NO. 2	CORE NA EXP.	-.396538E-02 DOLLARS
COMPONENT NO. 3	ABOVE-CORE NA EXP.	-.394841E-02 DOLLARS
COMPONENT NO. 4	ROD-BANK EXP., L1	-.157741E-02 DOLLARS
COMPONENT NO. 5	ROD-BANK EXP., L2	-.421164E-03 DOLLARS
COMPONENT NO. 6	ROD-BANK EXP., L3	-.685374E-04 DOLLARS
COMPONENT NO. 7	ROD-BANK EXP., L4	-.151948E-03 DOLLARS
	COMBINED EFFECT	-.208672E-01 DOLLARS

#### SUBTOTALS

COMPONENTS 2 TO 3	-.791379E-02 DOLLARS
COMPONENTS 4 TO 7	-.221906E-02 DOLLARS

TIME= 7.00

COMPONENT NO. 1	AXIAL FUEL EXP.	-.113615E-01	DOLLARS
COMPONENT NO. 2	CORE NA EXP.	-.410769F-02	DOLLARS
COMPONENT NO. 3	ABOVE-CORE NA EXP.	-.418195F-02	DOLLARS
COMPONENT NO. 4	ROD-BANK EXP., L1	-.167097F-02	DOLLARS
COMPONENT NO. 5	ROD-BANK EXP., L2	-.453895F-03	DOLLARS
COMPONENT NO. 6	ROD-BANK EXP., L3	-.85A577F-04	DOLLARS
COMPONENT NO. 7	ROD-BANK EXP., L4	-.185542E-03	DOLLARS
	COMRINED EFFECT	-.221374F-01	DOLLARS

## SUBTOTALS

COMPONENTS 2 TO 3	-,837964E-02	DOLLARS
COMPONENTS 4 TO 7	-,239626E-02	DOLLARS

TIME= 8.00

COMPONENT NO. 1	AXIAL FUEL EXP.	-.119429E-01	DOLLARS
COMPONENT NO. 2	CORE NA EXP.	-.441304F-02	DOLLARS
COMPONENT NO. 3	ABOVE-CORE NA EXP.	-.439845E-02	DOLLARS
COMPONENT NO. 4	ROD-BANK EXP., L1	-.175770F-02	DOLLARS
COMPONENT NO. 5	ROD-BANK EXP., L2	-.483438E-03	DOLLARS
COMPONENT NO. 6	ROD-BANK EXP., L3	-.103804F-03	DOLLARS
COMPONENT NO. 7	ROD-BANK EXP., L4	-.218806E-03	DOLLARS

COMRINED EFFECT	-.233181E-01	DOLLARS
-----------------	--------------	---------

## SUBTOTALS

COMPONENTS 2 TO 3	-,881151E-02	DOLLARS
COMPONENTS 4 TO 7	-,256375E-02	DOLLARS

TIME= 9.00

COMPONENT NO. 1	AXIAL FUEL EXP.	-.124818E-01 DOLLARS
COMPONENT NO. 2	CORE NA EXP.	-.461269E-02 DOLLARS
COMPONENT NO. 3	ABOVE-CORE NA EXP.	-.459917E-02 DOLLARS
COMPONENT NO. 4	ROD-BANK EXP., L1	-.183811E-02 DOLLARS
COMPONENT NO. 5	ROD-BANK EXP., L2	-.510416E-03 DOLLARS
COMPONENT NO. 6	ROD-BANK EXP., L3	-.122215E-03 DOLLARS
COMPONENT NO. 7	ROD-BANK EXP., L4	-.251453E-03 DOLLARS
	COMBINED EFFECT	-.244159E-01 DOLLARS

SUBTOTALS

COMPONENTS 2 TO 3	-.921186E-02 DOLLARS
COMPONENTS 4 TO 7	-,272219E-02 DOLLARS

TIME= 10.00

COMPONENT NO. 1	AXIAL FUEL EXP.	-.129815E-01 DOLLARS
COMPONENT NO. 2	CORE NA EXP.	-.479777E-02 DOLLARS
COMPONENT NO. 3	ABOVE-CORE NA EXP.	-.478523E-02 DOLLARS
COMPONENT NO. 4	ROD-BANK EXP., L1	-.191265E-02 DOLLARS
COMPONENT NO. 5	ROD-BANK EXP., L2	-.535216E-03 DOLLARS
COMPONENT NO. 6	ROD-BANK EXP., L3	-.146964E-03 DOLLARS
COMPONENT NO. 7	ROD-BANK EXP., L4	-.283286E-03 DOLLARS
	COMBINED EFFECT	-.254366E-01 DOLLARS

SUBTOTALS

COMPONENTS 2 TO 3	-.958301E-02 DOLLARS
COMPONENTS 4 TO 7	-,287211E-02 DOLLARS

## REVIEW OF RESULTS

T= .100000E 00	-.102829E-02 DOLLARS
T= .200000E 00	-.371544E-02 DOLLARS
T= .400000E 00	-.892931E-02 DOLLARS
T= .600000E 00	-.111456E-01 DOLLARS
T= .800000E 00	-.121613E-01 DOLLARS
T= .100000E 01	-.127600E-01 DOLLARS
T= .200000E 01	-.147255E-01 DOLLARS
T= .300000E 01	-.164412E-01 DOLLARS
T= .400000E 01	-.180284E-01 DOLLARS
T= .500000E 01	-.195003E-01 DOLLARS
T= .600000E 01	-.208672E-01 DOLLARS
T= .700000E 01	-.221374E-01 DOLLARS
T= .800000E 01	-.233181E-01 DOLLARS
T= .900000E 01	-.244159E-01 DOLLARS
T= .100000E 02	-.254366E-01 DOLLARS

#### ACKNOWLEDGMENT

I wish to thank T. R. Bump for discussions of his BOW II program and D. A. Kucera for the programming of BOW III, PROFILE, and DYNAMIC.

## REFERENCES

1. R. A. Cushman, *The Effect of Radial Heat Transfer on the Temperature Distribution in EBR-II Stainless-Steel Reflector Subassemblies*, Trans. Am. Nucl. Soc. 10, 661 (1967).
2. T. R. Bump, *Effect of Reactor Temperatures on Bowing of EBR-II Subassemblies*, Trans. Am. Nucl. Soc. 10, 661 (1967).  
R. R. Smith, P. J. Persiani, D. A. Meneley, J. T. Madell, J. K. Long, F. S. Kirn, R. W. Hyndman, R. A. Cushman, T. R. Bump, J. C. Beitel, and D. A. Kucera, *EBR-II Run 25 and 26A Interim Report*, ANL internal memorandum (1968).
3. L. J. Koch, W. B. Loewenstein, and H. O. Monson, *Addendum to Hazard Summary Report, Experimental Breeder Reactor-II (EBR-II)*, ANL-5719 (Addendum) (June 1962).
4. P. J. Persiani, T. R. Bump, R. A. Cushman, J. Long, and D. Kucera, *Analysis of the Variation in the EBR-II Power Coefficient Due to Blanket Change*, Trans. Am. Nucl. Soc. 11, 282 (1968).
5. T. R. Bump, *Bow II: A Code for Calculating Deflections of Closely Spaced Parallel Beams, Each with Limited-pivot Support at One End, Possible Beam Interactions at Other End and at One Intermediate Position, and Arbitrary Temperature Distribution*, ANL-7528 (to be published).
6. P. J. Persiani, J. Kallfelz, F. Kirn, J. K. Long, and R. Smith, *EBR-II Power Coefficient Variations During Operational Run 26*, Trans. Am. Nucl. Soc. 11, 281 (1968).
7. R. Hyndman, private communication, ANL Idaho Division (Rod-drop Power Time Curve).
8. J. A. DeShong, Jr., *Power Transfer Functions of the EBWR Obtained Using A Sinusoidal Reactivity Driving Function*, ANL-5798 (Jan 1958).
9. J. A. DeShong, Jr. and W. C. Lipinski, *Analyses of Experimental Power-reactivity Feedback Transfer Functions for a Natural Circulation Boiling Water Reactor*, ANL-5850 (July 1958).
10. R. J. Roark, *Formulas for Stress and Strain*, McGraw-Hill (1965), Table III, p. 104.
11. P. Laurson and W. Cox, *Properties and Mechanics of Materials*, John Wiley and Sons (1931), p. 255.
12. S. Timoshenko, *Theory of Plates and Shells*, 2nd Edition, McGraw-Hill (1959), p. 206.
13. F. Jones and E. Oberg, *Machinery's Handbook*, The Industrial Press, New York (1937), p. 346.

